STUDIES OF CONFORMATIONAL CHANGES AND THE EFFECT OF ANTIBODY AND RECEPTOR BINDING ON CANINE PARVOVIRUS

A Dissertation

Presented to the Faculty of the Graduate School

of Cornell University

In Partial Fulfillment of the Requirements for the Degree of

Doctor of Philosophy

by

Christian Nelson

January 2009

STUDIES OF CONFORMATIONAL CHANGES AND THE EFFECT OF ANTIBODY AND RECEPTOR BINDING ON CANINE PARVOVIRUS

Christian Nelson, Ph. D.

Cornell University 2009

To be successful as pathogens, the capsids of nonenveloped viruses must balance two opposing roles: they must be structurally robust in order to protect the encapsulated genome from environmental insults outside of the host cell, yet metastable to allow release of the viral genome upon infection.

A goal of these studies was to further characterize the antibody response directed against canine parvovirus (CPV), and to understand the interplay between receptor and antibody binding to the capsid. Another goal was to understand the conformational changes that occur in the structure of the CPV capsid during infection, and to understand the biological significance of these changes.

A panel of eight antibodies directed against the virus were shown to be neutralizing as intact immunoglobulin G proteins (IgGs). However the fragment antigen binding domains (Fabs) of these IgGs differed greatly in their ability to neutralize CPV. These eight Fabs compete for receptor binding on the surface of cells, and compete with soluble receptor in solution, although the neutralizing Fabs competed for binding at significantly lower Fab to capsid ratios. Structural analysis of those Fabs demonstrated that most accessible areas of the capsid were able to generate an immune response and participate in antibody binding.

CPV is a highly stable virus, and many harsh conditions do not cause large structural changes in the virus. By biochemical and biophysical assays presented here, the viral capsid was unchanged until pH 4 and is thermally stable to temperatures of 70°C. Conditions that the virus would encounter during infection, such as low pH and

calcium removal, did not have direct structural effects on the CPV capsid. Furthermore, transferrin receptor or antibody binding did not cause detectable changes to the capsid structure.

These studies show that CPV is an extremely robust pathogen, due to its highly stable capsid. The capsid has clearly evolved to persist in harsh environmental conditions outside of the cell, and infect in the presence of circulating antibodies.

BIOGRAPHICAL SKETCH

Christian D.S. Nelson was born in Pittsford NY, a suburb just southeast of Rochester NY, in June of 1982. He attended public school in the Pittsford central school district, and graduated from Pittsford Sutherland High School in 2000. He then attended the University of Rochester for a semester, and majored in biomedical engineering, before enrolling at Cornell University the following spring. At Cornell, he completed a bachelors of science in biological sciences with a minor in biochemistry and graduated in 2004. While at Cornell, he performed undergraduate research in the laboratory of Dr. Colin Parrish, and stayed on for a year after graduation to work as a technician. The following year he was accepted to the graduate studies program in the College of Veterinary Medicine, and worked again for Dr. Colin Parrish.

After graduation he will work as a post-doctoral research associate in the laboratory of Dr. Walter Atwood at Brown University. There he will study the mechanisms by which non-enveloped human polyomaviruses bind, enter, and uncoat in host cells. This will hopefully constitute the next step in the long process of becoming an independent research scientist.

For Melissa

ACKNOWLEDGMENTS

There is an extremely long list of people who have contributed to my graduate training, in one way or another. Dr. Colin Parrish has given me tremendous guidance and confidence in my research over the years, and I would most certainly not be pursing this career without his continued support. He was willing to train me at a time when I had no clear direction, and for that I am eternally grateful. Drs. Theodore Clark, Linda Nicholson, and Robert Oswald of my special committee have been excellent, and I appreciate the thoughtful input and support that they have given to me. Dr. John Parker has also been extraordinarily helpful, and I appreciate the many discussions we have had.

It has been a joy to work with everyone in the Parrish lab. I must especially thank Wendy Weichert, who beyond providing advice and assistance over the years, has been a great friend. Virgiana Scarpino has also done a fantastic job keeping up with my voracious appetite for purified virus and receptor. Other current and past members have also provided an enjoyable working environment and include Laura Palermo, Karla Stucker, Carole Harbison, Karin Hoelzer, Nell Bond, Tyler Lillie, Shelagh Johnson, and Gail Sullivan. Of course, I must also thank my fellow graduate student and officemate Robert "Oz" Ossiboff for his support and companionship.

I would also like to thank my collaborators. The Rossmann laboratory, and Dr. Susan Hafenstein in particular, have been extremely patient in explaining basic concepts of structural biology, a concept of which I knew little about. Dr. Brian Bothner has also been extremely helpful beyond the physical work of our collaboration, by explaining protein dynamics and suggesting meaningful experiments and controls to strengthen my work.

I owe much of my accomplishments to my parents, Edward and Deborah

Nelson, who constantly supported me in my work, and encouraged me to ask questions. Finally, I must thank by beautiful wife Melissa, who has been a mainstay of support through this entire degree process. Without her unwavering optimism, this thesis would not have been completed.

TABLE OF CONTENTS

LIST OF FIGURES

LIST OF TABLES

CHAPTER ONE

Introduction

1.1 Parvovirus characteristics.

Canine parvovirus (CPV) belongs to the Parvoviridae family, the characteristic traits of which are a small nonenveloped icosahedral capsid, and a DNA genome of roughly 5kb which is linear, self priming, and single-stranded. Sixty copies of several isoforms of the same capsid protein encase this genome, to form a capsid of around 25 nm diameter. Transcription will not occur off of the ssDNA, and therefore parvoviruses likely wait for a cell to begin S-phase to allow DNA fill-in so that replication and transcription can occur (47, 124, 187).

1.2 CPV emergence and pathogenesis.

Canine parvovirus is a relatively new pathogen of canines, first detected in 1978 and having emerged ~4-10 years earlier (128, 157). CPV most likely evolved from a closely related virus of cats, feline panleukopenia virus (FPV) (67, 123, 124, 127, 176). CPV generally infects naïve dogs and newborn puppies, and causes enteritis or myocarditis in infected animals (134). The frequency of symptomatic infection is believed to be small, since reactive sera is recovered from many animals that have not presented symptoms of CPV infection. The natural course of transmission is through the fecal-oral route, and CPV is believed to initially infect epithelial or immune cells of the tonsils. CPV uses the transferrin receptor (TfR) to bind and enter cells, and as mentioned, requires cells to be in S-phase in order to replicate its DNA (122, 139, 140). This restricts susceptible cells to those that are actively dividing, and those that show upregulation of TfR expression. Infection of the tonsils results in viral sheding into the lymphatics and blood, and the establishment of a viremia that then infects other lymph nodes, other immune tissues including the thymus and bone marrow, and eventually the crypt cells of the small intestinal villi (183). In young puppies, infection of the rapidly dividing cells of the myocardium

leads to myocarditis. Enteric symptoms are the result of infection of crypt cells, which cause a loss of the intestinal epithelium and intestinal integrity, and leakage of large amounts of sera into the intestinal contents. Virus is shed in this diarrhea in titers as high as 10^9 infectious doses per ml. Persistent infection is not seen in CPV, and most infections are now seen in young puppies that have lost maternal antibody protection around 8 to 12 weeks of age (125, 134).

1.3 Splicing of primary transcripts and capsid composition.

The currently recognized capsid proteins of CPV, termed Viral Protein 1 and 2 (VP1 and VP2), are generated from the same primary transcript, which is transcribed from the promoter at map unit 38 of the CPV genome (36, 133). Alternate splicing of this transcript leads to different mRNAs corresponding to VP1 or VP2, and splicing efficiency of VP1 results in approximately 25% of the capsid protein in an infected cell to be VP1 and the remaining to be VP2 (78). These protein ratios are not reflected in the composition of the capsid, where 5-6 of the 60 copies of capsid protein are VP1, and which indicates that factors other protein abundance may dictate the relative protein ratios within the CPV capsid (174). VP1 (767 residues, 80.3 kda) contains the VP2 sequence (584 residues, 64.7 kda) plus an additional 143 amino acids on its N-terminus, termed the VP1 unique region (VP1ur). Within the VP1ur is a phospholipase A2 (PLA2) domain and several groups of basic amino acids that can act as nuclear localization sequences (NLS), and both motifs are critical for infection (193, 203)(Figure 1.1a). VP2 expressed alone can form virus-like particles (VLPs), implying that VP2 contains all the necessary information for capsid assembly (72, 151). These VP2-only capsids are able to package DNA, implying that there are no special sequences within VP1 necessary for DNA packaging (188). It is not known how VP1 and VP2 are arrayed within the capsid. Research within the related

Figure 1.1a.

Transcriptional layout of CPV-2 and features of VP1 and VP2. Transcription from the promoter at P38 leads to the capsid protein precursor mRNA. Alternative splicing results in mRNAs for either VP1 or VP2. Alternative splicing of the VP2 mRNA removes the start codon of VP1, and translation of VP2 starts at a second start codon ~400 nt downstream. A schematic diagram of VP1 and VP2 are shown. VP1 contains an additional 143 residues that contain a PLA2 domain and NLS.

VP1/2 mRNA transcription and alternative splicing

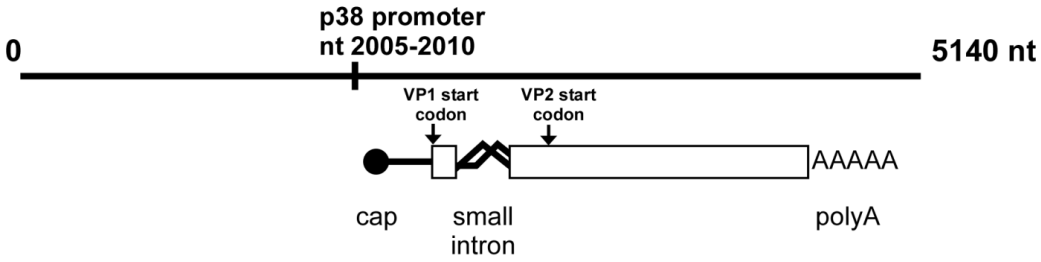

VP1/2 protein features

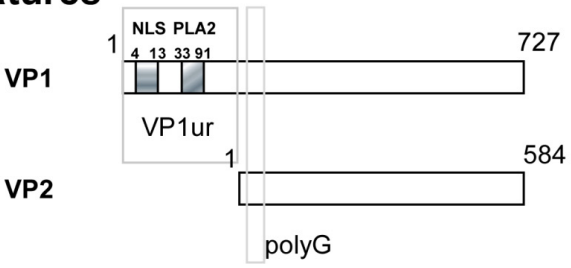

parvovirus H1 suggests that VP1 may be clustered within the capsid, since chemical cross-linking results in a higher than expect proportion of VP1-VP1 linkages (120).

1.4 Capsid structure of CPV.

The atomic structures have been solved for CPV, FPV, and related mutants, and VP1 and VP2 contain extensive secondary structure (Figure 1.1b). VP1 and VP2 also share the same core structural feature, an anti-parallel beta (β) barrel motif (3, 61, 187, 202) (Figure 1.2a). This motif is present in many other nonenveloped viruses, including the well-studied picornaviridae family, although CPV contains two additional β-strands (150).

In this beta barrel, β-strands BIDG (plus the extra strands βA and βB) line the interior of the capsid, while the CHEF strands fill volume between the interior and exterior surfaces. The exterior surface of the capsid is composed of the loops that connect the strands of the β-barrel. Some of these loops are quite large and complex, with the GH loop being the largest at 221 amino acids (187). These loops are responsible for many of the functions associated with viral functions, host interactions and cell infection, such as receptor and antibody binding (71, 160, 169, 179).

CPV is one of the smallest viruses, with the intact capsid having a diameter of 260Å at its widest point. The 60 VP1 and VP2 monomers that comprise the capsid show a T=1 icosahedral symmetry (Figure 1.2b)(187). The symmetry elements are six 5-fold axes of symmetry, fifteen 2-fold axes of symmetry, and ten 3-fold axes of symmetry (these numbers are doubled if you count the structures on either side of the axis, rather than the axis itself). Analysis of the crystal structure shows that the GH loops from adjacent monomers around the 3-fold axis inter-digitate to form a large raised region over the 3-fold axis. The calculated free energy of formation of the 3-fold axis is large (-201 kJ per mol subunit), indicating that this structure is much

Figure 1.1b.

Secondary structure representation of the VP2 capsid structure. Loops are colored based on structural features. These colors are consistent with Figure 1.2a. The core β-barrel is colored in red. The surface loop 1 (BC strands) is colored in orange, loop 2 (EF strands) is colored in blue, and loop 3-4 (GH strands) are colored in purple. The beta ribbon forming the 5-fold pore (DE) is colored in green.

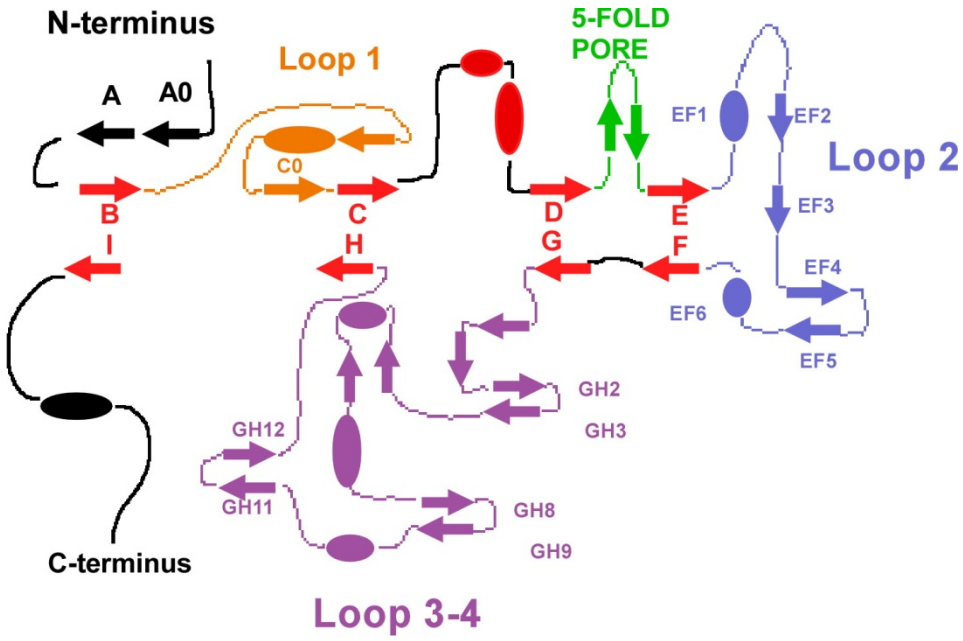
N-terminus
A
A0
Loop 1
C0
5-FOLD
PORE
EF1
EF2
Loop 2
EF3
EF4
EF5
EF6
B
I
C
H
D
G
E
F
GH2
GH3
GH12
GH11
GH8
GH9
C-terminus
Loop 3-4

Figure 1.2a.

Three dimensional structure of the VP2 capsid protein structure. The alpha carbon backbone is rendered as a cartoon and the structure is colored according to its different features. The core β-barrel is colored in red. The surface loop 1 (BC strands) is colored in orange, loop 2 (EF strands) is colored in blue, and loop 3-4 (GH strands) are colored in purple. The beta ribbon forming the 5-fold pore (DE) is colored in green.

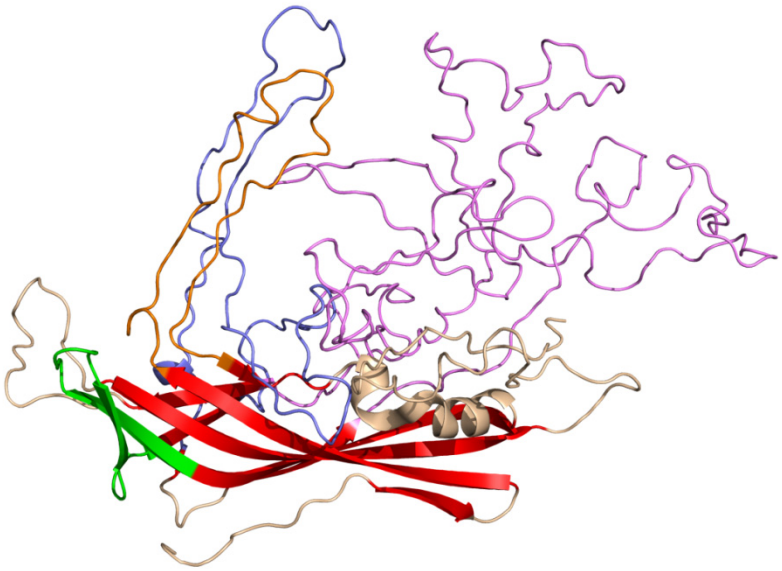

Figure 1.2b.

The assembled capsid structure of CPV. The capsid is surface rendered, and three VP2 monomers are differentially colored to display their orientation in the capsid. The asymmetric unit is overlaid onto the capsid. The 5-fold, 3-fold, and 2-fold axes of symmetry are indicated by a pentagon, triangle, and oval, respectively.

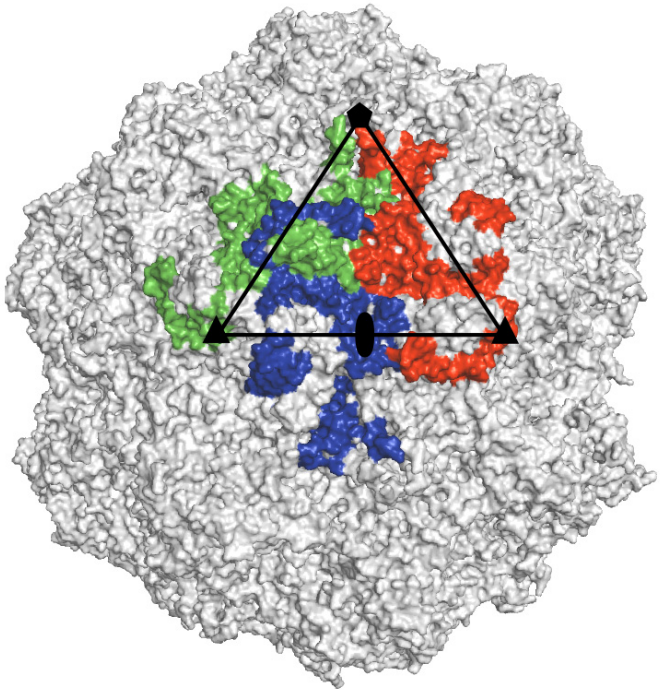

more stable than the pentamers (-75 kJ per mol subunit) or dimers (-37 kJ per mol subunit) (202). This raised region around the 3-fold axis is termed the 3-fold spike and is a prominent structural feature of the viral capsid, measuring 70Å wide and 22Å high (1).

Another major feature of the capsid of CPV is the ~10 Å wide pore that are present at each 5-fold axis of symmetry that extends to the interior of the capsid. This pore is formed by β ribbons of the DE loops of each of the 5 surrounding monomers which form a cylinder. It is believed that the N-termini of the VP2 capsid proteins are externalized through these pores, and the 5'-end of the viral DNA is believed to be left exposed from the capsid through one pore after it is packaged (202). A glycine-rich region between resides 22 and 39 (VP2 numbering) is shared by both VP1 and VP2, and this region is believed to reside within the pore for ~11 of the VP2s in full (but not empty) capsids (2, 45, 202). Occupancy of the 5-fold pore by this stretch of glycines and other residues with small side-chains causes only minor steric clashes with the wall of the pore. However, externalization of the N-terminal ~20 amino acids would require an enlargement of the pore, as the bulky side chains in that sequence would cause significant clashes as they pass through the pore (202). The actual diameter of this pore in solution is therefore not known, but it is assumed that the β-strands comprising the pore and the surrounding residues are dynamic and able to separate and allow the pore to expand. In accordance with this hypothesis, there are cavities surrounding the 5-fold pore that may be compressed to allow room for the expansion of the pore (28). The compression of cavities in viral proteins during the infectious cycle has been demonstrated in other viruses (29, 33).

1.5 VP1 unique region.

1.5a Phosopholipase A2 (PLA2) domain.

Sequence analysis of most parvoviruses shows a series of conserved residues in the VP1ur (residues 33-91 in CPV). These residues constitute a functional PLA2 enzyme, which is in the same class as the calcium dependant secretory PLA2s (203). Phospholipases are classified based on the bond they hydrolyze, and PLA2 enzymes hydrolyze the ester bonds at the *sn*-2 position of phospholipids (201). PLA2 is further classified into more than ten groups based on their enzymatic and structural characteristics, with the parvovirus PLA2s belonging to group XIII (26). The parvovirus PLA2s differ greatly in their specific activity, but all have similar substrate specificities and pH sensitivities (178). In addition, all of these parvovirus PLA2s require millimolar calcium concentrations to function.

The active site of parvovirus PLA2 consists of a histidine-aspartic acid (HD) dyad, which is highly conserved among the different viruses (203). The unprotonated His residue polarizes a water molecule, which then attacks the carbonyl bond at the *sn-2* position of the phospholipid (178). PLA2 of parvoviruses are most active at pH 6-7 (203). This is most likely a result of deprotonation of the histadine residue in the HD dyad. This deprotonation is necessary to coordinate the water molecule that is responsible for the nucleophilic cleavage of the phosopholipid. The PLA2 of CPV is believed to be similar to most secretory phospholipases that do not dissociate from the membrane after hydrolysis, and instead move along the membrane to cleave the next phospholipid (201). All parvovirus PLA2s studied so far are able to bind efficiently to the zwitterionic phosphatidylcholine lipids that make up the majority of the external leaflet of the plasma membrane, and also are the predominant lipid in the internal leaflet of endosomes (26).

PLA2 is critical for infection, as point mutants that render PLA2 inactivate render the virus non-infectious, and these mutant virions are seen to accumulate in endosomes near the perinuclear regions of cells similar to wild type particle (56, 59, 203). This indicates that PLA2 deficient particles are able to bind, enter, and traffic through cells similar to wildtype particles. The lack of infectivity is thought to be a failure of virions to escape from these perinuclear endosomes or lysosomes, and the mutant virions are subsequently degraded. Also, infection of CPV in the presence of PLA2 inhibitors reduced infection, although the effect of these inhibitors on cell division was not examined and whether they have direct effects on the viral infection is not clear (171). In the closely related parvovirus minute virus of mice (MVM), a mutant PLA2 deficit was complemented in trans by addition of bee venom PLA2, indicating that covalent linkage of the capsids and PLA2 are not necessary for infection (56). Since this class of phospholipase requires levels of calcium that are approximately 1000-fold higher than the cytoplasm, it is likely that this enzyme acts in the extracellular space or in organelles with relatively high calcium levels (178). The CPV capsid coordinates 120 or 180 calcium ions (depending on the variant) and it is possible that those ions are released in the endosome and enhance enzyme activity. The VP1 encoded PLA2 domain is not accessible on the surface of the virus before infection, and is enzymatically inactive prior to externalization (203). During infection, this domain becomes accessible, and this externalization is believed to be a critical point in infection (171).

1.5b Nuclear localization signals (NLS).

Amino acid residues 4-13 of VP1 act as a functional NLS for the CPV particle (188, 192). When synthetic peptides corresponding to these residues were attached to fluorescently labeled bovine serum albumin, the localization of the albumin was

changed from cytoplasmic to nuclear. Furthermore it was shown that this process of nuclear localization was receptor mediated and energy dependant, as either excess unconjugated peptides or energy poisons blocked this process (192). Finally, point mutations within this sequence resulted in virions that were less infectious (196). Additional sequences between residues 109-130 of VP1 also resemble NLS, but their significance is less well understood, since peptide-albumin conjugates of these residues do not traffic to the nucleus (94, 192). The VP1ur that contains this NLS is believed to be contained within the capsid and becomes externalized during infection (195). To date however, there is no clear mechanistic understanding as to how these NLS sequences become accessible or engaged by the cellular transport machinery (47). Presumably, exposure of this NLS would engage the karyopherin transport machinery and result in trafficking of the particle through the nuclear pore, allowing the viral genome to gain access to the host polymerases that are necessary for viral transcription.

1.6 Localization of N-termini of VP1 and VP2.

The atomic resolution structures of all parvoviruses solved to date do not show the N-termini of either the VP1 or VP2. For CPV, the protein is resolved started at amino acid 38 (VP2 numbering) (187). The inability to detect significant electron density associated with the N-terminus of VP1 or VP2 indicates that this area of the capsid is disordered in the crystal structure, and is likely dynamic in solution. In most crystal structures of full capsids, weak electron density is seen in the pore at the 5-fold axis of symmetry and that is believed to correspond to the Gly-rich sequence near the N-terminus (presumably of VP2). Based on electron density calculations in the 2.9 Å structure of DNA containing capsids, at least 60 percent of the pores are filled with polypeptides from VP2 (202). Since the pore is large enough to accommodate a single

polypeptide chain, it is believed that these VP2 N-termini alternate in their occupancy of the pore. There are however, no direct measurements of the rates of externalization of these N-termini reported.

The extra-capsid accessibility of the N-terminus VP2 appears to be important for successful nuclear export of the assembled full capsids of MVM. Normal infection produces a proportion of capsids that lack DNA, and in those empty capsids the N-terminus of VP2 is sequestered within the capsid. This N-terminus is accessible in full capsids with packaged DNA, implying that the packaging process results in the extrusion of these N-termini, or alternatively that in empty particles the N-termini withdraw into the particle. Since the capsid may be packaged under pressure, DNA packaging may force some of N-termini to an exterior position (45, 46). Within the N-terminus of VP2 is a nuclear export signal (NES). For MVM, when that peptide is synthesized and conjugated to fluorescently labeled bovine serum albumin it can result in trafficking of the albumin out of the nucleus (101). Full MVM particles that lack this NES remain localized in the nucleus very late in infection (101). MVM contains several serine residues in this NES, and phosphorylation of these residues is important for export. It is believed that the CRM-1 export pathway is important for this process, but the exact interactions between this molecule and the capsid have not been demonstrated (95, 101).

The N-terminus of VP1 is also not resolved in the atomic resolution structure of CPV (202). This is not surprising as VP1 represents 10% of the capsid protein and would not be able to fully occupy any of the symmetry positions on the capsid. Since 60-fold icosahedral averaging was used to solve the crystal structure of CPV, this asymmetrically distributed electron density would be averaged out when solving the structure. Attempts at producing VP1-only particles have not been successful, as those particles do not assemble (151). The N-terminus of VP1 is not accessible in

newly formed virions of either full or empty capsids, as determined by probing with VP1-specific antibodies against the N-terminus (195). The PLA2 domain within the VP1ur is also not enzymatically active, indicating that the PLA2 is sequestered from its substrate, does not have Ca^{2+} required for its activity, or is in a form that renders it inactive (171). During infection or heating *in vitro*, this N-terminus becomes accessible to VP1 antibodies (195). There is however some debate as to whether VP1ur occupies an internal position within the capsid and this may differ between viruses. In the related parvovirus B19, the VP1ur is initially not accessible to antibodies, but after mild treatments capsids can be immunoprecipitated by polyclonal sera against the N-terminus (147). Other studies however, have shown that VP1 N-terminus can be immunoprecipitated, and recombinant B19 virions that have either lysozyme or GFP added to their N-termini are either enzymatically active, or can be immunoprecipitated with antibodies against GFP, respectively (148, 110). If the N-terminus of VP1 of B19 is normally exposed, it is unclear whether this is an exception to the parvovirus family or a more common trait. A possibility remains that the N-terminus of VP1 is also external to the capsid but in a denatured form that is not reactive to antibodies, or may be on the outside of the capsid but be sequestered in the canyon which lies directly around the 5-fold axis and therefore is sequestered from antibody binding and PLA2 substrate.

1.7 Sialic acid and lipid binding.

CPV binds to sialic acid using structures near the two fold axis of symmetry, most notable Arg 377, Glu 396, and 397 Arg (179, 10). The virus appears to preferentially bind to sialic acid of the N-glycolyl neuraminic acid form (179). However, the role of sialic acid binding in infection remains unclear. Treatment of cells with neuraminidase, which removes the sialic acids, delays the kinetics of

binding, but does not prevent infection (179). Furthermore, mutant viruses that are not able to bind to sialic acid are not reduced in their infectivity, and cells that express only N-glycolyl neuraminic acid but not transferrin receptor are not permissive for infection (10, 194). It is therefore believed that sialic acid serves as a viral attachment factor for cells. Sialic acid binding may however be important for productive binding and entry during in vivo infection of canines. CPV has been reported to interact with sphingomyelin and other phosphoinositides, and lipids may co-purify with the virus (117, 171). It is not clear what effect this binding has on the infectious life cycle of the virus.

1.8 Transferrin Receptor.

CPV uses TfR for binding and uptake into cells (122). CPV cannot bind or enter Chinese hamster ovary (CHO) cells that either express the hamster TfR, or that do not express any TfR (the TRVb cell line), but expression of feline or canine TfRs in these cells allows binding and infection. Addition of a polyclonal anti-TfR anti-sera to the TRVb cells expressing feline TfR before addition of virus inhibits binding and uptake. This sera also inhibits binding and uptake of viruses to HeLa cells that normally express human TfR (122). Microinjection of a monoclonal antibody against the TfR cytoplasmic tail prevents infection. Finally the virus has been shown to bind directly to the purified TfR ectodomain in biochemical assays (118).

The TfR is a homodimeric type II membrane protein that contains several functional regions, the cytoplasmic, transmembrane sequences, a stalk that raises the receptor above the membrane, and an ectodomain that contains 3 smaller domains, the helical, protease-like, and apical domains. A soluble portion of the ectodomain (sTfR) can be generated by treatment of cells with trypsin, which releases the ectodomain starting at residue 119, and a similar sTfR can also be produced *in vitro* by baculovirus

expression, expressing a protein corresponding to amino acid residues 119-770 (69, 90). The crystal structure of this soluble ectodomin for human TfR has been solved (89), and that shares 79% identity with the feline receptor (the feline and canine receptor differ by 11%). Homology modeling can therefore be used to visualize important domains on the surface of the feline or canine TfR (Figure 1.3). Structural and biochemical evidence suggests that the receptor is always present as a dimer on the surface of cells (156). TfR contains two interchain disulfide bonds, which are not necessary for dimerization, and are not included in sTfR (7, 77). The interface between these monomers is localized between the helical domains of the two subunits which form an extensive and stable hydrophobic interaction, having a solvent inaccessible surface area of 4100Å (89). Cryo-EM studies of TfR:Tf complexes show that Tf binds to areas of the helical and protease-like domain, on the plasma membrane proximal side of the receptor (34). TfR contains significant post-translational modifications including disulfide bonds between dimers, and addition of multiple glycans. The human TfR has 3 N-linked glycosylation sites, and glycosylation of some of those sites are necessary for correct folding and surface expression. Mutations of the human TfR glycosylation sites results in little or no expression of correctly folded TfR (24). The feline TfR has four glycosylation sites and the canine TfR has five, with the extra glycosylation site important for discriminating binding between CPV and FPV (119).

1.9 Endocytosis of TfR into cells.

Endocytosis of TfR and transferrin is well characterized, and is among the best characterized examples of clathrin-mediated endocytosis (CME). TfR controls iron homeostasis in the cell through binding and uptake of its natural ligand, iron-loaded

Figure 1.3.

Homology structure model of the dimeric feline transferrin receptor soluble ectodomain, based on the solved human TfR crystal structure. The stalk, transmembrane, and cytoplasmic domain are included to orient the ecotdomain with respect to the plasma membrane, and are colored orange. The helical domain, protease-like domain, and apical domain are colored green, blue, and red respectively.

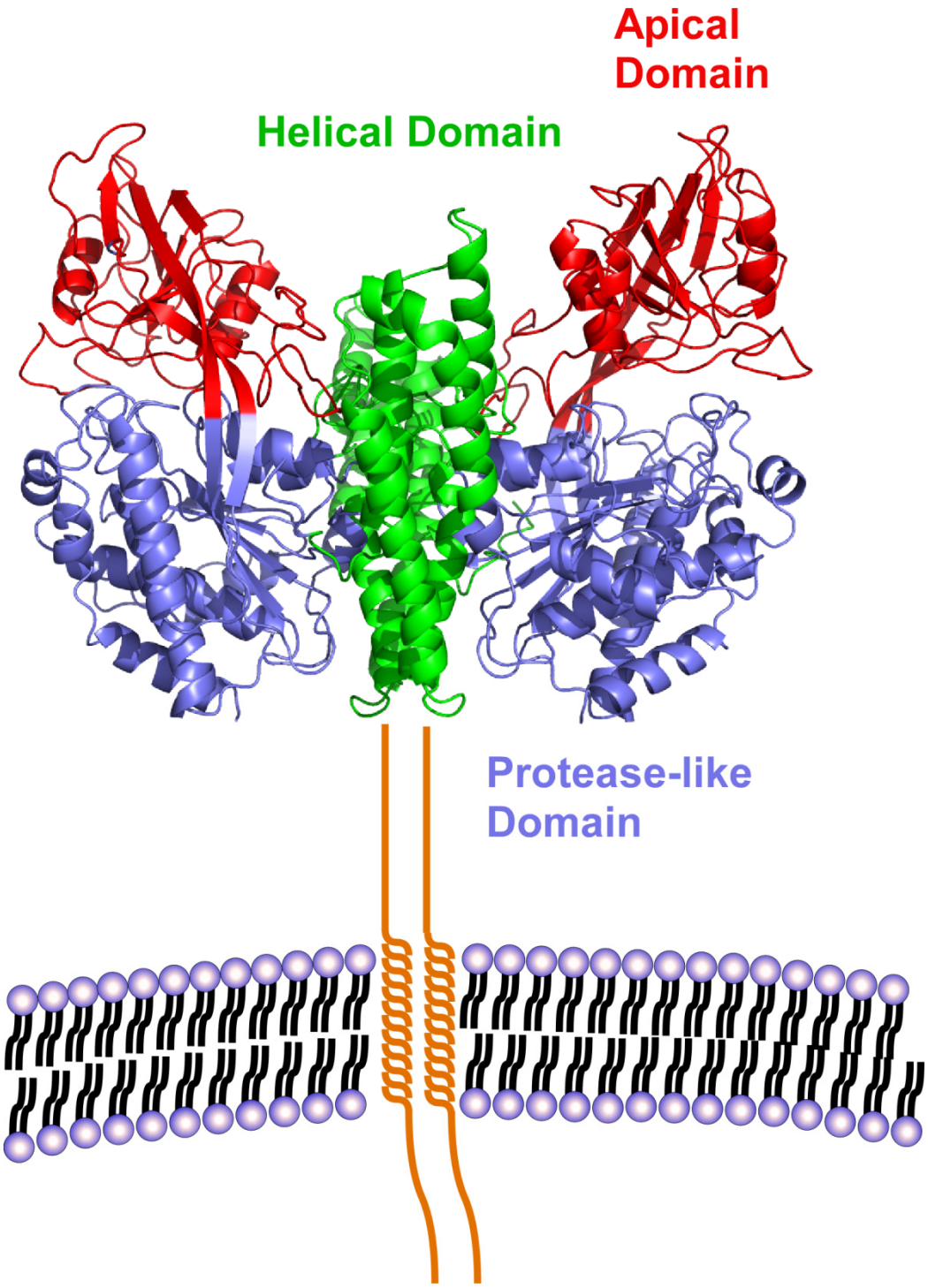
Apical
Domain
Helical Domain
Protease-like
Domain

transferrin (Tf), which bivalently binds iron (54). Uptake of TfR is a constitutive process in the cell, and binding of ligands are not necessary to induce endocytosis (81). The process of CME itself is complex, with a number of accessory proteins playing a role in cargo sorting and internalization (161). Endocytosis begins with clustering of TfR into clathrin coated pits, due to the accumulation of cytosolic proteins under the plasma membrane, one protein of which is clathrin (54). Within the cytoplasmic tail of TfR is the YTRF domain, which binds the medium chain of adapter protein 2 (AP2). AP2 binds clathrin and oligermization of clathrin forms cage-like structures which cause membrane bending and invagination. The coiled protein dynamin is then recruited and forms a collar structure at the proximal side of the plasma membrane (83). This GTPase is responsible for pinching off the vesicle (42).

The TfR-Tf complex is then delivered to acidic endosomes, and ultimately recycles back to the plasma membrane. The process of TfR-Tf entry and recycling is fast, with the iron delivery to low pH endosomes and recycling completed in as little as 15 min (175). The TfR/Tf complex is trafficked to the mildly acidic early endosomes that are enriched in the proteins Rab4, Rab5, and EEA-1. Here the low pH causes dissociation of iron from Tf, while remaining associated with TfR. Most of the TfR then accumulates in Rab 11 positive recycling endosomes. Clustering in these endosomes promotes recycling back to the surface, where apo-Tf dissociates back into the extracellular space. Two routes of recycling may be followed, one that is faster and those appear to involve the Rab11 recycling compartment, and more direct recycling from the early endosome that involves Rab4. At early times after Tf addition to cells, 90% of Tf was associated with Rab4 positive endosomes, and 64% was associated with Rab4 endosomes at 30 min after Tf addition (167). A slower process occurs through a perinuclear recycling component, in endosomes enriched in Rab 11 (158).

1.10 Binding, entry, and uncoating of CPV in cells.

1.10a CPV interactions with TfR.

Binding of TfR is necessary and most likely sufficient, along with its associated endocytic machinery, for viral binding and entry into cells. Specific interactions between CPV and TfR is necessary for infection, as replacement of the ectodomain of TfR with other capsid-binding ligands such as an anti-CPV single chain antibody fragment of the variable domain (scFv) binds capsids to cells but does not mediate infection (69). It was not determined in this assay whether scFv-Tfr chimeras were able to internalize virus. By flow cytometry, there is no obvious competition between CPV and Tf for binding to TfR (70). Since FPV capsids are unable to bind to the canine TfR, chimeras between the canine and feline TfRs can be used to identify specific receptor regions or structures that control virus binding. This approach showed that residues in the apical domain of the TfR affect binding to CPV and FPV (119). In addition, changing residue 221 in the TfR from a Leu to Lys resulted in a mutant TfR that was able to bind to CPV, but allowed only low levels of infectivity (119). This suggests that successful infection depends on specific interaction between CPV and TfR, as other receptors that bind CPV do not allow infection. However, the specific mechanisms that mediate infection through CPV and TfR binding are still not understood.

The interactions between CPV and the soluble feline TfR ectodomain (sfTfR) have been analyzed by cryo-electron (cryoEM) microscopy and three dimensional image reconstructions. This co-structure has been solved to 27Å and has allowed for the mapping of a sfTfR footprint on the surface of the CPV capsid (63). sfTfR and CPV were shown to have extensive molecular interactions, with approximately 1000 Å of surface area contact. It is possible that higher resolution reconstructions would result in a smaller footprint on the virus.

1.10b Trafficking of CPV within the cell.

Correct trafficking of CPV capsids within the endosomal system of the host cell is thought to be required to ensure infection. One hypothesis for the high particle to infectious unit ratio seen for many animal viruses is a result of incorrect trafficking of many particles within the cell (184). This high particle to infectivity ratio also makes it extremely difficult to identify which particle, or which compartment within the cell is responsible for infection. It is also likely that CPV can use multiple pathways to infect a cell (65).

Canine parvovirus begins infection by interacting with TfR on the surface of host cells. Similar to TfR bound to Tf, the CPV-TfR complex associates with clathrin coated pits, and dominant negative forms of dynamin prevent infection (121). Binding to TfR and entry to the cell through CME enables efficient and rapid entry into cells, and the endocytosis within the cells allows the particles to bypass the dense cortical actin that lies directly below the plasma membrane. Other pathways of endocytosis may also be used for uptake, and removal of the YTRF motif from the cytoplamic tail of TfR reduced the rate of uptake from the cell surface, but did not greatly reduce infection, indicating that the virus can still infect cells without using CME (69).

CPV particles entering the cells initially follow the normal trafficking pattern of Tf/TfR, with virus associating with Rab5 positive early endosomes shortly after addition of virus. Unlike the Tf/TfR complexes, which recycle efficiently back to the cell surface, the TfR/CPV complexes become associated with Rab7-positive late endosomes and lysosomes (21, 171). Furthermore, microinjected antibodies against the cytoplasmic tail of TfR inhibit CPV infection between 2 and 4 hours after internalization (122), indicating that the virus must remain bound to TfR for a number of hours after binding to the surface of cells. CPV rapidly traffics to a perinuclear region, and can still be detected in that location 10 hours post uptake (172). The

perinuclear vesicles may be recycling endosomes, late endosomes or lysosomes as they do not co-localize with a golgi marker TGN-38, or the ER marker PDI (172). The virus-containing vesicles are believed to traffic to this perinuclear region along microtubules, as treatment of cells with nocodazole prevented this localization (196). Trafficking of CPV within the cell is most likely not spatially and temporally separated within distinct compartments, and live-cell imaging of the dynamic process shows that particles co-localize within various types of endosomes at early times after uptake, and do not necessarily proceed in a strictly stepwise manner (Carole Harbison, unpublished results).

How does CPV remain associated with TfR for so long but apparently not recycle? It is thought that clustering of TfR can change the sorting of the receptor and its cargo to different pathways. Uptake of chemically oligermized Tf causes re-distribution of the cargo to a longer lived recycling endosome or late endosome, slows down recycling, and results in increased degradation (102). It is possible that clustering of the dimeric TfR by binding and cross-linking the multivalent causes a redistribution of the receptor-capsid complex to late endosomes and lysosomes, and this may be a productive step in infection (171). Thus, although CPV rapidly enters cells and seems to traffic to many distinct compartments it is not completely clear which compartment or endocytic route is critical for infection.

1.10c Capsid conformational changes associated with infection.

The parvovirus capsid is a very robust structure, and while it is generally believed that a conformational change in the CPV capsid is critical for infection, the nature of any structural changes that occur are unknown. It is presumed that an important conformational change required for infection is the release of VP1ur from its internal position in the capsid. Exposure of this domain would expose the active PLA2

enzyme that would modify the endosomal membrane, an event that appears required for particle escape or to allow re-direction of endosomes, while the exposure of NLS signals would allow trafficking to the nucleus. CPV likely traffics through a late endosome or lysosome since low pH is necessary for infection (122, 171). However, it is not clear whether the low pH acts directly to change the structure of the virus, or whether this low pH is important in the activation of other cellular events such as vesicular trafficking and fusion, or for the activity of low pH-dependent proteases. The structures of CPV or FPV at pH 7.5, 6.2 and 5.5 have been solved by X-ray diffraction of viral crystals, and only minor changes are seen at low pH. There is however an interplay between low pH and calcium binding (31, 160, 187). For FPV, the flexible loop between residues 360 and 373 becomes increasingly disordered at low pH in part due to loss of one of the bound Ca^{2+} ions, along with the loss of hydrogen bonds. Treatment with EGTA removes all of the Ca^{2+} ions and this releases two loops so that they change positions, and the 360-373 loop is completely disordered in the structure (Figure 1.4). It is not known what physiological effects this increased loop flexibility has on CPV or FPV. This region is in the area where TfR and sialic acids bind, and may therefore be important for allowing the capsids to disengage from the receptor once inside the cell (63). Besides this flexible loop, there are no other structural changes that have been observed at low pH or calcium levels.

Low pH may also affect the release of some N-termini of VP1. Studies of MVM capsids show that low pH prevents exposure of VP1ur in an *in vitro* system devoid of any other components (55). In contrast, for B19 low pH causes externalization of VP1ur and capsids can be immunoprecipitated with antibodies against this domain (147). In cells, drugs that prevent acidification of endosomes will prevent release of VP1ur as detectable by IFA (99). Whether these differences are the result of experimental differences, or intrinsic differences between viruses is not clear.

Figure 1.4.

Changes in parvovirus capsid flexibility and calcium binding at low pH and addition of EGTA. FPV at pH 7.5 coordinates three Ca^{+2} ions. Lowering the pH to 6.5 causes loss of secondary structure in the 361-374 loop, and displacement of one Ca^{+2} ion. Removal of the remaining Ca+2 ions by EGTA treatment causes the 36-374 loop to be disordered. Coordinated Ca^{+2} ions are indicated by red circles.

FPV pH 7.5 (PDB 1C8F)

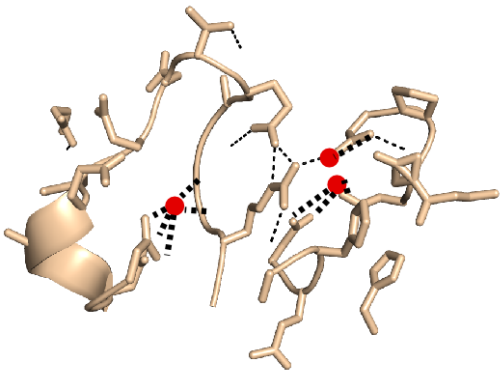

FPV pH 6.2 (pbd 1C8G)

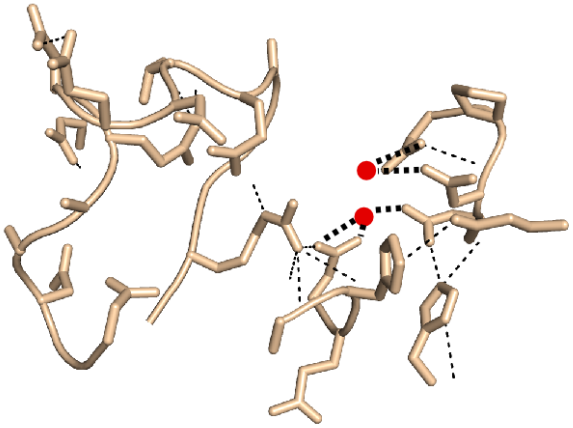

FPV ph 6.2 + EGTA (pdb 1C8E)

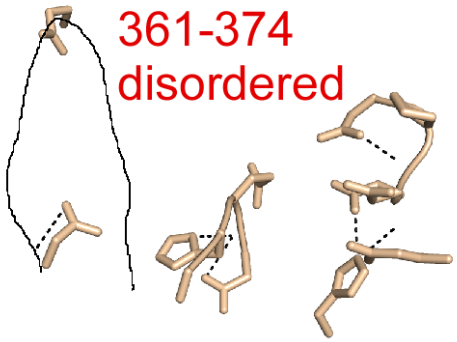

The effect of low pH on VP1ur exposure is difficult to interpret in terms of the atomic resolution structure of CPV, since the 5-fold pore of CPV is not expanded at low pH, and the temperature factor is not greatly changed, indicating that this area may not be more flexible at lower pH. Also, VP1ur exposure is not the only critical step in infection. Particles that were heated to expose VP1ur and then added to cells whose endosomal pH was raised by treatment with Bafilomyacin A1 were not infectious. Also CPV particles that were treated with low pH and then microinjected into cells were not infectious. These results indicates that other steps in viral entry besides VP1ur exposure require low pH (171).

Low pH may be important for activation of low pH proteases in late endosomes and lysosomes. All proteases examined so far will convert VP2 to VP3 *in vitro*, and this cleavage is also seen during infection of cells (37, 197). It is believed that proteolysis of VP2 is an essential precursor step for the externalization of VP1ur. For MVM full capsids conversion of VP2 to VP3 by proteases allows immunoprecipitation with anti-VP1ur antibodies at lower temperatures than uncleaved capsids, starting at 45 degrees (55). Particles that are not treated with proteases must be heated to approximately 60°C before VP1ur can be detected, and heating CPV to 60°C also releases VP1 (55, 195). This indicates that the conversion of VP2 to VP3 promotes externalization of VP1ur. Other laboratories however, have reported by immunofluorescence, that empty particles (where VP2 cannot be converted to VP3) can still release VP1ur, and it is possible that other factors encountered during infection also help to release VP1ur (99). The endosomal proteases such as cathepsins are most likely to be responsible for the VP2 to VP3 cleavage, and those are activated by low pH and inhibition of this pH abrogates viral infectivity (74). Yeast two-hybrid study of binding partners for the capsid protein of another parvovirus, adeno-associated virus (AAV), identified cathepsins B and L as important in AAV 2 and 8

infection, and these proteases will cleave capsids without disassembling them (6). *In vitro* treatment of CPV with cathepsins converts VP2 to VP3, but showed no further cleavage of capsid protein (197). There is only one disulfide bond in the structure of CPV, and it is unlikely that reducing conditions would have a large impact on the structure of CPV.

CPV binding to TfR may also cause conformational changes in the capsid. Cryo-EM and 3D asymmetric image reconstruction along with biochemical studies showed that only a small number of purified feline TfR ectodomain molecules bound to each capsid, despite an excess of the receptor in those samples (63). Modeling the structure of TfR onto the CPV capsid demonstrates that between 20 and 24 receptors should be able to bind to the virus without steric clashes (in this case 2 receptors at each 3-fold or 5-fold axis, respectively). Purification of CPV:feline TfR complexes showed only 7 or fewer receptors bound per virus, as determined by quantative slot blots. Also, soluble TfR competed with cellular TfR for binding to CPV at concentrations as low as 3 sTfR per capsid. This suggests that binding of TfR may induce a conformational change in the virus that precludes binding of other receptor molecules, or that there are a limited number of available binding sites on each capsid. The resolution of the cryo-EM reconstruction, was not great enough to detect any conformational changes. Another possibility is that there is inherent structural asymmetry in the virus that would allow receptor binding to only a limited number of sites on the surface of the virus.

1.10d Penetration of endosomes by CPV.

CPV is believed to escape from endosomes by use of its PLA2 domain within VP1ur. The highest activity of these PLA2 at pH 6-7 along with the need for millimolar amounts of calcium, suggests that if this enzyme is necessary for escape

from endosomes, then it would most likely occur in a relatively early endosome, or in a moderately low pH endosome (such as a recycling endosome).

How exactly any membrane modification by the CPV PLA2 leads to particle penetration is still not well understood. Cellular PLA2 promotes exocytosis by causing fusion of exosomes to the plasma membrane, and can fuse *in vitro* (19, 111, 114). Annexins are proteins that bind to phospholipids and promote fusion, and their activity requires arachidonic acid. Therefore, liberation of arachidonic acid by PLA2 is believed to be responsible for this membrane fusion (108). Since parvovirus PLA2s will liberate arachidonic acid from mammalian cells, it is possible that modification of membranes and fusion of endosomes by the PLA2 is involved in the infectious process (15).

The PLA2 domain, along with the rest of VP1ur is believed to be externalized from the 5-fold pore, in a partially or completely unfolded form. Unlike most other secretory PLA2s, the PLA2 of CPV lacks disulfide bonds, and this may help in the externalization of this domain through the narrow pore (203). Alternatively the pore may expand to allow passage of the folded domain, as apparently occurs when the VP2-N terminus is externalized. As VP1ur is externalized in endosomes, it is believed that the PLA2 is active at this point or a later step (99). The PLA2 domain however does not appear to cause complete lysis of endosomes, as determined by co-incubation of CPV with FITC labeled dextrans (171). After release from the endosome, the virion may engage components of the microtubule trafficking system including dynein, and move to the perinuclear region before entry to the nucleus.

1.10e Cytoplasmic trafficking and entry of CPV into the nucleus.

The CPV genome must enter the nucleus for productive infection, however the steps leading up to this event are still not well characterized. CPV is believed to be

directly exposed to the cytoplasm after escape from endosomes, as microinjection of anti-capsid antibodies into the cytosol will block infection by virus added to the cells (196). Capsids display NLS motifs in the VP1ur, and the virus is small enough to enter through the nuclear pore complex, with the help of the karyopherin transport system (43, 64). An alternate mechanism of nuclear entry has been proposed, where parvoviruses capsids would directly perforate the nuclear membrane by an unknown mechanism, thereby bypassing the nuclear pore complex (38, 39).

1.10f DNA release.

The 3' end of the DNA is not initially accessible in intact virions, yet it must become exposed during infection to engage the host DNA polymerase. To date, no structural or biochemical studies have determined the location of the 3' end of the DNA or how accessibility to the 3' end is accomplished. It appears that the DNA can become exposed from the particle without disassembly as *in vitro* studies of MVM and B19 show that the capsids remain intact while the DNA can be accessed by DNA polymerases at temperatures above 60°C for MVM, or 50°C for B19 (45, 146). By a microscopy based approach using biotinylated nucleotide probes, MVM virions were shown to expose the 3' end of the viral DNA in endosomes (99).

1.11 Viral entry and uncoating of other nonenveloped viruses.

The steps leading to membrane penetration by the viral particle can be conceptually divided into four phases (reviewed in (184)). The particle must first enter the cell and traffic to the site of membrane penetration. Next the virus must undergo a conformational change that activates or exposes a membrane-modification or disruption activity. This newly exposed factor then disrupts the membrane, and the particle crosses the membrane to enter the cytoplasm.

While some enveloped viruses can fuse directly at the plasma membrane, most nonenveloped viruses require endocytosis (104). This is most likely because endocytosis allows viruses to sense the presence of the cell interior, to bypass the dense cortical actin network that lies directly under the plasma membrane, and to traffic within the cell (25, 103). Various viruses are taken into cells by most known endocytic pathways including macropinocytosis (adenovirus), clathrin-independent endocytosis (arenaviruses and influenza), clathrin-mediated endocytosis (parvovirus, adenovirus, influenza), and caveolar and related entry pathways (SV40, coxsakie B, echo virus 1) (reviewed (104))(85-87, 100, 109, 132, 144, 145, 159). These pathways are often not exclusive for a given virus, and many viruses can use multiple pathways (48, 152). Poliovirus is endocytosed by a clathrin- and caveolin-independent pathway, and has been demonstrated to release its genome within the 100-200 nm of the plasma membrane, in response to unidentified host factors (17, 50, 73). Since poliovirus replicates in the cytoplasm, the virus does not need access to the nucleus, and therefore the cortical actin and the endosomal membrane likely offer the main barriers to viral entry. Other viruses must undergo trafficking to reach the correct site of uncoating. For example, SV40, a polyomavirus, binds to the glycolipid GM1 (and possibly MHC class I) on the surface of cells (8, 18, 185). After binding, SV40 diffuses laterally on the surface of cells until it localizes to caveolin-enriched lipid rafts (131). Once in these rafts, signaling occurs that results in pinching off of cavolae, and trafficking to tubular-vesicular endosomes called caveosomes within the cell (130, 131, 173). From the caveosomes, SV40 is pinched off in vesicles that lack caveolin-1, and those traffic to and fuse with the smooth ER along microtubules, where SV40 translocates across the ER membrane. Entry of adenoviruses appears to use both clathrin mediated endocytosis and macropinocytosis (reviewed in (104)). Adenovirus binds to the coxsakie virus adenovirus receptor (CAR) with its fiber

protein, and also to integrins using an RGD motif within the penton (11, 143, 198). After endocytosis, release of the virus is triggered to allow escape into the cytosol (199).

After trafficking to the correct location within the cell, the nonenveloped virus capsid must undergo conformational changes that result in the release of membrane lytic or of membrane modifying factors, and these can involve various mechanisms including receptor binding, redox chemistry, low pH, and protease digestion. For poliovirus, binding to PVR either *in vitro* or on the surface of cells catalyzes conformational changes in the capsid that results in swelling of the particle (reviewed in (66))(49, 57, 186). The ultimate result of these conformational changes is the exposure of the N-terminus of VP4 to the outside of the particle, which was previously sequestered within the particle (58). This N-terminus is myristoylated, and inserts into membranes upon exposure (35, 106, 189). SV40 undergoes conformational changes when it reaches the smooth ER. In the ER, SV40 and the closely related Py virus utilizes protein folding and disulfide isomerization machinery to uncoat (98, 155). Particle stability is accomplished through changes in disulfide bonds between capsid subunits controlled by the isomerization protein ERp57 in the lumen of the ER, which acts to break and reform the disulfide linkages and similar changes are seen *in vitro* by treatment with DTT and EGTA (14-16, 40, 75). This isomerization activity, coupled with calcium removal from the capsids results in removal of approximately 12 of 72 pentamers from the capsid (155). Isomerization of disulfide bonds and calcium removal are also important for the exposure of VP2 and VP3, which are normally located on the interior of the capsid. The N-terminus of VP2 is myristoylated and it is thought to insert into membranes to create pores (84, 170). Adenovirus enters cells and comes in contact with low pH endosomes (reviewed in (91)). This low pH activates a viral protease that cleaves some capsid proteins, destabilizing the capsid

and liberating a number of capsid proteins (62, 199). Protein VI is normally sequestered within capsids, but upon exposure will lyse endosomes through the use of its amphipathic N-terminus. This allows escape of adenovirus to the cytoplasm where it will traffic to the nucleus to replicate. Finally, reoviruses undergo conformational changes after protease processing outside the cell or in late endosomes. After endocytosis, capthepsins B and L cleave the outer capsid protein σ3 to generate intermediate subviral particles (ISVPs) (9, 51). Those intermediate particles are further processed to release the N terminus of the μ1 protein (called μ1N), which is normally buried within the capsid (30). The release of μ1N is accomplished by dramatic conformational changes to the capsid (204). The released μ1N reacts *in trans* with other intermediate particles to release more μ1N in a positive feedback loop (5). The released μ1N is myristoylated at its N-terminus and is responsible for inserting into membranes and causing pore formation (76).

Penetration and crossing membranes by enveloped viruses is a more straightforward process than for nonenveloped viruses, since fusion of the viral envelope to the host membrane will result in the release of the nucleocapsid across the barrier (184). For nonenveloped particles, the particles must lyse membranous organelles, hijack the host protein translocation machinery, or modify membranes in a way that allows trafficking of the particle or genome across the membrane. One suggested mechanism that is often observed is through the formation of pores by viral proteins. The VP4 N-terminus of poliovirus for example, inserts into membranes after PVR-induced exposure (189). Recent cryo-EM or cryo tomography and image reconstructions have visualized poliovirus bound to PVR-decorated liposomes (13, 20). These models show the binding of five PVR molecules around the 5-fold axis of symmetry and disruption of membrane below this axis, possibly as a result of insertion of the VP4 N-terminus into the membrane. The insertion of the N-terminus of VP4 is

thought to destabilize the membranes and allow release of the RNA into the cytoplasm. The μ1N of reovirus has also been shown to induce pore formation in both lipsomes and in resealed red blood cell ghosts (4). However, the average pore size formed is on the order of 4-9 nm, which is around one tenth the size of the reovirus particle. Since the entire particle is believed to be released into the cytosol, it is thought that osmotic pressure may lyse the endosome, or the pore may be expanded by other unidentified factors. SV40 and the closely related mouse polyoma virus (Py) have been shown to hijack host transport machinery to gain access to the cytosol. These viruses appear to use the ER-associated degradation (ERAD) pathway, which normally functions to retrotranslocate misfolded proteins back to the cytosol for degradation (92, 155). However, interaction of SV40 and Py with ERp57 also causes exposure of the myristoylated N-terminus of VP2, which inserts into membranes (136), and at this point it is not clear whether VP2 or the ERAD pathway is responsible for trafficking of particles across the ER membrane.

1.12 Host range of CPV and FPV.

CPV is a new virus of domestic dogs and related canines, emerging in the late 1960s from feline FPV or a related virus of other members of the Carnivora. FPV and CPV are >99% related in amino acid sequence identity and show conserved differences of 9 amino acids in the VP2 sequences (107, 126). Binding to TfR is a primary determinant of host range, although there is some complexity in the connection between receptor binding and host specificity. Both CPV and FPV bind to the feline TfR, but only CPV capsids are able to bind to the canine TfR (70). However, early strains of CPV (termed CPV type-2, isolated in 1978) are able to infect feline cells but do productively infect cats (124, 183). FPV isolates can replicate in cells in the thymus of dogs in experimental infection, indicating that there

are additional constraints to host range besides simple TfR binding (181, 183). A mutant of FPV that contains residues 93 and 323 of CPV is able to bind to canine TfR, and residues 80, 564 and 568 were also shown to affect the success of CPV in dogs (68, 180, 182). CPV-2a, which emerged in 1979 as a variant of the ancestral CPV-2 regained the ability to infect cats, and capsid protein changes were involved in this gain of function (22, 44, 105, 112, 129, 153, 181). Comparison of the atomic resolution structures of FPV and CPV-2 capsids showed only small differences between the two viruses (61). The capsids of FPV coordinate an additional calcium ion and additional hydrogen bonds in the capsid protein controlled by the host range determining sequences (residue 93), and may therefore have less flexibility in several surface loops compared to CPV ((128)). It is not clear how these changes affect host range, but they may influence the interaction of the capsid with feline and canine TfRs and with other host factors. The canine TfR has an extra glycosylation site, and removal of this modification allows that receptor to bind to FPV capsids (119). It is likely that part of the evolution of FPV to CPV was a gain in the ability to more favorably interact with this extra glycan.

1.13 Neutralization of viruses.

A detailed understanding of the host immune response to viral infection is critical for development of new anti-viral therapeutics and vaccines. Antibodies (Abs) play major roles in protection of the host from infection and clearance of viremia during systemic infections (23). The full spectrum of Ab responses against viruses is large and complex. Since this complexity makes a detailed understanding of Ab protection difficult, *in vitro* studies using monoclonal antibodies (MAb) offer a tractable way to study a subset of the Ab response (137). As used here, the term neutralization refers to the ability of an Ab to block viral infection *in vitro* by binding

directly to the virus (79). Other mechanisms of antibody-mediated viral inactivation can include cellular effector functions such as complement fixation, antibody dependant cellular cytotoxicity, opsinization, or Fc mediated phagocytosis. It is likely that mechanisms of neutralization seen in *in vitro* studies would also function similarly in an infected animal as part of the defense against or recovery from infection.

Extensive research has been done on neutralization of nonenveloped viruses; however many of the mechanisms of neutralization are still not well understood. In the early studies problems included the use of polyclonal and intact (multivalent) Abs which made it difficult to identify the viral epitopes and often confused Ab binding constants (162). Examining the effects of fragment, antigen binding (Fab) of MAbs allows the combination of structural and biochemical data into a mechanistic understanding of capsid-antibody interactions. X-ray diffraction on icosahedral capsid-Fab complexes yields the greatest amount of structural information, however the growth of crystals of such complexes has been difficult, with human rhinovirus 14 and an Fab fragment being the only successfully solved complex (165). Cryo-EM and 3D image reconstructions can readily image capsid-Fab complexes, but sofar provide lower resolution models than crystallographic data. To increase the effective resolution of cryo-EM models, pseudo-atomic resolution structures may be used, where the atomic resolution structures of each component (solved separately by X-ray diffraction) are fitted into the electron density maps of reconstructed cryo-EM models (149). This allows the interpretation of Ab footprints on the surface of the virus, and in some cases has been successful in identifying conformational changes after Ab binding (93, 162). Other attempts at understanding the virus-antibody interaction have relied on crystallizing Fabs with peptides that resemble the antigenic sites on the virus (191), although there may then be concerns that the peptides do not form the same conformation as the assembled capsid protein.

The mechanisms by which Abs neutralize viruses are becoming increasingly clear. In some models the Fabs of IgGs appear to neutralize viruses by blocking receptor binding, by preventing conformational changes necessary for infection before or after the virion binds cells, by causing conformational changes to the virus, or by preventing correct endocytosis of the virus by blocking virus-induced cell signaling or co-receptor binding (32, 52, 53, 60, 82, 97, 115, 116, 190). Intact IgGs also neutralize virus by aggregation of capsids to lower the effective number of infectious units, and in some cases the IgG can bivalently bind to a single particle to increase the apparent affinity or prevent viral uncoating (23, 80). While all of these mechanisms are possible, a survey of recent structural and biochemical data suggests that many Abs act to prevent binding of virions to host cells through simple steric hindrance of the virus-receptor interaction (162).

Human rhinovirus (HRV) is a well-studied example of capsid-Fab interactions. The structure of a neutralizing MAb bound to HRV14 has been determine by cryo-EM and image reconstructions and also by X-ray diffraction on intact capsid-Fab complexes. Both of these structures showed that large conformational changes did not occur in the capsid after Fab binding (163, 164, 166), but instead structural changes occur to the CDR3 of the Fab, which allowed it to bind better to the capsid (163). This Fab also binds in the same area of the capsid as the cellular receptor, and competes for receptor binding (41). In this case the intact IgG binds bivalently to the virus across a twofold axis of symmetry, but it is not clear whether this is necessary for neutralization, or acts by increasing the Ab affinity (166). Interestingly, Fab binding acts to stabilize the virus and prevents some movements that occur in the viral proteins (breathing) in way similar to anti-viral compounds (138). This study indicates part of the complexity of studying neutralization: even though this Fab may neutralize primarily by preventing receptor binding, other mechanisms such as

stabilization of capsids may also aid in neutralization. Neutralization by steric hindrances occurs for many other nonenvelped viruses including reoviruses (113), adenoviruses (168), possibly papillomaviruses (12), foot and mouth disease virus, caliciviruses (177), and parvoviruses (200).

1.14. Immune responses during CPV infection.

Antibodies are believed to play a critical role in preventing CPV infection. Puppies that acquire maternal immunity are protected from infection, and they become susceptible only when the antibodies wane to low titers. In many cases there are still detectable levels of antibody present when the pups are infected. In laboratory experiments, passive transfer of sera from immunized animals to naïve puppies will protect the recipients from infection (134). Also maternal antibodies will interfere with administration of the live-attenuated CPV vaccine, indicating that antibodies also inhibit replication of the vaccine virus (27). It is not known what role T-cells play in clearance of viral infection, although several T-cell epitopes near the C-terminus and the N-terminus of VP1 have been described (141, 142)

The CPV capsid itself is highly immunogenic, and vaccination of dogs with formalin inactivated CPV induces serum antibody titers that persist up to either 20 week (with no boost immunization) or 50 weeks (with booster) (135). Vaccination with a live attenuated strain of CPV protected dogs for at least 24 months and induced persistently high antibody titers (27). In addition, baculovirus-produced VP2-only viral like particles (VLPs) are able to fully protect animals with a dose of as little as one microgram. Most of the B-cell epitopes identified are within the VP2 region of the capsid (88, 96, 142, 169). This is in contrast to B19, where major neutralizing epitopes are present in VP1ur, and this difference may be the result of difference in surface accessibility of this region (154). Several studies have identified linear B-cell

epitopes of CPV using synthetic peptides or protein fragments expressed in bacteria. These studies demonstrated that the amino terminus of VP2 (residues 1-23) is a functional B-cell epitope, as well as residues near the C-terminus (residues 549 and 573, VP2 numbering), and other residues that are believed to be on or near the surface of the virus (residues 91, 172, 283, 297, and 498, VP2 numbering) (96). A variety of antibody epitopes on CPV were identified by escape mutant analysis (169), which clustered into two sites, termed site A and site B. While these were mouse monoclonal antibodies, it is likely that the rodent response was similar to the natural canine antibody response to CPV infection. Residues which affected binding of MAbs to site A are 93, 222, 224, and 426, while for site B, residues 299, 300, and 302 were important. Those residues were identified by escape mutant analysis, and it is possible that mutation of these residues would have an allosteric effect on the capsid, and the actual antibody epitopes are located elsewhere on the capsid. However, the clustering of the changes into two small regions suggest that those are within the footprints of the antibodies. In all the studies to date the antibodies studied were immunoglobulin G proteins (IgG), which represent the high affinity antibodies that develop against the virus. It is not known whether the earlier and lower affinity IgM antibodies would bind to different areas of the capsid. Analysis of antibody binding to CPV is complicated by the fact that many mutations affect more than one function - for example the Lys to Asn change of VP2 residue 93 changed both the antigenic structure of the capsid and the specificity of binding to TfR that controls canine host range. The sites A and B may be the structures on the capsid that can establish interactions with other proteins, and therefore bind both the TfR and antibodies. It is more likely that there is a complex interplay between receptor and antibody binding, as the footprints of TfR and Fabs overlap (Figure 1.5). A practical implication of this

Figure 1.5.

The interplay between receptor and antibody binding. Residues important for receptor binding are shaded in green. Residues important for binding site A antibodies are shaded red and site B are shaded blue. Shared residues between receptor and site A are shaded in yellow, and residues shared between receptor and site B are shaded in teal.

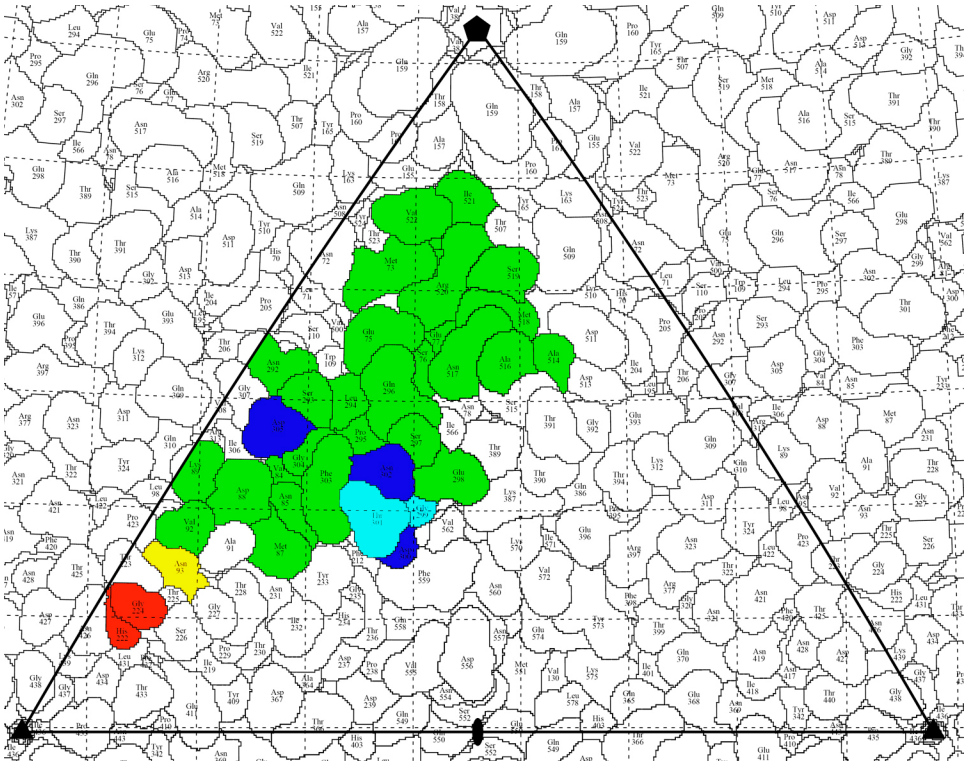

interplay is that it is extremely difficult to understand whether naturally arising mutation in the virus are a result of antibody selection or receptor binding, or both.

1.15 Thesis overview.

This thesis will explore the biochemical effects of conditions that mimic the entry of CPV into cells. It will also examine the relationship between receptor and antibody binding, and the effect of that binding on the structure of the virus.

Chapter 2 will discuss the mechanisms of neutralization of CPV by intact IgGs or Fabs of monoclonal antibodies. The competition between Fabs and TfR will also be examined.

Chapter 3 will describe the visualization of antibody footprints on the virus by Cryo-EM and image reconstruction techniques. I will describe these footprints and their relationship to viral epitopes.

Chapter 4 will describe the effects of low pH, calcium removal, increased temperature, and ligand binding on the structure of the capsid.

Chapter 5 will summarize the work presented here and offer insights into potential future research projects.

REFERENCES

1. **Agbandje-McKenna, M.** 2006. Atomic structure of viral particles. Oxford University Press, New York.
2. **Agbandje-McKenna, M., A. L. Llamas-Saiz, F. Wang, P. Tattersall, and M. G. Rossmann.** 1998. Functional implications of the structure of the murine parvovirus, minute virus of mice. Structure **6:**1369-1381.
3. **Agbandje, M., R. McKenna, M. G. Rossmann, M. L. Strassheim, and C. R. Parrish.** 1993. Structure determination of feline panleukopenia virus empty particles. Proteins **16:** 155-171.
4. **Agosto, M. A., T. Ivanovic, and M. L. Nibert.** 2006. Mammalian reovirus, a nonfusogenic nonenveloped virus, forms size-selective pores in a model membrane. Proceedings of the National Academy of Sciences of the United States of America **103:**16496-501.
5. **Agosto, M. A., K. S. Myers, T. Ivanovic, and M. L. Nibert.** 2008. A positive-feedback mechanism promotes reovirus particle conversion to the intermediate associated with membrane penetration. Proc Natl Acad Sci U S A **105:**10571-6.
6. **Akache, B., D. Grimm, X. Shen, S. Fuess, S. R. Yant, D. S. Glazer, J. Park, and M. A. Kay.** 2007. A two-hybrid screen identifies cathepsins B and L as uncoating factors for adeno-associated virus 2 and 8. Mol Ther **15:**330-9.
7. **Alvarez, E., N. Girones, and R. J. Davis.** 1989. Intermolecular disulfide bonds are not required for the expression of the dimeric state and functional activity of the transferrin receptor. Embo J **8:**2231-2240.
8. **Atwood, W. J., and L. C. Norkin.** 1989. Class I major histocompatibility proteins as cell surface receptors for simian virus 40. J Virol **63:**4474-7.

9. **Baer, G. S., and T. S. Dermody.** 1997. Mutations in reovirus outer-capsid protein sigma3 selected during persistent infections of L cells confer resistance to protease inhibitor E64. J Virol **71:**4921-4928.

10. **Barbis, D. P., S.-F. Chang, and C. R. Parrish.** 1992. Mutations adjacent to the dimple of canine parvovirus capsid structure affect sialic acid binding. Virology **191:**301-308.

11. **Bergelson, J. M., J. A. Cunningham, G. Droguett, E. A. Kurt-Jones, A. Krithivas, J. S. Hong, M. S. Horwitz, R. L. Crowell, and R. W. Finberg.** 1997. Isolation of a common receptor for Coxsackie B viruses and adenoviruses 2 and 5. Science **275:**1320-3.

12. **Booy, F. P., R. B. Roden, H. L. Greenstone, J. T. Schiller, and B. L. Trus.** 1998. Two antibodies that neutralize papillomavirus by different mechanisms show distinct binding patterns at 13 A resolution. J Mol Biol **281:**95-106.

13. **Bostina, M., D. Bubeck, C. Schwartz, D. Nicastro, D. J. Filman, and J. M. Hogle.** 2007. Single particle cryoelectron tomography characterization of the structure and structural variability of poliovirus-receptor-membrane complex at 30 A resolution. J Struct Biol **160:**200-10.

14. **Brady, J. N., J. D. Kendall, and R. A. Consigli.** 1979. In vitro reassembly of infectious polyoma virions. J Virol **32:**640-7.

15. **Brady, J. N., V. D. Winston, and R. A. Consigli.** 1978. Characterization of a DNA-protein complex and capsomere subunits derived from polyoma virus by treatment with ethyleneglycol-bis-N,N'-tetraacetic acid and dithiothreitol. J Virol **27:**193-204.

16. **Brady, J. N., V. D. Winston, and R. A. Consigli.** 1977. Dissociation of polyoma virus by the chelation of calcium ions found associated with purified virions. J Virol **23:**717-24.

17. **Brandenburg, B., L. Y. Lee, M. Lakadamyali, M. J. Rust, X. Zhuang, and J. M. Hogle.** 2007. Imaging Poliovirus Entry in Live Cells. PLoS Biol **5:**e183.

18. **Breau, W. C., W. J. Atwood, and L. C. Norkin.** 1992. Class I major histocompatibility proteins are an essential component of the simian virus 40 receptor. J Virol **66:**2037-45.

19. **Brown, W. J., K. Chambers, and A. Doody.** 2003. Phospholipase A2 (PLA2) enzymes in membrane trafficking: mediators of membrane shape and function. Traffic **4:**214-21.

20. **Bubeck, D., D. J. Filman, and J. M. Hogle.** 2005. Cryo-electron microscopy reconstruction of a poliovirus-receptor-membrane complex. Nat Struct Mol Biol **12:**615-8.

21. **Bucci, C., P. Thomsen, P. Nicoziani, J. McCarthy, and B. van Deurs.** 2000. Rab7: a key to lysosome biogenesis. Mol Biol Cell **11:**467-80.

22. **Buonavoglia, D., A. Cavalli, A. Pratelli, V. Martella, G. Greco, M. Tempesta, and C. Buonavoglia.** 2000. Antigenic analysis of canine parvovirus strains isolated in Italy. New Microbiol **23:**93-6.

23. **Burton, D. R.** 2002. Antibodies, viruses and vaccines. Nat Rev Immunol **2:**706-13.

24. **Byrne, S. L., R. Leverence, J. S. Klein, A. M. Giannetti, V. C. Smith, R. T. MacGillivray, I. A. Kaltashov, and A. B. Mason.** 2006. Effect of glycosylation on the function of a soluble, recombinant form of the transferrin receptor. Biochemistry **45:**6663-73.

25. **Campbell, E. M., R. Nunez, and T. J. Hope.** 2004. Disruption of the actin cytoskeleton can complement the ability of Nef to enhance human immunodeficiency virus type 1 infectivity. J Virol **78:**5745-55.

26. **Canaan, S., Z. Zadori, F. Ghomashchi, J. Bollinger, M. Sadilek, M. E. Moreau, P. Tijssen, and M. H. Gelb.** 2004. Interfacial enzymology of parvovirus phospholipases A2. J Biol Chem.

27. **Carmichael, L. E., J. C. Joubert, and R. V. H. Pollock.** 1983. A modified canine parvovirus vaccine 2. Immune response. Cornell Vet. **73:**13-29.

28. **Carreira, A., and M. G. Mateu.** 2006. Structural tolerance versus functional intolerance to mutation of hydrophobic core residues surrounding cavities in a parvovirus capsid. Journal of molecular biology **360:**1081-93.

29. **Chan, D. C., D. Fass, J. M. Berger, and P. S. Kim.** 1997. Core structure of gp41 from the HIV envelope glycoprotein. Cell **89:**263-73.

30. **Chandran, K., J. S. Parker, M. Ehrlich, T. Kirchhausen, and M. L. Nibert.** 2003. The delta region of outer-capsid protein micro 1 undergoes conformational change and release from reovirus particles during cell entry. Journal of virology **77:**13361-75.

31. **Chapman, M. S.** 1996. Structural refinement of the DNA-containing capsid of canine parvovirus using RSRef, a resolution-dependent stereochemically restrained real-space refinement method. Acta Crystallogr D Biol Crystallogr **52:**129-42.

32. **Che, Z., N. H. Olson, D. Leippe, W. M. Lee, A. G. Mosser, R. R. Rueckert, T. S. Baker, and T. J. Smith.** 1998. Antibody-mediated neutralization of human rhinovirus 14 explored by means of cryoelectron microscopy and X-ray crystallography of virus-Fab complexes. J Virol **72:**4610-22.

33. **Chen, J., K. H. Lee, D. A. Steinhauer, D. J. Stevens, J. J. Skehel, and D. C. Wiley.** 1998. Structure of the hemagglutinin precursor cleavage site, a determinant of influenza pathogenicity and the origin of the labile conformation. Cell **95:**409-17.

34. **Cheng, Y., O. Zak, P. Aisen, S. C. Harrison, and T. Walz.** 2004. Structure of the human transferrin receptor-transferrin complex. Cell **116:**565-576.

35. **Chow, M., J. F. Newman, D. Filman, J. M. Hogle, D. J. Rowlands, and F. Brown.** 1987. Myristylation of picornavirus capsid protein VP4 and its structural significance. Nature **327:**482-6.

36. **Clemens, K. E., and D. J. Pintel.** 1988. The two transcription units of the autonomous parvovirus minute virus of mice are transcribed in a temporal order. J.Virol. **62:**1448-1451.

37. **Clinton, G., and M. Hayashi.** 1976. The parvovirus MVM: a comparison of heavy and light particle infectivity and their density conversion in vitro. Virology **74:**57-63.

38. **Cohen, S., A. R. Behzad, J. B. Carroll, and N. Pante.** 2006. Parvoviral nuclear import: bypassing the host nuclear-transport machinery. The Journal of general virology **87:**3209-13.

39. **Cohen, S., and N. Pante.** 2005. Pushing the envelope: microinjection of Minute virus of mice into Xenopus oocytes causes damage to the nuclear envelope. J Gen Virol **86:**3243-52.

40. **Colomar, M. C., C. Degoumois-Sahli, and P. Beard.** 1993. Opening and refolding of simian virus 40 and in vitro packaging of foreign DNA. J. Virol **67:**2779-2786.

41. **Colonno, R. J., P. L. Callahan, D. M. Leippe, R. R. Rueckert, and J. E. Tomassini.** 1989. Inhibition of rhinovirus attachment by neutralizing monoclonal antibodies and their Fab fragments. J Virol **63:**36-42.

42. **Conner, S. D., and S. L. Schmid.** 2003. Regulated portals of entry into the cell. Nature **422:**37-44.

43. **Cook, A., F. Bono, M. Jinek, and E. Conti.** 2007. Structural biology of nucleocytoplasmic transport. Annu Rev Biochem **76:**647-71.

44. **Costa, A. P., J. P. Leite, N. V. Labarthe, and R. C. Garcia.** 2005. Genomic typing of canine parvovirus circulating in the state of rio de janeiro, Brazil from 1995 to 2001 using polymerase chain reaction assay. Vet Res Commun **29:**735-43.

45. **Cotmore, S. F., M. D'Abramo A, C. M. Ticknor, and P. Tattersall.** 1999. Controlled conformational transitions in the MVM virion expose the VP1 N-terminus and viral genome without particle disassembly. Virology **254:**169-181.

46. **Cotmore, S. F., and P. Tattersall.** 2005. Encapsidation of minute virus of mice DNA: aspects of the translocation mechanism revealed by the structure of partially packaged genomes. Virology **336:**100-12.

47. **Cotmore, S. F., and P. Tattersall.** 2007. Parvoviral host range and cell entry mechanisms. Adv Virus Res **70:**183-232.

48. **Damm, E. M., L. Pelkmans, J. Kartenbeck, A. Mezzacasa, T. Kurzchalia, and A. Helenius.** 2005. Clathrin- and caveolin-1-independent endocytosis: entry of simian virus 40 into cells devoid of caveolae. J Cell Biol **168:**477-88.

49. **De Sena, J., and B. Mandel.** 1977. Studies on the in vitro uncoating of poliovirus. II. Characteristics of the membrane-modified particle. Virology **78:**554-66.

50. **DeTulleo, L., and T. Kirchhausen.** 1998. The clathrin endocytic pathway in viral infection. Embo J **17:**4585-93.

51. **Ebert, D. H., J. Deussing, C. Peters, and T. S. Dermody.** 2002. Cathepsin L and cathepsin B mediate reovirus disassembly in murine fibroblast cells. J Biol Chem **277:**24609-17.

52. **Edwards, M. J., and N. J. Dimmock.** 2001. A haemagglutinin (HA1)-specific FAb neutralizes influenza A virus by inhibiting fusion activity. J Gen Virol **82:**1387-1395.

53. **Edwards, M. J., and N. J. Dimmock.** 2001. Hemagglutinin 1-specific immunoglobulin G and Fab molecules mediate postattachment neutralization of influenza A virus by inhibition of an early fusion event. J Virol **75:**10208-10218.

54. **Enns, C. A.** 2002. The transferrin receptor, p. 71-94. *In* D. M. Templeton (ed.), Molecular and cellular iron transport. Marcel Dekker, New York.

55. **Farr, G. A., S. F. Cotmore, and P. Tattersall.** 2006. VP2 cleavage and the leucine ring at the base of the fivefold cylinder control pH-dependent externalization of both the VP1 N terminus and the genome of minute virus of mice. J Virol **80:**161-71.

56. **Farr, G. A., L. G. Zhang, and P. Tattersall.** 2005. Parvoviral virions deploy a capsid-tethered lipolytic enzyme to breach the endosomal membrane during cell entry. Proc Natl Acad Sci U S A **102:**17148-53.

57. **Fenwick, M. L., and P. D. Cooper.** 1962. Early interactions between poliovirus and ERK cells: some observations on the nature and significance of the rejected particles. Virology **18:**212-23.

58. **Fricks, C. E., and J. M. Hogle.** 1990. Cell-induced conformational change in poliovirus: externalization of the amino terminus of VP1 is responsible for liposome binding. J Virol **64:**1934-1945.

59. **Girod, A., C. E. Wobus, Z. Zadori, M. Ried, K. Leike, P. Tijssen, J. A. Kleinschmidt, and M. Hallek.** 2002. The VP1 capsid protein of adeno-associated virus type 2 is carrying a phospholipase A2 domain required for virus infectivity. J Gen Virol **83:**973-8.

60. **Gomez-Puertas, P., F. Rodriguez, J. M. Oviedo, F. Ramiro-Ibanez, F. Ruiz-Gonzalvo, C. Alonso, and J. M. Escribano.** 1996. Neutralizing antibodies to different proteins of African swine fever virus inhibit both virus attachment and internalization. J Virol **70:**5689-94.

61. **Govindasamy, L., K. Hueffer, C. R. Parrish, and M. Agbandje-McKenna.** 2003. Structures of host range-controlling regions of the capsids of canine and feline parvoviruses and mutants. J Virol **77:**12211-21.

62. **Greber, U. F., Willetts, M., Webster, P., Helenius, A.** 1993. Stepwise dismantling of adenovirus 2 during entry into cells. Cell **75:**477-486.

63. **Hafenstein, S., L. M. Palermo, V. A. Kostyuchenko, C. Xiao, M. C. Morais, C. D. Nelson, V. D. Bowman, A. J. Battisti, P. R. Chipman, C. R. Parrish, and M. G. Rossmann.** 2007. Asymmetric binding of transferrin receptor to parvovirus capsids. Proc Natl Acad Sci U S A **104:**6585-9.

64. **Hansen, J., K. Qing, and A. Srivastava.** 2001. Infection of purified nuclei by adeno-associated virus 2. Mol Ther **4:**289-96.

65. **Harbison, C. E., J. A. Chiorini, and C. R. Parrish.** 2008. The parvovirus capsid odyssey: from the cell surface to the nucleus. Trends Microbiol **16:**208-14.

66. **Hogle, J. M.** 2002. Poliovirus cell entry: common structural themes in viral cell entry pathways. Annu Rev Microbiol **56:**677-702.

67. **Horiuchi, M., H. Goto, N. Ishiguro, and M. Shinagawa.** 1994. Mapping of determinants of the host range for canine cells in the genome of canine parvovirus using canine parvovirus/mink enteritis virus chimeric viruses. J Gen Virol **75:**1319-1328.

68. **Hueffer, K., L. Govindasamy, M. Agbandje-McKenna, and C. R. Parrish.** 2003. Combinations of two capsid regions controlling canine host range

determine canine transferrin receptor binding by canine and feline parvoviruses. J Virol **77:**10099-10105.

69. **Hueffer, K., L. M. Palermo, and C. R. Parrish.** 2004. Parvovirus infection of cells by using variants of the feline transferrin receptor altering clathrin-mediated endocytosis, membrane domain localization, and capsid-binding domains. J Virol **78:**5601-5611.

70. **Hueffer, K., J. S. Parker, W. S. Weichert, R. E. Geisel, J. Y. Sgro, and C. R. Parrish.** 2003. The natural host range shift and subsequent evolution of canine parvovirus resulted from virus-specific binding to the canine transferrin receptor. J. Virol. **77:**1718-1726.

71. **Hueffer, K., and C. R. Parrish.** 2003. Parvovirus host range, cell tropism and evolution. Curr Opin Microbiol **6:**392-398.

72. **Hurtado, A., P. Rueda, J. Nowicky, J. Sarraseca, and J. I. Casal.** 1996. Identification of domains in canine parvovirus VP2 essential for the assembly of virus-like particles. J Virol **70:**5422-9.

73. **Irurzun, A., and L. Carrasco.** 2001. Entry of poliovirus into cells is blocked by valinomycin and concanamycin A. Biochemistry **40:**3589-600.

74. **Ishidoh, K., and E. Kominami.** 2002. Processing and activation of lysosomal proteinases. Biol Chem **383:**1827-31.

75. **Ishizu, K. I., H. Watanabe, S. I. Han, S. N. Kanesashi, M. Hoque, H. Yajima, K. Kataoka, and H. Handa.** 2001. Roles of disulfide linkage and calcium ion-mediated interactions in assembly and disassembly of virus-like particles composed of simian virus 40 VP1 capsid protein. J Virol **75:**61-72.

76. **Ivanovic, T., M. A. Agosto, L. Zhang, K. Chandran, S. C. Harrison, and M. L. Nibert.** 2008. Peptides released from reovirus outer capsid form membrane pores that recruit virus particles. Embo J **27:**1289-98.

77. **Jing, S. Q., and I. S. Trowbridge.** 1987. Identification of the intermolecular disulfide bonds of the human transferrin receptor and its lipid-attachment site. Embo J **6:**327-31.

78. **Jongeneel, C. V., R. Sahli, G. K. McMaster, and B. Hirt.** 1986. A precise map of splice junctions in the mRNAs of minute virus of mice, an autonomous parvovirus. J Virol **59:**564-573.

79. **Klasse, P. J., and Q. J. Sattentau.** 2001. Mechanisms of virus neutralization by antibody. Curr Top Microbiol Immunol **260:**87-108.

80. **Klasse, P. J., and Q. J. Sattentau.** 2002. Occupancy and mechanism in antibody-mediated neutralization of animal viruses. J Gen Virol **83:**2091-108.

81. **Klausner, R. D., G. Ashwell, J. van Renswoude, J. B. Harford, and K. R. Bridges.** 1983. Binding of apotransferrin to K562 cells: explanation of the transferrin cycle. Proc Natl Acad Sci U S A **80:**2263-6.

82. **Knossow, M., M. Gaudier, A. Douglas, B. Barrere, T. Bizebard, C. Barbey, B. Gigant, and J. J. Skehel.** 2002. Mechanism of neutralization of influenza virus infectivity by antibodies. Virology **302:**294-8.

83. **Koenig, J. H., and K. Ikeda.** 1989. Disappearance and reformation of synaptic vesicle membrane upon transmitter release observed under reversible blockage of membrane retrieval. J Neurosci **9:**3844-60.

84. **Krauzewicz, N., C. H. Streuli, N. Stuart-Smith, M. D. Jones, S. Wallace, and B. E. Griffin.** 1990. Myristylated polyomavirus VP2: role in the life cycle of the virus. J Virol **64:**4414-20.

85. **Lakadamyali, M., M. J. Rust, H. P. Babcock, and X. Zhuang.** 2003. Visualizing infection of individual influenza viruses. Proc Natl Acad Sci U S A **100:**9280-5.

86. **Lakadamyali, M., M. J. Rust, and X. Zhuang.** 2004. Endocytosis of influenza viruses. Microbes Infect **6:**929-36.

87. **Lakadamyali, M., M. J. Rust, and X. Zhuang.** 2006. Ligands for clathrin-mediated endocytosis are differentially sorted into distinct populations of early endosomes. Cell **124:**997-1009.

88. **Langeveld, J. P., J. I. Casal, C. Vela, K. Dalsgaard, S. H. Smale, W. C. Puijk, and R. H. Meloen.** 1993. B-cell epitopes of canine parvovirus: distribution on the primary structure and exposure on the viral surface. J Virol **67:**765-772.

89. **Lawrence, C. M., S. Ray, M. Babyonyshev, R. Galluser, D. W. Borhani, and S. C. Harrison.** 1999. Crystal structure of the ectodomain of human transferrin receptor. Science **286:**779-782.

90. **Lebron, J. A., M. J. Bennett, D. E. Vaughn, A. J. Chirino, P. M. Snow, G. A. Mintier, J. N. Feder, and P. J. Bjorkman.** 1998. Crystal structure of the hemochromatosis protein HFE and characterization of its interaction with transferrin receptor. Cell **93:**111-23.

91. **Leopold, P. L., and R. G. Crystal.** 2007. Intracellular trafficking of adenovirus: many means to many ends. Adv Drug Deliv Rev **59:**810-21.

92. **Lilley, B. N., J. M. Gilbert, H. L. Ploegh, and T. L. Benjamin.** 2006. Murine polyomavirus requires the endoplasmic reticulum protein Derlin-2 to initiate infection. J Virol **80:**8739-44.

93. **Lok, S. M., V. Kostyuchenko, G. E. Nybakken, H. A. Holdaway, A. J. Battisti, S. Sukupolvi-Petty, D. Sedlak, D. H. Fremont, P. R. Chipman, J. T. Roehrig, M. S. Diamond, R. J. Kuhn, and M. G. Rossmann.** 2008. Binding of a neutralizing antibody to dengue virus alters the arrangement of surface glycoproteins. Nat Struct Mol Biol **15:**312-7.

94. **Lombardo, E., J. C. Ramirez, J. Garcia, and J. M. Almendral.** 2002. Complementary roles of multiple nuclear targeting signals in the capsid proteins of the parvovirus minute virus of mice during assembly and onset of infection. J Virol **76:**7049-59.

95. **Lopez-Bueno, A., N. Valle, J. M. Gallego, J. Perez, and J. M. Almendral.** 2004. Enhanced cytoplasmic sequestration of the nuclear export receptor CRM1 by NS2 mutations developed in the host regulates parvovirus fitness. J Virol **78:**10674-84.

96. **Lopez de Turiso, J. A., E. Cortez, A. Ranz, J. Garcia, A. Sanz, C. Vela, and J. I. Casal.** 1991. Fine mapping of canine parvovirus B cell epitopes. J Gen Virol **72:**2445-2456.

97. **Ludert, J. E., M. C. Ruiz, C. Hidalgo, and F. Liprandi.** 2002. Antibodies to rotavirus outer capsid glycoprotein VP7 neutralize infectivity by inhibiting virion decapsidation. J Virol **76:**6643-51.

98. **Magnuson, B., E. K. Rainey, T. Benjamin, M. Baryshev, S. Mkrtchian, and B. Tsai.** 2005. ERp29 triggers a conformational change in polyomavirus to stimulate membrane binding. Mol Cell **20:**289-300.

99. **Mani, B., C. Baltzer, N. Valle, J. M. Almendral, C. Kempf, and C. Ros.** 2006. Low pH-dependent endosomal processing of the incoming parvovirus minute virus of mice virion leads to externalization of the VP1 N-terminal sequence (N-VP1), N-VP2 cleavage, and uncoating of the full-length genome. J Virol **80:**1015-24.

100. **Marjomaki, V., V. Pietiainen, H. Matilainen, P. Upla, J. Ivaska, L. Nissinen, H. Reunanen, P. Huttunen, T. Hyypia, and J. Heino.** 2002. Internalization of echovirus 1 in caveolae. J Virol **76:**1856-65.

101. **Maroto, B., N. Valle, R. Saffrich, and J. M. Almendral.** 2004. Nuclear export of the nonenveloped parvovirus virion is directed by an unordered protein signal exposed on the capsid surface. J Virol **78:**10685-94.

102. **Marsh, E. W., P. L. Leopold, N. L. Jones, and F. R. Maxfield.** 1995. Oligomerized transferrin receptors are selectively retained by a lumenal sorting signal in a long-lived endocytic recycling compartment. J Cell Biol **129:**1509-1522.

103. **Marsh, M., and R. Bron.** 1997. SFV infection in CHO cells: cell-type specific restrictions to productive virus entry at the cell surface. J. Cell Sci. **110:**95-103.

104. **Marsh, M., and A. Helenius.** 2006. Virus entry: open sesame. Cell **124:**729-40.

105. **Martella, V., A. Cavalli, A. Pratelli, G. Bozzo, M. Camero, D. Buonavoglia, D. Narcisi, M. Tempesta, and C. Buonavoglia.** 2004. A canine parvovirus mutant is spreading in Italy. J Clin Microbiol **42:**1333-6.

106. **Martin-Belmonte, F., J. A. Lopez-Guerrero, L. Carrasco, and M. A. Alonso.** 2000. The amino-terminal nine amino acid sequence of poliovirus capsid VP4 protein is sufficient to confer N-myristoylation and targeting to detergent-insoluble membranes. Biochemistry **39:**1083-90.

107. **Martyn, J. C., B. E. Davidson, and M. J. Studdert.** 1990. Nucleotide sequence of feline panleukopenia virus: comparison with canine parvovirus identifies host-specific differences. J Gen Virol **71:**2747-2753.

108. **Mayorga, L. S., W. Beron, M. N. Sarrouf, M. I. Colombo, C. Creutz, and P. D. Stahl.** 1994. Calcium-dependent fusion among endosomes. J Biol Chem **269:**30927-34.

109. **Meier, O., K. Boucke, S. V. Hammer, S. Keller, R. P. Stidwill, S. Hemmi, and U. F. Greber.** 2002. Adenovirus triggers macropinocytosis and endosomal leakage together with its clathrin-mediated uptake. J Cell Biol **158:**1119-31.

110. **Miyamura, K., S. Kajigaya, M. Momoeda, S. J. Smith-Gill, and N. S. Young.** 1994. Parvovirus particles as platforms for protein presentation. Proc Natl Acad Sci U S A **91:**8507-8511.

111. **Nagao, T., T. Kubo, R. Fujimoto, H. Nishio, T. Takeuchi, and F. Hata.** 1995. Ca(2+)-independent fusion of secretory granules with phospholipase A2-treated plasma membranes in vitro. Biochem J **307 (Pt 2):**563-9.

112. **Nakamura, M., Y. Tohya, T. Miyazawa, M. Mochizuki, H. T. Phung, N. H. Nguyen, L. M. Huynh, L. T. Nguyen, P. N. Nguyen, P. V. Nguyen, N. P. Nguyen, and H. Akashi.** 2004. A novel antigenic variant of canine parvovirus from a Vietnamese dog. Arch Virol **149:**2261-9.

113. **Nason, E. L., J. D. Wetzel, S. K. Mukherjee, E. S. Barton, B. V. Prasad, and T. S. Dermody.** 2001. A monoclonal antibody specific for reovirus outer-capsid protein sigma3 inhibits sigma1-mediated hemagglutination by steric hindrance. J Virol **75:**6625-34.

114. **Nishio, H., T. Takeuchi, F. Hata, and O. Yagasaki.** 1996. Ca(2+)-independent fusion of synaptic vesicles with phospholipase A2-treated presynaptic membranes in vitro. Biochem J **318 (Pt 3):**981-7.

115. **Nybakken, G. E., T. Oliphant, S. Johnson, S. Burke, M. S. Diamond, and D. H. Fremont.** 2005. Structural basis of West Nile virus neutralization by a therapeutic antibody. Nature **437:**764-9.

116. **Osiowy, C., and R. Anderson.** 1995. Neutralization of respiratory syncytial virus after cell attachment. J Virol **69:**1271-4.

117. **Pakkanen, K., J. Karttunen, S. Virtanen, and M. Vuento.** 2008. Sphingomyelin induces structural alteration in canine parvovirus capsid. Virus Res **132:**187-91.

118. **Palermo, L. M., S. L. Hafenstein, and C. R. Parrish.** 2006. Purified feline and canine transferrin receptors reveal complex interactions with the capsids of canine and feline parvoviruses that correspond to their host ranges. Journal of virology **80:**8482-92.

119. **Palermo, L. M., K. Hueffer, and C. R. Parrish.** 2003. Residues in the apical domain of the feline and canine transferrin receptors control host-specific binding and cell infection of canine and feline parvoviruses. J Virol **77:**8915-8923.

120. **Paradiso, P. R.** 1983. Analysis of the protein-protein interactions in the parvovirus H-1 capsid. J.Virol. **46:**94-102.

121. **Parker, J. S., and C. R. Parrish.** 2000. Cellular uptake and infection by canine parvovirus involves rapid dynamin-regulated clathrin-mediated endocytosis, followed by slower intracellular trafficking. J Virol **74:**1919-1930.

122. **Parker, J. S. L., W. J. Murphy, D. Wang, S. J. O'Brien, and C. R. Parrish.** 2001. Canine and feline parvoviruses can use human or feline transferrin receptors to bind, enter, and infect cells. J. Virol. **75:**3896-3902.

123. **Parrish, C. R.** 1990. Emergence, natural history, and variation of canine, mink, and feline parvoviruses. Adv Virus Res **38:**403-450.

124. **Parrish, C. R.** 1991. Mapping specific functions in the capsid structure of canine parvovirus and feline panleukopenia virus using infectious plasmid clones. Virology **183:**195-205.

125. **Parrish, C. R.** 1995. Pathogenesis of feline panleukopenia virus and canine parvovirus. Baillieres Clin Haematol **8:**57-71.

126. **Parrish, C. R., C. F. Aquadro, and L. E. Carmichael.** 1988. Canine host range and a specific epitope map along with variant sequences in the capsid protein gene of canine parvovirus and related feline, mink and raccoon parvoviruses. Virology **166:**293-307.

127. **Parrish, C. R., P. Have, W. J. Foreyt, J. F. Evermann, M. Senda, and L. E. Carmichael.** 1988. The global spread and replacement of canine parvovirus strains. J Gen Virol **69 (Pt 5):**1111-6.

128. **Parrish, C. R., and Y. Kawaoka.** 2005. The origins of new pandemic viruses: the acquisition of new host ranges by canine parvovirus and influenza A viruses. Annu Rev Microbiol **59:**553-86.

129. **Parrish, C. R., P. H. O'Connell, J. F. Evermann, and L. E. Carmichael.** 1985. Natural variation of canine parvovirus. Science **230:**1046-1048.

130. **Pelkmans, L., and A. Helenius.** 2002. Endocytosis via caveolae. Traffic **3:**311-20.

131. **Pelkmans, L., J. Kartenbeck, and A. Helenius.** 2001. Caveolar endocytosis of simian virus 40 reveals a new two-step vesicular-transport pathway to the ER. Nat Cell Biol **3:**473-83.

132. **Pietiainen, V., V. Marjomaki, P. Upla, L. Pelkmans, A. Helenius, and T. Hyypia.** 2004. Echovirus 1 endocytosis into caveosomes requires lipid rafts, dynamin II, and signaling events. Mol Biol Cell **15:**4911-25.

133. **Pintel, D., A. Gersappe, D. Haut, and J. Pearson.** 1995. Determinants that govern alternative splicing of parvovirus pre-mRNAs. Seminars in Virology **6:**283-291.

134. **Pollock, R. V. H., and L. E. Carmichael.** 1990. The canine parvoviruses, p. 113-134. *In* P. Tijssen (ed.), CRC handbook of parvoviruses, vol. 2. CRC Press, Inc., Boca Raton.

135. **Pollock, R. V. H., and L. E. Carmichael.** 1982. Dog response to inactivated canine parvovirus and feline panleucopenia virus vaccines. Cornell Vet. **72:**16-35.

136. **Rainey-Barger, E. K., B. Magnuson, and B. Tsai.** 2007. A chaperone-activated nonenveloped virus perforates the physiologically relevant endoplasmic reticulum membrane. J Virol **81:**12996-3004.

137. **Reading, S. A., and N. J. Dimmock.** 2007. Neutralization of animal virus infectivity by antibody. Arch Virol **152:**1047-59.

138. **Reisdorph, N., J. J. Thomas, U. Katpally, E. Chase, K. Harris, G. Siuzdak, and T. J. Smith.** 2003. Human rhinovirus capsid dynamics is controlled by canyon flexibility. Virology **314:**34-44.

139. **Rhode III, S. L.** 1974. Replication progress of the parvovirus H-1; III. factors affecting H-1 RF DNA synthesis. J. Virol. **14:**791-801.

140. **Rhode, S. L. I.** 1973. Replication process of the parvovirus H-1 I. Kinetics in a parasynchronous cell system. J Virol **11:**856-861.

141. **Rimmelzwaan, G. F., M. C. Poelen, R. H. Meloen, J. Carlson, F. G. UytdeHaag, and A. D. Osterhaus.** 1990. Delineation of canine parvovirus T cell epitopes with peripheral blood mononuclear cells and T cell clones from immunized dogs. J Gen Virol **71:**2312-2329.

142. **Rimmelzwaan, G. F., R. W. J. van der Heijden, E. Tijhaar, M. C. M. Poelen, J. Carlson, A. D. M. E. Osterhaus, and F. G. C. M. UytdeHaag.** 1990. Establishment and characterization of canine parvovirus-specific murine

CD4+ T cel clones and their use for the delineation of T cell epitopes. J. Gen. Virol. **71:**1095-1102.

143. **Roelvink, P. W., A. Lizonova, J. G. Lee, Y. Li, J. M. Bergelson, R. W. Finberg, D. E. Brough, I. Kovesdi, and T. J. Wickham.** 1998. The coxsackievirus-adenovirus receptor protein can function as a cellular attachment protein for adenovirus serotypes from subgroups A, C, D, E, and F. J Virol **72:**7909-15.

144. **Rojek, J. M., and S. Kunz.** 2008. Cell entry by human pathogenic arenaviruses. Cell Microbiol **10:**828-35.

145. **Rojek, J. M., A. B. Sanchez, N. T. Nguyen, J. C. de la Torre, and S. Kunz.** 2008. Different mechanisms of cell entry by human-pathogenic Old World and New World arenaviruses. J Virol **82:**7677-87.

146. **Ros, C., C. Baltzer, B. Mani, and C. Kempf.** 2005. Parvovirus uncoating in vitro reveals a mechanism of DNA release without capsid disassembly and striking differences in encapsidated DNA stability. Virology **345:**137-147.

147. **Ros, C., M. Gerber, and C. Kempf.** 2006. Conformational changes in the VP1-unique region of native human parvovirus B19 lead to exposure of internal sequences that play a role in virus neutralization and infectivity. Journal of virology **80:**12017-24.

148. **Rosenfeld, S. J., K. Yoshimoto, S. Kajigaya, S. Anderson, N. S. Young, A. Field, P. Warrener, G. Bansal, and M. S. Collett.** 1992. Unique region of the minor capsid protein of human parvovirus B19 is exposed on the virion surface. J Clin Invest **89:**2023-2029.

149. **Rossmann, M. G.** 2000. Fitting atomic models into electron-microscopy maps. Acta Crystallogr D Biol Crystallogr **56:**1341-1349.

150. **Rossmann, M. G., and J. E. Johnson.** 1989. Icosahedral RNA virus structure. Ann Rev Biochem **58:**533-573.

151. **Ruffing, M., H. Zentgraf, and J. A. Kleinschmidt.** 1992. Assembly of viruslike particles by recombinant structural proteins of adeno-associated virus type 2 in insect cells. J Virol **66:**6922-6930.

152. **Rust, M. J., M. Lakadamyali, F. Zhang, and X. Zhuang.** 2004. Assembly of endocytic machinery around individual influenza viruses during viral entry. Nat Struct Mol Biol **11:**567-73.

153. **Sagazio, P., M. Tempesta, D. Buonavoglia, F. Cirone, and C. Buonavoglia.** 1998. Antigenic characterization of canine parvovirus strains isolated in Italy. J Virol Methods **73:**197-200.

154. **Saikawa, T., S. Anderson, M. Momoeda, S. Kajigaya, and N. S. Young.** 1993. Neutralizing linear epitopes of B19 parvovirus cluster in the VP1 unique and VP1-VP2 junction regions. J Virol **67:**3004-3009.

155. **Schelhaas, M., J. Malmstrom, L. Pelkmans, J. Haugstetter, L. Ellgaard, K. Grunewald, and A. Helenius.** 2007. Simian Virus 40 depends on ER protein folding and quality control factors for entry into host cells. Cell **131:**516-29.

156. **Schneider, C., R. Sutherland, R. Newman, and M. Greaves.** 1982. Structural features of the cell surface receptor for transferrin that is recognized by the monoclonal antibody OKT9. J Biol Chem **257:**8516-22.

157. **Shackelton, L. A., C. R. Parrish, U. Truyen, and E. C. Holmes.** 2005. High rate of viral evolution associated with the emergence of carnivore parvovirus. Proc Natl Acad Sci U S A **102:**379-384.

158. **Sheff, D. R., E. A. Daro, M. Hull, and I. Mellman.** 1999. The receptor recycling pathway contains two distinct populations of early endosomes with different sorting functions. J Cell Biol **145:**123-139.

159. **Sieczkarski, S. B., and G. R. Whittaker.** 2002. Influenza virus can enter and infect cells in the absence of clathrin-mediated endocytosis. J Virol **76:**10455-64.

160. **Simpson, A. A., V. Chandrasekar, B. Hebert, G. M. Sullivan, M. G. Rossmann, and C. R. Parrish.** 2000. Host range and variability of calcium binding by surface loops in the capsids of canine and feline parvoviruses. J Mol Biol **300:**597-610.

161. **Slepnev, V. I., and P. De Camilli.** 2000. Accessory factors in clathrin-dependent synaptic vesicle endocytosis. Nat Rev Neurosci **1:**161-72.

162. **Smith, T. J.** 2003. Structural studies on antibody-virus complexes. Adv Protein Chem **64:**409-53.

163. **Smith, T. J., E. S. Chase, T. J. Schmidt, N. H. Olson, and T. S. Baker.** 1996. Neutralizing antibody to human rhinovirus 14 penetrates the receptor-binding canyon. Nature **383:**350-4.

164. **Smith, T. J., N. H. Olson, R. H. Cheng, E. S. Chase, and T. S. Baker.** 1993. Structure of a human rhinovirus-bivalently bound antibody complex: implications for viral neutralization and antbody flexibility. Proc. Natl. Acad. Sci. USA **90:**7015-7018.

165. **Smith, T. J., N. H. Olson, R. H. Cheng, E. S. Chase, and T. S. Baker.** 1993. Structure of a human rhinovirus-bivalently bound antibody complex: implications for viral neutralization and antibody flexibility. Proc Natl Acad Sci U S A **90:**7015-8.

166. **Smith, T. J., N. H. Olson, R. H. Cheng, H. Liu, E. S. Chase, W. M. Lee, D. M. Leippe, A. G. Mosser, R. R. Rueckert, and T. S. Baker.** 1993. Structure of human rhinovirus complexed with Fab fragments from a neutralizing antibody. J Virol **67:**1148-58.

167. **Sonnichsen, B., S. De Renzis, E. Nielsen, J. Rietdorf, and M. Zerial.** 2000. Distinct membrane domains on endosomes in the recycling pathway visualized by multicolor imaging of Rab4, Rab5, and Rab11. J Cell Biol **149:**901-14.

168. **Stewart, P. L., C. Y. Chiu, S. Huang, T. Muir, Y. Zhao, B. Chait, P. Mathias, and G. R. Nemerow.** 1997. Cryo-EM visualization of an exposed RGD epitope on adenovirus that escapes antibody neutralization. Embo J **16:**1189-98.

169. **Strassheim, L. S., A. Gruenberg, P. Veijalainen, J.-Y. Sgro, and C. R. Parrish.** 1994. Two dominant neutralizing antigenic determinants of canine parvovirus are found on the threefold spike of the virus capsid. Virology **198:**175-184.

170. **Streuli, C. H., and B. E. Griffin.** 1987. Myristic acid is coupled to a structural protein of polyoma virus and SV40. Nature **326:**619-22.

171. **Suikkanen, S., M. Antila, A. Jaatinen, M. Vihinen-Ranta, and M. Vuento.** 2003. Release of canine parvovirus from endocytic vesicles. Virology **316:**267-80.

172. **Suikkanen, S., K. Saajarvi, J. Hirsimaki, O. Valilehto, H. Reunanen, M. Vihinen-Ranta, and M. Vuento.** 2002. Role of recycling endosomes and lysosomes in dynein-dependent entry of canine parvovirus. J Virol **76:**4401-11.

173. **Tagawa, A., A. Mezzacasa, A. Hayer, A. Longatti, L. Pelkmans, and A. Helenius.** 2005. Assembly and trafficking of caveolar domains in the cell: caveolae as stable, cargo-triggered, vesicular transporters. J Cell Biol **170:**769-79.

174. **Tattersall, P., A. J. Shatkin, and D. C. Ward.** 1977. Sequence homology between the structural polypeptides of minute virus of mice. J Mol Biol **111:**775-794.

175. **Teeters, C. L.** 1986. Transferrin and Apotransferrin: pH-dependent Conformational Changes Associated with Receptor-mediated Uptake. Annals of the New York Academy of Sciences **463:**403-407.

176. **Thomas, N. J., W. J. Foreyt, J. F. Evermann, L. A. Windberg, and F. F. Knowlton.** 1984. Seroprevalence of canine parvovirus in wild coyotes from Texas, Utah, and Idaho (1972 to 1983). J Am Vet Med Assoc **185:**1283-7.

177. **Thouvenin, E., S. Laurent, M. F. Madelaine, D. Rasschaert, J. F. Vautherot, and E. A. Hewat.** 1997. Bivalent binding of a neutralising antibody to a calicivirus involves the torsional flexibility of the antibody hinge. J Mol Biol **270:**238-46.

178. **Tijssen, P., J. Szelei, and Z. Zadori.** 2006. Phospholipase A2 domains in structural proteins of parvoviruses, p. 95-107. *In* R. J. Kerr, S. F. Cotmore, M. E. Bloom, R. M. Linden, and C. R. Parrish (ed.), Parvoviruses. Oxford University Press Inc., New York.

179. **Tresnan, D. B., L. Southard, W. Weichert, J. Y. Sgro, and C. R. Parrish.** 1995. Analysis of the cell and erythrocyte binding activities of the dimple and canyon regions of the canine parvovirus capsid. Virology **211:**123-132.

180. **Truyen, U., M. Agbandje, and C. R. Parrish.** 1994. Characterization of the feline host range and a specific epitope of feline panleukopenia virus. Virology **200:**494-503.

181. **Truyen, U., J. F. Evermann, E. Vieler, and C. R. Parrish.** 1996. Evolution of canine parvovirus involved loss and gain of feline host range. Virology **215:**186-189.

182. **Truyen, U., A. Gruenberg, S. F. Chang, B. Obermaier, P. Veijalainen, and C. R. Parrish.** 1995. Evolution of the feline-subgroup parvoviruses and the control of canine host range in vivo. J. Virol. **69:**4702-4710.

183. **Truyen, U., and C. R. Parrish.** 1992. Canine and feline host ranges of canine parvovirus and feline panleukopenia virus: distinct host cell tropisms of each virus in vitro and in vivo. J Virol **66:**5399-5408.

184. **Tsai, B.** 2007. Penetration of nonenveloped viruses into the cytoplasm. Annu Rev Cell Dev Biol **23:**23-43.

185. **Tsai, B., J. M. Gilbert, T. Stehle, W. Lencer, T. L. Benjamin, and T. A. Rapoport.** 2003. Gangliosides are receptors for murine polyoma virus and SV40. Embo J **22:**4346-55.

186. **Tsang, S. K., B. M. McDermott, V. R. Racaniello, and J. M. Hogle.** 2001. Kinetic analysis of the effect of poliovirus receptor on viral uncoating: the receptor as a catalyst. J Virol **75:**4984-9.

187. **Tsao, J., M. S. Chapman, M. Agbandje, W. Keller, K. Smith, H. Wu, M. Luo, T. J. Smith, M. G. Rossmann, R. W. Compans, and C. R. Parrish.** 1991. The three-dimensional structure of canine parvovirus and its functional implications. Science **251:**1456-1464.

188. **Tullis, G. E., L. R. Burger, and D. J. Pintel.** 1993. The minor capsid protein VP1 of the autonomous parvovirus minute virus of mice is dispensible for encapsidation of progeny single stranded DNA but is required for infectivity. J. Virol. **67:**131-141.

189. **Tuthill, T. J., D. Bubeck, D. J. Rowlands, and J. M. Hogle.** 2006. Characterization of early steps in the poliovirus infection process: receptor-decorated liposomes induce conversion of the virus to membrane-anchored entry-intermediate particles. Journal of virology **80:**172-80.

190. **Varghese, R., Y. Mikyas, P. L. Stewart, and R. Ralston.** 2004. Postentry neutralization of adenovirus type 5 by an antihexon antibody. J Virol **78:**12320-32.

191. **Verdaguer, N., M. G. Mateu, D. Andreu, E. Giralt, E. Domingo, and I. Fita.** 1995. Structure of the major antigenic loop of foot-and-mouth disease virus complexed with a neutralizing antibody: direct involvement of the Arg-Gly-Asp motif in the interaction. Embo J **14:**1690-6.

192. **Vihinen-Ranta, M., L. Kakkola, A. Kalela, P. Vilja, and M. Vuento.** 1997. Characterization of a nuclear localization signal of canine parvovirus capsid proteins. Eur J Biochem **250:**389-394.

193. **Vihinen-Ranta, M., A. Kalela, P. Makinen, L. Kakkola, V. Marjomaki, and M. Vuento.** 1998. Intracellular route of canine parvovirus entry. J Virol **72:**802-806.

194. **Vihinen-Ranta, M., S. Suikkanen, and C. R. Parrish.** 2004. Pathways of cell infection by parvoviruses and adeno-associated viruses. J Virol **78:**6709-14.

195. **Vihinen-Ranta, M., D. Wang, W. S. Weichert, and C. R. Parrish.** 2002. The VP1 N-terminal sequence of canine parvovirus affects nuclear transport of capsids and efficient cell infection. J Virol **76:**1884-91.

196. **Vihinen-Ranta, M., W. Yuan, and C. R. Parrish.** 2000. Cytoplasmic trafficking of the canine parvovirus capsid and its role in infection and nuclear transport. J Virol **74:**4853-4859.

197. **Weichert, W. S., J. S. Parker, A. T. Wahid, S. F. Chang, E. Meier, and C. R. Parrish.** 1998. Assaying for structural variation in the parvovirus capsid and its role in infection. Virology **250:**106-17.

198. **Wickham, T. J., P. Mathias, D. A. Cheresh, and G. R. Nemerow.** 1993. Integrins alphaVbeta3 and alphavbeta5 promote adenovirus internalization but not virus attachment. Cell **73:**309-319.

199. **Wiethoff, C. M., H. Wodrich, L. Gerace, and G. R. Nemerow.** 2005. Adenovirus protein VI mediates membrane disruption following capsid disassembly. J Virol **79:**1992-2000.

200. **Wikoff, W. R., G. Wang, C. R. Parrish, R. H. Cheng, M. L. Strassheim, T. S. Baker, and M. G. Rossmann.** 1994. The structure of a neutralized virus: canine parvovirus complexed with neutralizing antibody fragment. Structure **2:**595-607.

201. **Wilton, D. C.** 2008. Phospholipases, 5 ed. Elsevier, Amsterdamn.

202. **Xie, Q., and M. S. Chapman.** 1996. Canine parvovirus capsid structure, analyzed at 2.9 Å resolution. J Mol Biol **264:**497-520.

203. **Zadori, Z., J. Szelei, M.-C. Lacoste, P. Raymond, M. Allaire, I. R. Nabi, and P. Tijssen.** 2001. A viral phospholipase A2 is required for parvovirus infectivity. Developmental Cell **1:**291-302.

204. **Zhang, L., K. Chandran, M. L. Nibert, and S. C. Harrison.** 2006. Reovirus mu1 structural rearrangements that mediate membrane penetration. Journal of virology **80:**12367-76.

CHAPTER TWO

Different mechanisms of antibody-mediated neutralization of parvoviruses revealed using the Fab fragments of monoclonal antibodies.

Christian D.S. Nelson, Laura S. Palermo, Susan L. Hafenstein, and Colin R. Parrish. 2007. Different mechanisms of antibody-mediated neutralization of parvoviruses revealed using the Fab fragments of monoclonal antibodies. Virology. (361) 283-293.

[Laura Palermo was a graduate student in Colin Parrish's laboratory who provided transferrin receptor for these experiments. Susan Hafenstein is a post-doctoral research associate in Michael Rossman's Laboratory who designed figure 2.7]

2.1 Abstract.

Antibody binding and neutralization are major host defenses against viruses, yet the mechanisms are often not well understood. Eight monoclonal antibodies and their Fab fragments were tested for neutralization of canine parvovirus and feline panleukopenia virus. All IgGs neutralized >90 percent of virus infectivity. Two Fabs neutralized when present at 5 nM, while the others gave little or no neutralization even at 20-100 nM. The antibodies bind two antigenic sites on the capsids which overlap the binding site of the host transferrin receptor (TfR). There was no correlation between Fab binding affinity and neutralization, indicating that the specific antibody epitope may be more important in determining neutralization. All Fabs reduced capsid binding of virus to purified feline TfR *in vitro*, but the highly neutralizing Fabs were more efficient competitors. All partially prevented binding and uptake of capsids by feline TfR on cells. The virus appears adapted to allow some infectivity in the presence of at least low levels of antibodies.

2.2 Introduction.

Protection and recovery from viral infection in animals are complex processes that involve many components of the innate and adaptive immune systems, and antibodies are a critical adaptive immune response against most viruses of vertebrates (6). Antibody neutralization is defined as the "abrogation of virus infectivity *in vitro* by the binding of antibodies to the virion" (31), and that binding may affect the virus at one or more stages in the viral infection cycle. In different models antibodies have been shown to crosslink and aggregate virions (10), prevent viral attachment to cells (32), block receptor binding by steric hindrance or by preventing viral conformational changes required for infection (10, 40), inactivate the virus before cell binding occurs (reviewed by (17))(16, 23, 50), or prevent infection after uptake into cells (49,

81)(reviewed in (31)). Additional antibody-mediated mechanisms occur *in vivo*, where they can cause Fc-mediated phagocytosis, complement binding and activation, opsonization, and antibody-dependant cellular cytotoxicity of infected cells (6).

Viruses and their hosts have been co-evolving for long periods, and the antigenic sites of viral structural proteins will be those that allow highest viral fitness in the face of antibody selection. Different viruses show various levels of antibody binding and differ in their ability to accommodate antigenic variation. Some viruses (such as rhinovirus, influenza, and HIV) either come in many serotypes or are able to tolerate amino acid variation to escape from or avoid the antibody responses of their hosts (21, 26, 37, 73). Other viruses (such as measles virus or polioviruses) are found as only 1 or a small number of antigenic types even after long periods of selection and are apparently unable to vary antigenically to escape preexisting antibodies (65, 66, 69, 70). These differences in antigenic structure and variation likely result from differences in the replication of the viruses, their modes of transmission, and the abilities of their structural proteins to accommodate antigenic change while still maintaining other viral properties (2, 83).

Although often considered a factor in antibody neutralization, the relationships between the antibody and receptor binding sites have only been examined directly in a few cases. Some receptor binding sites are conserved and buried in clefts or other protected structures that are at least partially inaccessible to antibodies (68), while other receptor binding sites are on prominent structures and show significant overlap with the antibody binding sites (15, 38).

Parvoviruses are small and have simple capsids made of essentially a single protein structure, and they do not appear to encode genes that can specifically manipulate the immune responses of their hosts. Despite this simplicity, they cause a variety of different types of disease, with acute infections in many cases. However,

several of the parvoviruses form persistent infections, indicating that they are able to persist in the face of host immunity. Canine parvovirus (CPV) and feline panleukopenia virus (FPV) have 25nm nonenveloped T=1 icosahedral capsids that are assembled from 60 copies of a mixture of viral proteins. The infectious capsids contain ~55 copies of VP2, and ~5 copies of the VP1 protein which in CPV and FPV contains both the VP2 sequence and an 143 additional N-terminal residues (80, 91). Full (DNA-containing) capsids have about 20 residues of some the VP2 N termini exposed on the outside of the capsid where they may be cleaved by host proteases to form VP3, and those N-termini are likely exposed through a pore at the five-fold axis of symmetry (86, 91). Elaborate loops forming most of the capsid surface make up most of the functional sites of the capsid, including those involved in receptor and antibody binding (1, 24, 27, 76, 80, 88).

The cell receptor for CPV and FPV is the transferrin receptor (TfR), and appropriate TfR binding leads to cell infection (29, 54). The TfR assembles as a stable homo-dimer, and each monomer is made up of 3 domains: a protease-like domain, an apical domain, and a helical domain. Transferrin and hereditary hemachromatosis protein bind to the membrane proximal portions of the protease-like and helical domains (12, 22, 36, 87) whereas CPV and FPV bind to the apical domain (53). Canine TfR binding to the CPV capsid is affected by residues in three positions on the threefold spike that are ~20-30Å apart, suggesting that the receptor binds to a broad surface of the capsid (24, 27).

There is variation among the CPV- and FPV-like viruses that is associated with differences in their host ranges. The original CPV strain (termed CPV type-2 (CPV-2)) emerged in 1978 due to a small number of mutations of an FPV-like virus which altered both receptor and antibody binding sites on the capsids. A further 4 or 5 mutations in the capsid protein gene of CPV-2 resulted in the emergence of a variant

virus (CPV type-2a (CPV-2a)) in 1979 which replaced CPV-2 worldwide within two years (56, 60, 61). CPV-2a differs from CPV-2 in affinity for the feline TfR and also in antigenic structure as defined by monoclonal antibody (MAb) binding (53, 56, 61). Those strains of virus also differ in canine and feline host ranges, as FPV infects cats but not dogs, CPV-2 strains infect dogs but not cats, while CPV-2a and later viruses infect both cats and dogs (45, 78, 79). Since 1980, variations of single residues in the capsid have become widely selected, including VP2 residue Asn426 to Asp (after 1984, designated the virus being designated CPV-2b (56)), VP2 residue Ser297 to Ala around 1990, and residue Asp426 to Glu after 2000 (4).

The antigenic structure of CPV and FPV has been examined by MAb binding, analysis of peptide binding by polyclonal sera, cryoelectron microscopic (cryoEM) analysis of capsid:Fab complexes, and analysis of natural and selected antigenic variants (7, 25, 34, 35, 57, 63, 76, 78, 88). Cross-competition studies of MAb binding and analysis of sequences that determine antigenic variations show that the epitopes can be divided among two major antigenic sites designated A and B (57, 76). Although site A is near the top of the threefold spike and site B is on the side (shoulder) of that structure, both epitopes are composed of multiple loops so that the binding sites are conformational in nature (76, 80, 88, 91). Although FPV or mink enteritis virus (MEV) isolates collected over many years show little antigenic variation (57, 59), both A and B site changes have been detected in CPV isolates from dogs and cats (42, 46, 47, 56, 61).

Panels of MAbs have been generated against FPV, CPV-2, and CPV-2b capsids, and all of those antibodies neutralized virus infectivity when tested as IgGs (76). When the antibody binding (variable) domains of two MAbs were expressed as single chain variable domains (scFvs), they neutralized infectivity, although at levels

lower than the corresponding IgGs, and that neutralization was in part due to cross-linking and aggregation of the capsids by dimeric forms of the scFv (92).

Here we examine the processes of antibody neutralization of canine and feline parvoviruses. We tested 8 different MAbs recognizing either site A or B for their abilities to neutralize the viruses as IgGs and Fabs. While all IgGs neutralized the viruses, only two of the Fabs recognizing site B efficiently neutralized viral infectivity, one was weakly neutralizing, and the other Fabs showed little or no neutralization. All Fabs at least partially inhibited the binding of capsids to the purified feline TfR, but the highly neutralizing antibodies showed the greatest inhibitory effect. There were only modest differences in the affinity of binding of the Fabs, but the highly neutralizing antibodies were not uniformly of higher affinity. Efficient neutralization by Fab binding likely results from either Fab-induced differences in the capsid-TfR interaction, or to effects on later stages of infection.

2.4 Materials and Methods.

Cells and viruses. Crandell Reese Feline Kidney Cells (CRFK) were grown in a 1:1 mixture of McCoy's 5A and Lebovitz L-15 media with 5% fetal calf serum (FCS). TRVb hamster cells which lack TfR were grown in Hams F-12 medium with 5% FCS, and were transfected with plasmids expressing the feline TfR (TRVb-fTfR) and selected with 400 μg/ml G418 (28) . FPV, CPV-2, and CPV-2b virus stocks were prepared from infectious clones transfected into CRFK cells as previously described (55), and stored at -80^{o}C in aliquots.

Purified Transferrin Receptor. Soluble TfR ectodomain was produced by baculovirus expression in insect cells as previously described (28, 52). The dimeric protein was isolated by size exclusion chromatography through a S300 column.

Capsid concentration measurements. Capsid concentrations in virus samples were determined using a capture ELISA. Purified rat anti-CPV (MAb F) bound to an ELISA plate was used to capture virus from the test samples or controls containing known amounts of purified virus. After 1 h the plate was washed with phosphate buffered saline with Tween 20 (PBST). The plates were incubated with a mouse anti-CPV (Mab 8), then with a specific goat anti-mouse HRP-conjugated antibody, and 2,2'-Azino-bis(3-ethyl bensthaxoline-6-sulfonic acid) (ABTS) substrate for 30 min.

Anti-CPV and FPV antibodies. Eight different hybridomas were chosen which produced IgG antibodies against CPV or FPV capsids (Table 2.1)(57, 58). Hybridomas were grown in 500 ml volumes in gas permeable bags (Nexell, Irving, CA) containing Dulbecco's minimal essential medium with 5% FCS, then the IgGs were purified using Protein G (GE Healthcare, Piscataway, NJ). Fabs were generated using papain digestion; the Fc portions removed with protein A (GE Healthcare), and the monomeric Fabs were purified by chromatography in a Sephadex G100 column in PBS. Protein concentrations were determined by A_{280} and by bicinchoninic acid (BCA) assay.

Virus neutralization assays. CRFK cells were seeded into 96 well trays at 1.28 x 10^4 cells per cm^2 and incubated overnight. 10^4 $TCID_{50}$ of virus and various amounts of IgG or Fab were mixed with DMEM to give a final volume of 0.4 ml. After 1 h at 37°C, each virus was diluted in 10-fold series, and 0.05ml added to replicate wells. After 1 h at 37°C, 0.1 ml of growth medium was added and cells were incubated for 48 hrs. After fixation the infected cells were detected by antibody staining as described (92), and the $TCID_{50}$ titers calculated.

Affinity of Fabs for CPV. Affinities of Fabs were determined by direct calibration ELISA (20). Three separate experiments were performed to obtain variables used in

determination of affinity. Unless otherwise noted100 ng of capsids and 10 ng of Fabs per well were used, Fabs were diluted in blocking buffer (PBST with 0.5% w/v ovalbumin), and plates washed six times with PBST between incubations. Fabs were detected with either an anti-mouse or anti-rat HRP-conjugated secondary antibody. Capsids were immobilized to Maxisorp plates (Nunc, Rochester, NY) in carbonate-bicarbonate buffer (pH 9.6) overnight at 4^{o}C. These plates were washed and then blocked with blocking buffer for 2.5 h before use in each experiment.

To determine the rate of Fab-CPV complex formation, *Kc*, Fabs and capsids were incubated for various times before the unbound Fabs were removed, wells washed and 100 µl of PBST was left in each well until the last time point was completed, when the bound Fabs detected. Non-linear regression analysis estimated the maximum absorbance for each Fab after infinite binding time. The absorbance correlates with the concentration of Fab-CPV complexes by an unknown calibration factor, *c*. The calibration factor was determined by incubating Fabs with immobilized capsids for varying times, and then serially transferred to more immobilized capsids. The amount of each Fab transferred or retained is determined by the transfer factor, F. After 4 transfers, the plates were washed, bound Fabs were detected, and F and *c* determined. The amount of CPV immobilized to the plate was determined by a saturation analysis. Fab concentrations ranging from 166 to 0.04 nM were allowed to interact with capsids for 3.5 hr, plates were washed and Fabs detected. Non linear regression analysis was used to determine the maximum binding that would occur with an infinite concentration of Fabs, and this was used to determine the immobilized CPV concentration by the calibration factor *c*. Affinities were determined by the equation $K_a = (1 - F)/(F * CPV_{immbolized})$.

TABLE 2.1.

Monoclonal antibodies used in these studies, along with the known specificity for particular viruses, and the escape mutants that affect their binding.

Antibody ID	**Source**	**Epitope recognized**	**Specificity**	**Escape mutations (residue in VP2 sequence)**
14	Mouse	Site A	CPV only	93 N-K, 224 G-R, 224 G-E, 222 H-Y
15	Mouse	Site B	CPV, FPV	299 G-E (300 A-D partial)
16	Mouse	Site B	CPV, FPV	299 G-E, 300 A-D, 302 N-D
6	Mouse	Site A	CPV, FPV	222 H-Y, 224 G-R, 224 G-E
8	Mouse	Site B	CPV, FPV	300 A-D, 302 N-D
B	Rat	Site A	CPV, FPV	222 H-Y, 224 G-R, 224 G-E
F	Rat	Site B	CPV, FPV	No escape mutant recovered
E	Rat	Site B	CPV, FPV	300 A-D

Competition with capsid binding to the feline TfR. The effects of the Fab on capsid binding to the feline TR were tested using *in vitro* binding assays. Purified feline TfR ectodomain was coated onto Maxisorp black plates (Nunc) in pH 9.6 carbonate buffer at 4^{o}C overnight. After washing the plates were incubated withblocking buffer for 1 h. The Fab fragments were incubated at various concentrations with the CPV-2 empty capsids labeled with Cy2, and then after 1 h the mixtures were added to the wells containing the feline TfR. Control Fabs were prepared from antibodies directed against the capsids of AAV-1 or AAV-5, which did not react with the CPV capsids. After 1 h incubation, the plates were washed and the capsid fluorescence bound determined in a fluorescence reader (Tecan Sapphire, Durham, NC).

Cell binding and uptake. Fluorescence microscopy was used to examine the ability of Fab bound capsids to bind and enter cells. Cy-2 labeled CPV-2 or FPV capsids were incubated with Fabs at ratios between 1:100 to 1:20 for 1 h at 37°C. CRFK cells, or TRVb- cells expressing the feline TfR were washed 3 times with DMEM containing 0.1% BSA, then incubated with Fab-CPV mixtures for 1 h at 37°C. Cells were washed with PBS, fixed in 2% paraformaldehyde (PFA) for 10 min, then washed and visualized under the fluorescent microscope. Images were collected at the same exposure in both phase contrast and fluorescence, and analyzed for virus fluorescence in each cell using Image J (Rasband, W.S., ImageJ, U. S. National Institutes of Health, Bethesda, Maryland, USA, http://rsb.info.nih.gov/ij/, 1997-2006). The area and regions of interest of cells were determined from the phase contrast image, and mean specific fluorescence values for each cell were determined for that same area in the fluorescent channel. Data is the result of at least 25 cells from each treatment, selected randomly using the phase contrast channel.

2.3 Results.

Antibody and Fab preparation and binding. Fab fragments of MAbs prepared by papain digestion were further purified by gel chromatography to ensure that only monomeric Fab proteins were used in these studies. All the Fabs bound to CPV-2 and FPV capsids in ELISA (Figure 2.1), except for the CPV-specific Fab14 which does not bind FPV (57)(Figure 2.1a). Direct calibration ELISA was used to determine the affinity of binding of the 8 Fabs to CPV-2 capsids (Figure 2.2) (20). Seven of the Fabs showed clear binding kinetics in the assays, and their affinities were readily determined (Table 2.2). Fab B showed low binding in the assays, and in the transfer assay showed increasing binding during the repeated transfers (Figure 2.2C), so that its affinity could not be calculated directly but was estimated to be around 8 x 10^{-9} nM. The binding affinities of 7 of the Fabs tested did not differ by more than 3-fold. The intact IgGs all showed higher avidities compared to the Fabs, as would be expected from their bivalent interactions (results not show).

Neutralization of FPV and CPV by IgG and Fabs. When tested as IgGs 7 of the antibodies neutralized >90% of CPV infectivity at 5nM and >99% CPV infectivity at 25nM, while MAb 14 neutralized only 88% of the infectivity at 100 nM (Figure 2.3A). FPV showed similar neutralization sensitivity, and >99% of the infectivity was also neutralized by 5nM of the 7 IgGs that reacted with the virus, but not by MAb 14 (Figure 2.3B). When the Fabs were tested, E and F neutralized >99% of the viral infectivity of both CPV and FPV at 5nM or lower concentrations, while Fab 16 neutralized at 25nM, and Fab 6 neutralized FPV only at 100nM (Figs. 2.4). By capture ELISA we determined that the capsids were present in the infectivity stocks used for the $TCID_{50}$ titrations at concentrations of ~6 μg/ml, so that the Fab:capsid ratios were ~100:1 at 5 nM (data not shown).

Figure 2.1.

Binding of Fabs for (A) CPV or (B) FPV capsids. The Fab fragments bound were detected with either an anti-mouse or anti-rat horseradish peroxidase conjugated secondary antibody as appropriate. Error bars show the standard error of the mean, comparing the results of 3 separate experiments.

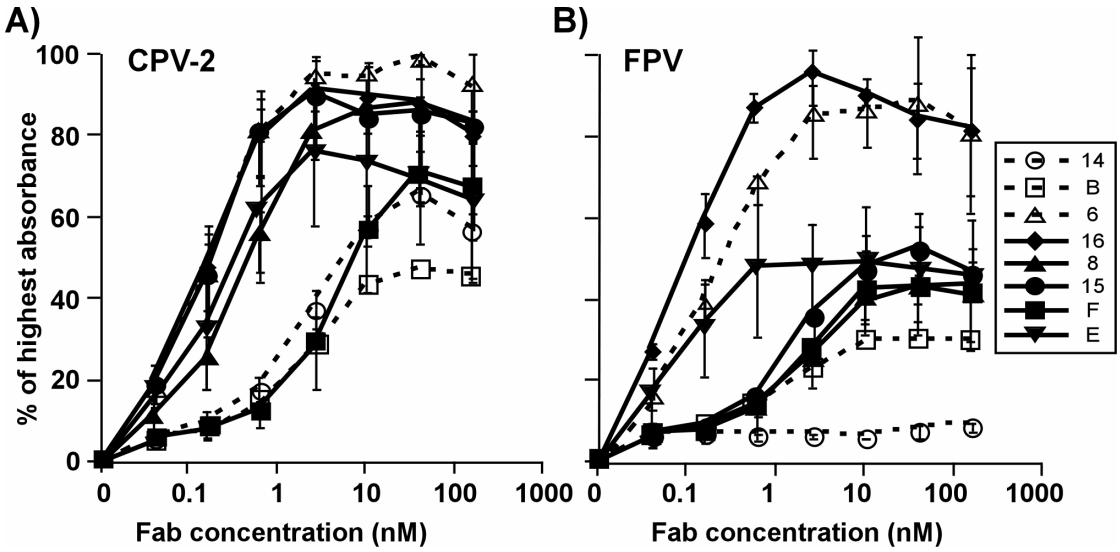
A)
CPV-2
% of highest absorbance
100
80
60
40
20
0
0
0.1
1
10
100
1000
Fab concentration (nM)
B)
FPV
0
0.1
1
10
100
1000
Fab concentration (nM)
14
B
6
16
8
15
F
E

Figure 2.2.

Determining the binding affinities of the 8 Fabs to the CPV capsids by measuring the kinetics of binding, the saturated binding level, and the degree of binding when the Fabs were incubated with the viral antigen and then transferred to a new well after various times; the 30 min transfer data is shown as an example. (A) The rate of Fab binding to the antigen, tested by allowing the Fabs to incubate for various times with the capsids before washing, then detecting with anti-mouse or anti-rat IgG HRPO conjugates. (B) The saturation of binding for the 8 different Fabs, showing the binding when the antigen was incubated with increasing amounts of the Fabs, allowing the saturated binding to be estimated. (C) The binding of each Fab in a transfer assay where the Fabs were incubated with the antigen for 30 min before transferring to a new well. This was repeated 4 times for various lengths of time; the 30 min data is shown here.

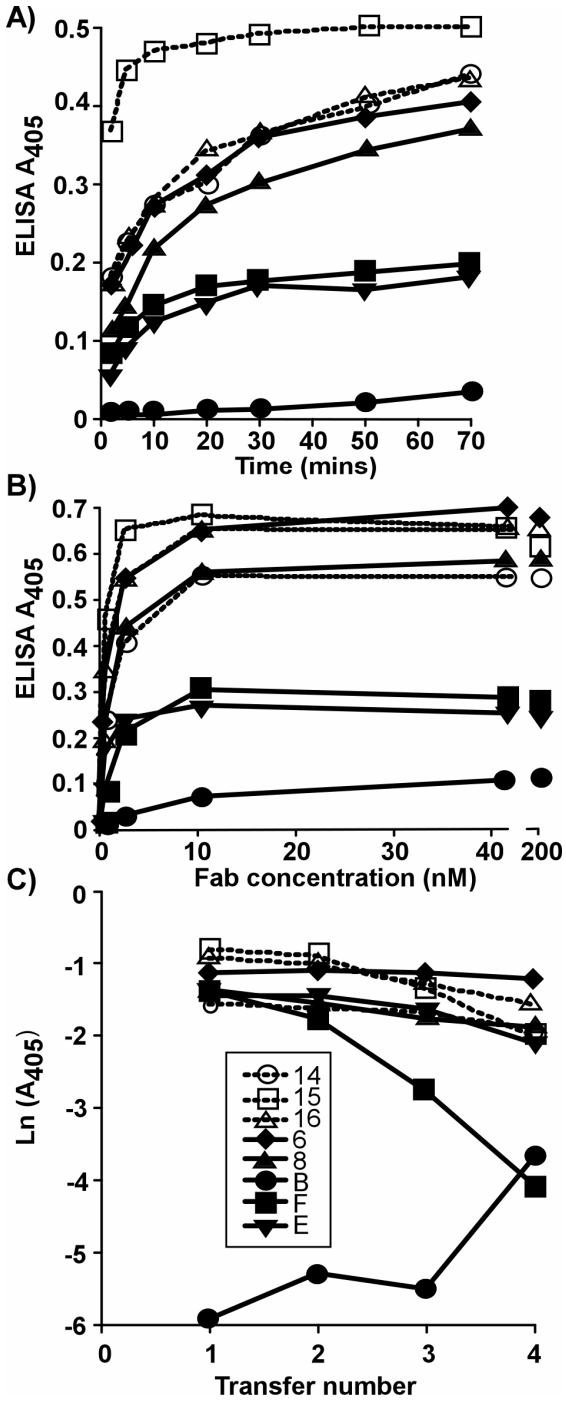
A)
ELISA A405
0.5
0.4
0.3
0.2
0.1
0
0 10 20 30 40 50 60 70
Time (mins)
B)
ELISA A405
0.7
0.6
0.5
0.4
0.3
0.2
0.1
0
0 10 20 30 40 200
Fab concentration (nM)
C)
Ln (A405)
0
-1
-2
-3
-4
-5
-6
0 1 2 3 4
Transfer number
14
15
16
6
8
B
F
E

Table 2.2.

Determination of the affinities of the Fabs examined here using the direct calibration ELISA method. The three components of the analysis are given, as well as the affinity calculated as the dissociation constant. We were unable to accurately determine the affinity of Fab B using this method. ND = not determined.

Antibody ID	**Rate of complex formation (Kc, s^{-1})**	**Calibration Factor (c, M)**	**Transfer Factor (F)**	**Dissociation constant (Kd, M)**
14	1.2×10^{-3}	7.0×10^{-10}	0.9	3.4×10^{-9}
15	3.4×10^{-3}	1.3×10^{-9}	0.7	2.1×10^{-9}
16	1.0×10^{-3}	8.6×10^{-10}	0.83	2.6×10^{-9}
6	1.3×10^{-3}	4.8×10^{-11}	0.99	3.2×10^{-9}
8	1.7×10^{-3}	1×10^{-9}	0.82	3.4×10^{-9}
B	ND	ND	ND	$\sim 6.1 \times 10^{-9}$
F	1.7×10^{-3}	8×10^{-9}	0.39	1.5×10^{-9}
E	8.5×10^{-4}	2×10^{-9}	0.8	1.7×10^{-9}

Figure 2.3.

The neutralization of (A) CPV-2 and (B) FPV infectivity by various amounts of the different IgGs of the 8 different MAb tested here. The IgGs were added to 10,000 $TCID_{50}$ of each virus at concentrations between 0 and 100 nM, incubated for 1 h at 37°C, then the surviving virus was diluted and tested for surviving $TCID_{50}$ in CRFK cells. The results are shown as the surviving infectivity in each culture compared to the titer of the control virus. Bars show the standard error of the mean, comparing the results of 3 separate experiments done on separate days.

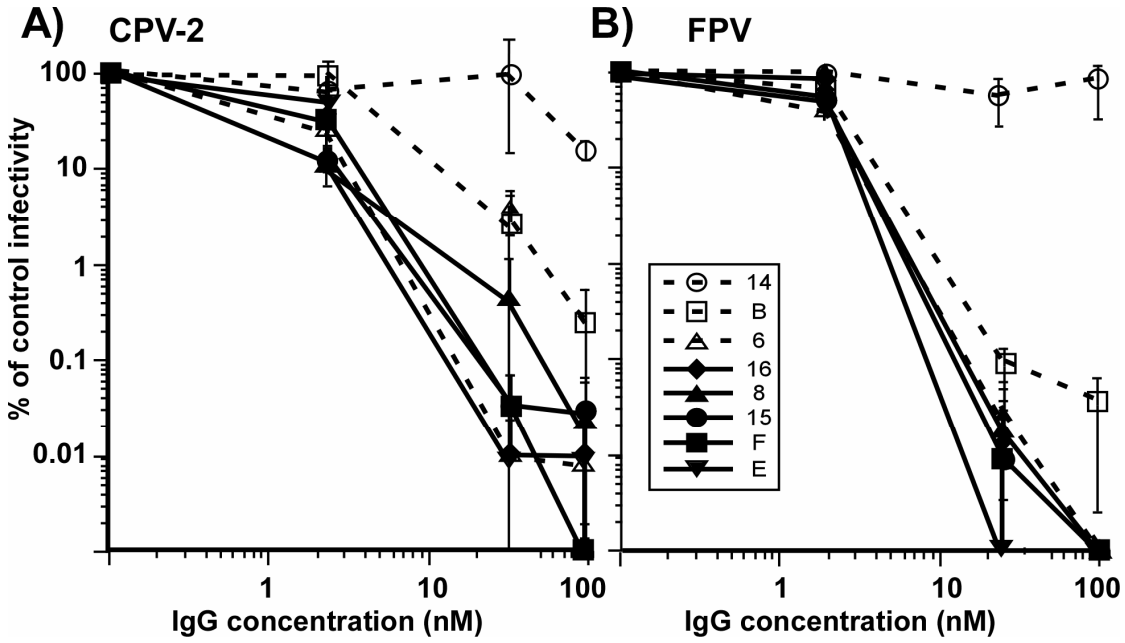
A)
CPV-2
B)
FPV
% of control infectivity
100
10
1
0.1
0.01
1
10
100
IgG concentration (nM)
14
B
6
16
8
15
F
E

Figure 2.4.

The neutralization of (A) CPV-2 and (B) FPV infectivity by the Fab fragments of the 8 different MAbs as shown for the IgGs in Figure 2.3. The results are shown as the surviving infectivity in each culture compared to the titer of the control virus. Bars show the standard error of the mean, comparing the results of 3 separate experiments done on separate days.

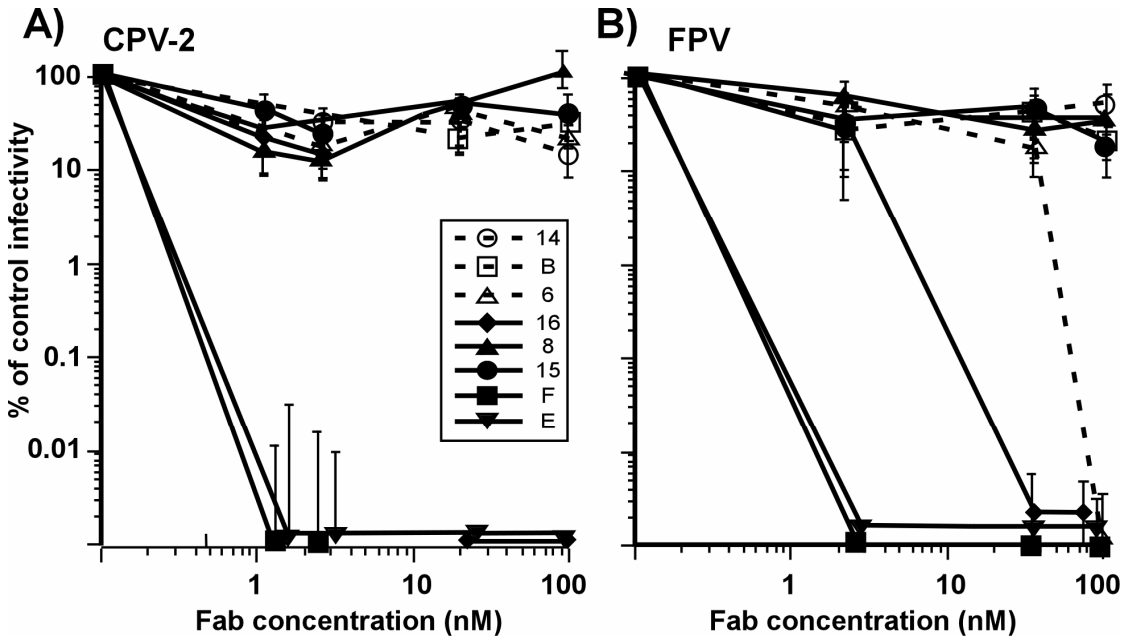
A)
CPV-2
100
10
1
0.1
0.01
% of control infectivity
14
B
6
16
8
15
F
E
1
10
100
Fab concentration (nM)
B)
FPV
1
10
100
Fab concentration (nM)

Fabs compete for receptor binding of the capsid. The CPV-2 capsids were labeled with Cy2 and bound to the purified ectodomain of feline TfR in a solid phase assay. All Fabs reduced capsid binding to the TfR at concentrations of 29 nM or greater (20 Fabs per capsid) (Figure 2.5). Fabs E and F showed the greatest competition, while Fab 6 did not completely block binding even at 100nM (Figure 2.5). Fab B also allowed some binding at 100 Fabs per capsid, perhaps due to its lower affinity relative to the other Fabs (Figure 2.2 and Table 2.2).

Fabs and viral attachment to cells. All Fabs were able to block the binding and uptake of a proportion of the capsids into TRVb cells expressing the feline TfR when tested at Fab:capsid ratios of up to 100:1 (Figure 2.6). However, all Fabs reduced binding and uptake to similar levels, and no specific distinction was seen between the highly neutralizing Fabs and the less or non-neutralizing Fabs.

2.5 Discussion.

Here we show that the parvovirus capsid interactions with antibodies are surprisingly complex and showed clear differences in viral neutralization despite the fact that they bind with similar affinities to most or all of the 60 sites on the capsid. Studies of escape mutations and competition assays have suggested that most antibodies generated against intact capsids recognize two dominant antigenic sites, described as site A near the top of the three fold axis and site B on the shoulder of that structure (76). The general features of those sites are shown in Figure 2.7, where the residues that affect the A and B sites in previous studies are displayed, along with projected Fab density from radial sections of Fab-virus cryoEM reconstructions Fab 14 bound to the A site while Fab 15 bound to the B site. In other studies, footprints of these Fabs have been defined by cryoEM reconstruction techniques which confirm the disposition of the two binding sites (25).

Figure 2.5.

Inhibition of binding of Cy2-labelled CPV-2 capsids to the feline TfR by the 8 Fabs tested here. The capsids were incubated with varying amounts of Fab per capsid, and then added to plates coated with the purified feline TfR ectodomain, and the bound capsids detected using a fluorescence plate reader. The amount of binding is shown as the percentage of the binding of the capsids without Fab added. Control Fabs against the capsids of adeno-associated viruses types 1 and 5 were tested at only 100 Fabs per capsid. The results are shown as the mean and standard error of three separate experiments.

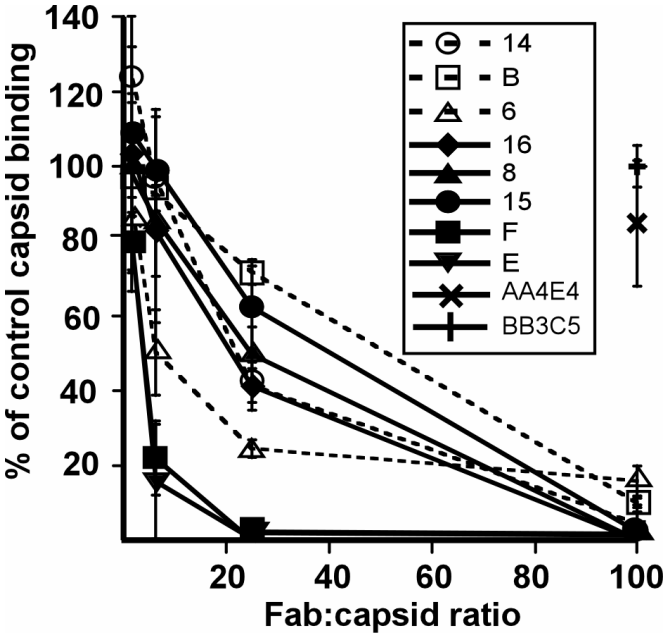
% of control capsid binding
140
120
100
80
60
40
20
20
40
60
80
100
Fab:capsid ratio
14
B
6
16
8
15
F
E
AA4E4
BB3C5

Figure 2.6.

Competition by Fabs for cell binding and uptake. CPV-2 capsids were incubated with varying amounts of the Fabs for 1 h at 37°C, then bound to TRVb cells expressing the feline TfR.

(A) Representative micrographs are shown for the no Fab control, and the Fabs against the A site (Fab 14) or the B site (Fab F).

(B) Total average cell-associated fluorescence (per cell) was determined for at least 20 cells at each concentration. Results are plotted as a percentage of the CPV bound to cells in the absence of any added Fabs. The control anti-AAV Fabs were tested at 100 Fabs/capsid.

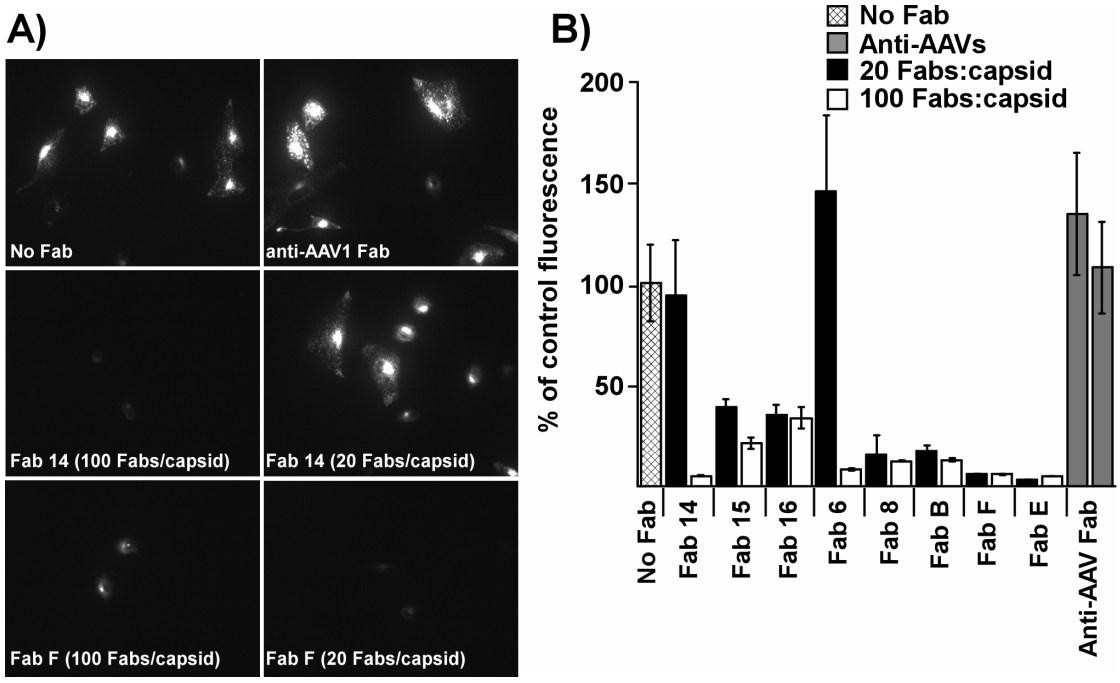
A)
No Fab
anti-AAV1 Fab
Fab 14 (100 Fabs/capsid)
Fab 14 (20 Fabs/capsid)
Fab F (100 Fabs/capsid)
Fab F (20 Fabs/capsid)
B)
No Fab
Anti-AAVs
20 Fabs:capsid
100 Fabs:capsid
% of control fluorescence
200
150
100
50
No Fab
Fab 14
Fab 15
Fab 16
Fab 6
Fab 8
Fab B
Fab F
Fab E
Anti-AAV Fab

Figure 2.7.

A roadmap showing the location of surface residues of CPV-2 that affect the binding of the different antibodies to the capsid structures. A single asymmetric unit of the capsid is shown. Two antigenic sites have been previously defined, and designated as (A) and (B) through the analysis of mutations that affected antibody binding or by cross-competition. Residues that affect antibody binding to some A-site antibodies are shown in red, and those affecting B-site antibodies are shown in blue. CryoEM density corresponding to Fab14 as bound to the A site and Fab15 as it interacts with the B site are projected to the surface of the virion and indicated as red (Fab14) or blue (Fab15). The projection of Fab density obtained from virus-Fab complex shows the A and B sites as previously described, but with some possible overlap between the antibodies binding to the two sites (25).

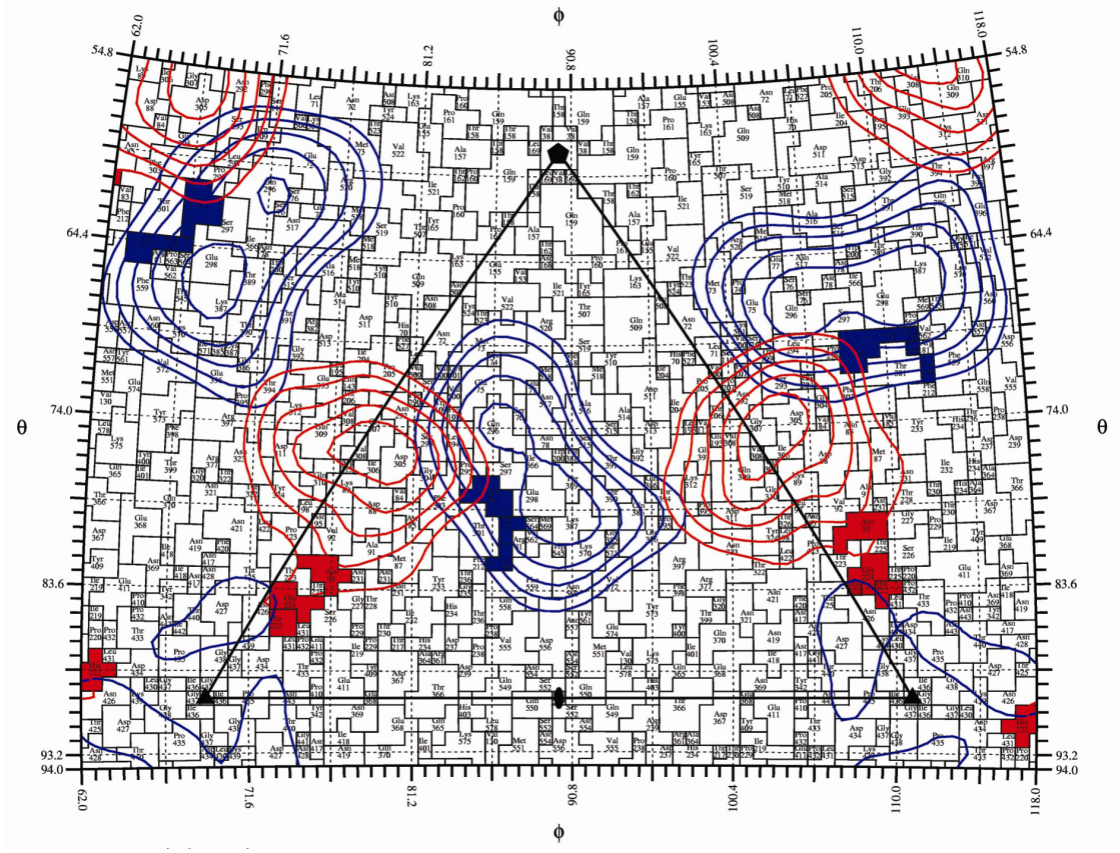
ϕ
62.0
71.6
81.2
90.8
100.4
110.0
118.0
54.8
64.4
74.0
83.6
93.2
94.0
θ

Although all 8 IgGs neutralized the viruses only two of the Fabs neutralized efficiently, and another was intermediate in neutralizing ability. Both neutralizing and non-neutralizing Fabs bound to the B site of the capsids, showing that neutralization depends on specific interactions of the Fabs with the capsid rather than being a result of simple Fab attachment to a particular site, and the neutralizing and non-neutralizing antibodies must therefore affect the cell infection processes differently. None of the A site Fabs tested here efficiently neutralized the virus.

Blockade of receptor binding is often suggested as a mechanism of viral neutralization, and here we were able to test for this effect using the purified receptor in *in vitro* assays, and by testing for binding to the receptor on cells. The results indicate that any neutralization differences due to effects on TfR binding would be rather subtle, since all of the Fabs inhibited binding to the purified receptor ectodomain when present in high enough concentrations. However, the highly neutralizing Fabs (E and F) blocked capsid binding to the TfR at the non-saturating concentration of 25 Fab per capsid, and even blocked 80% of the binding at a ratio of 6.25 Fab per capsid. This suggests a mechanism of neutralization that results from a direct effect of small numbers of Fabs on the capsid that blocks TfR binding to the remaining sites on the capsid, perhaps through some allosteric change induced in the capsid. However, in limited studies we have not been able to directly demonstrate any change in the capsid (results not shown). The less efficiently neutralizing or non-neutralizing Fabs also inhibited capsid binding to the feline TfR when added at higher concentrations, indicating that they would not have the same structural effect on the capsids, and that they must leave sufficient binding sites available at lower antibody concentrations for cell binding and endocytosis allowing infection. The TfR is very efficiently taken up by clathrin-mediated endocytosis (19), and even the low affinity binding of the capsid to the canine TfR allows efficient infection of cells (52).

The antibodies against the CPV and FPV capsids recognize only a limited number of structural sites (25), suggesting that those sites are particularly efficient at selecting high affinity antibodies and are the result of selection to allow the most efficient replication and transmission in the presence of antibodies. The capsid structures of the parvoviruses infecting vertebrates show a variety of prominent regions at or surrounding the threefold spikes (9, 30, 43, 51, 84, 90), and epitopes that have been mapped mostly fall on those structures (14, 39, 76, 89). Insect parvoviruses are not under antibody selection, and have smoother surfaces (3, 71), suggesting that the prominent structures benefit the vertebrate viruses when targeted by antibodies, perhaps because the limited number of sites inducing high affinity antibodies allows them to regulate the effects of the antibody binding during infection.

What selects for changes in the viral antigenic structure? Although natural antigenic variants have been seen among the CPV- and FPV-like viruses, most of those changes simultaneously alter TfR receptor binding (27, 29, 52), and in this case it appears that antigenic variation is a side-effect of capsid changes that alter receptor binding to mediate host adaptation. FPV and MEV have been in long association with their hosts and are also antigenically conserved, with only a single antigenic variant being identified among MEV isolates due to the change of residue 300 from Ala to Ser (57, 59). The natural antigenic variants of CPV fall within both the A and B sites of the capsid. The change of VP2 residue 93 from Lys to Asn during the emergence of CPV was required for canine TfR binding and canine host range determination, and that also altered antigenic site A (8, 27, 29). That difference would not have been subject to selection by preexisting immunity as CPV-2 could not infect cats, so the selection of that site was for host range variation alone. Some combination of the changes between CPV-2 and CPV-2a of VP2 residues 87, 101, 300, and 305 also reduced the affinity of CPV-2a binding of CPV-2a to the feline TfR (52), and allowed

the CPV-2a and the more recent strains to infect cats (77). Those changes also altered antigenic site B causing the loss of binding to some antibodies that bound CPV-2 and FPV, and creating the CPV-2a specific antigenic sites (56). That variation also reduced the affinity of the virus for the feline TfR and likely determined the host range for cats, again making it likely that receptor binding was the most important property being selected.

Other antigenic variants have emerged in the CPV-2a background; after 1983 the change of VP2 residue 426 from Asn to Asp was found worldwide, giving the CPV-2b variant (56). That mutation is still seen at various levels among dogs around the world, suggesting that the selection on that site prevents it becoming fixed (5, 13, 67, 75). Since the year 2000, viruses containing the VP2 residue 426 to Glu replacement have been seen in various parts of the world, and that variant is increasing in frequency (42, 48). Residue 426 is within the TfR binding site, but effects of those mutations on TfR binding have not been described.

Antibody and receptor binding have overlapping effects on the pathogenesis and epidemiology of these viruses. Antibodies in infected and recovered animals protect for life against re-infection, so that the viruses are maintained in nature as a series of acute infections of puppies or kittens which have waning or no maternal immunity. This continual turnover of the virus population allows mutations to be selected within the global populations of hosts over short time periods. Host infection is oro-nasal, and the virus then circulates systemically to infect cells in many lymphoid tissues and the small intestine, and the virus is vulnerable to both mucosal and plasma antibodies during this process. Ability to infect hosts with low levels of maternal antibodies may be a selected property of these viruses (18, 41, 62, 85). In addition, although anti-viral antibodies are important for recovery from infection,

some viremia continues for a short period in the presence of the developing antibody response (44).

The interactions between viruses, host receptors and antibodies can be complex, even for the simple parvovirus capsids. The extensive overlap between the TfR and antibody binding sites results in many mutations in the capsid surface that affect the binding of both ligands simultaneously. The antibody-capsid interactions of these parvoviruses may share features with other virus-receptor-antibody interactions. The foot and mouth disease virus also shows overlap between the integrin binding sequence and antibody epitopes on the G-H loop of the virus, although the Arg-Gly-Asp binding sequence is quite small and may be conserved while the surrounding epitopes can vary (15, 82). In other cases the receptor binding and antigenic sites are largely distinct. Some picornaviruses bind their receptors through a lowered region of the capsids (canyon), while most of the antigenic sites are on raised regions (although some antibodies may be able to access the receptor site) (64, 74). For the influenza virus hemagglutinin the sialic acids bind in relatively conserved pockets while the antigenic sites are on surface regions which can readily accommodate variation (72, 73). In HIV the receptor binding sites on the gp120 are protected from antibody by a variety of strategies including overlapping carbohydrate structures and rapid variability, while the conserved chemokine receptor binding site is buried within the structure and not revealed until after CD4 binding (11, 33). Most viruses of vertebrates are under strong antibody selection and many different solutions are used to allow their success. Since these interactions are key to effective protective antiviral immunity, a better understanding of the processes involved would help in the design of better vaccines in the future.

2.6 Acknowledgements.

Gail Sullivan and Wendy Weichert provided excellent technical support, and Alex Maltsev helped with data analysis. Supported by grants AI 28385 and AI 33468 from the National Institutes of Health to C.R.P..

REFERENCES

1. **Agbandje, M., R. McKenna, M. G. Rossmann, M. L. Strassheim, and C. R. Parrish.** 1993. Structure determination of feline panleukopenia virus empty particles. Proteins **16:** 155-171.
2. **Bailey, J., J. N. Blankson, M. Wind-Rotolo, and R. F. Siliciano.** 2004. Mechanisms of HIV-1 escape from immune responses and antiretroviral drugs. Curr Opin Immunol **16:**470-6.
3. **Bruemmer, A., F. Scholari, M. Lopez-Ferber, J. F. Conway, and E. A. Hewat.** 2005. Structure of an insect parvovirus (Junonia coenia Densovirus) determined by cryo-electron microscopy. J Mol Biol **347:**791-801.
4. **Buonavoglia, C., V. Martella, A. Pratelli, M. Tempesta, A. Cavalli, D. Buonavoglia, G. Bozzo, G. Elia, N. Decaro, and L. Carmichael.** 2001. Evidence for evolution of canine parvovirus type 2 in Italy. J Gen Virol **82:**3021-5.
5. **Buonavoglia, D., A. Cavalli, A. Pratelli, V. Martella, G. Greco, M. Tempesta, and C. Buonavoglia.** 2000. Antigenic analysis of canine parvovirus strains isolated in Italy. New Microbiol **23:**93-6.
6. **Burton, D. R.** 2002. Antibodies, viruses and vaccines. Nat Rev Immunol **2:**706-13.
7. **Casal, J. I., J. P. Langeveld, E. Cortes, W. W. Schaaper, E. van Dijk, C. Vela, S. Kamstrup, and R. H. Meloen.** 1995. Peptide vaccine against canine parvovirus: identification of two neutralization subsites in the N terminus of VP2 and optimization of the amino acid sequence. J Virol **69:**7274-7277.
8. **Chang, S. F., J. Y. Sgro, and C. R. Parrish.** 1992. Multiple amino acids in the capsid structure of canine parvovirus coordinately determine the canine

host range and specific antigenic and hemagglutination properties. J Virol **66:**6858-6567.

9. **Chapman, M. S.** 1996. Structural refinement of the DNA-containing capsid of canine parvovirus using RSRef, a resolution-dependent stereochemically restrained real-space refinement method. Acta Crystallogr D Biol Crystallogr **52:**129-42.

10. **Che, Z., N. H. Olson, D. Leippe, W. M. Lee, A. G. Mosser, R. R. Rueckert, T. S. Baker, and T. J. Smith.** 1998. Antibody-mediated neutralization of human rhinovirus 14 explored by means of cryoelectron microscopy and X-ray crystallography of virus-Fab complexes. J Virol **72:**4610-22.

11. **Chen, B., E. M. Vogan, H. Gong, J. J. Skehel, D. C. Wiley, and S. C. Harrison.** 2005. Structure of an unliganded simian immunodeficiency virus gp120 core. Nature **433:**834-41.

12. **Cheng, Y., O. Zak, P. Aisen, S. C. Harrison, and T. Walz.** 2004. Structure of the human transferrin receptor-transferrin complex. Cell **116:**565-576.

13. **Costa, A. P., J. P. Leite, N. V. Labarthe, and R. C. Garcia.** 2005. Genomic typing of canine parvovirus circulating in the state of rio de janeiro, Brazil from 1995 to 2001 using polymerase chain reaction assay. Vet Res Commun **29:**735-43.

14. **Costello, F., N. Steenfos, K. T. Jensen, J. Christensen, E. Gottschalck, A. Holm, and B. Aasted.** 1999. Epitope mapping of Aleutian mink disease parvovirus virion protein VP1 and 2. Scand J Immunol **49:**347-54.

15. **Domingo, E., N. Verdaguer, W. F. Ochoa, C. M. Ruiz-Jarabo, N. Sevilla, E. Baranowski, M. G. Mateu, and I. Fita.** 1999. Biochemical and structural studies with neutralizing antibodies raised against foot-and-mouth disease virus. Virus Res **62:**169-175.

16. **Edwards, M. J., and N. J. Dimmock.** 2001. A haemagglutinin (HA1)-specific FAb neutralizes influenza A virus by inhibiting fusion activity. J Gen Virol **82:**1387-1395.

17. **Edwards, M. J., and N. J. Dimmock.** 2001. Hemagglutinin 1-specific immunoglobulin G and Fab molecules mediate postattachment neutralization of influenza A virus by inhibition of an early fusion event. J Virol **75:**10208-10218.

18. **Elia, G., A. Cavalli, F. Cirone, E. Lorusso, M. Camero, D. Buonavoglia, and M. Tempesta.** 2005. Antibody levels and protection to canine parvovirus type 2. J Vet Med B Infect Dis Vet Public Health **52:**320-2.

19. **Enns, C. A.** 2002. The transferrin receptor, p. 71-94. *In* D. M. Templeton (ed.), Molecular and cellular iron transport. Marcel Dekker, New York.

20. **Fuchs, H., G. Orberger, R. Tauber, and R. Gessner.** 1995. Direct calibration ELISA: a rapid method for the simplified determination of association constants of unlabeled biological molecules. J Immunol Methods **188:**197-208.

21. **Gao, G., M. R. Alvira, S. Somanathan, Y. Lu, L. H. Vandenberghe, J. J. Rux, R. Calcedo, J. Sanmiguel, Z. Abbas, and J. M. Wilson.** 2003. Adeno-associated viruses undergo substantial evolution in primates during natural infections. Proc Natl Acad Sci U S A **100:**6081-6.

22. **Giannetti, A. M., P. M. Snow, O. Zak, and P. J. Bjorkman.** 2003. Mechanism for multiple ligand recognition by the human transferrin receptor. PLoS Biol **1:**E51.

23. **Gomez-Puertas, P., F. Rodriguez, J. M. Oviedo, F. Ramiro-Ibanez, F. Ruiz-Gonzalvo, C. Alonso, and J. M. Escribano.** 1996. Neutralizing

antibodies to different proteins of African swine fever virus inhibit both virus attachment and internalization. J Virol **70:**5689-94.

24. **Govindasamy, L., K. Hueffer, C. R. Parrish, and M. Agbandje-McKenna.** 2003. Structures of host range-controlling regions of the capsids of canine and feline parvoviruses and mutants. J Virol **77:**12211-21.

25. **Hafenstein, S., M. G. Rossmann, L. M. Palermo, and C. R. Parrish.** 2006. unpublished results.

26. **Holguin, A., J. Hernandez, M. A. Martinez, M. G. Mateu, and E. Domingo.** 1997. Differential restrictions on antigenic variation among antigenic sites of foot-and-mouth disease virus in the absence of antibody selection. J Gen Virol **78 (Pt 3):**601-9.

27. **Hueffer, K., L. Govindasamy, M. Agbandje-McKenna, and C. R. Parrish.** 2003. Combinations of two capsid regions controlling canine host range determine canine transferrin receptor binding by canine and feline parvoviruses. J Virol **77:**10099-10105.

28. **Hueffer, K., L. M. Palermo, and C. R. Parrish.** 2004. Parvovirus infection of cells by using variants of the feline transferrin receptor altering clathrin-mediated endocytosis, membrane domain localization, and capsid-binding domains. J Virol **78:**5601-5611.

29. **Hueffer, K., J. S. Parker, W. S. Weichert, R. E. Geisel, J. Y. Sgro, and C. R. Parrish.** 2003. The natural host range shift and subsequent evolution of canine parvovirus resulted from virus-specific binding to the canine transferrin receptor. J. Virol. **77:**1718-1726.

30. **Kaufmann, B., A. A. Simpson, and M. G. Rossmann.** 2004. The structure of human parvovirus B19. Proc Natl Acad Sci U S A **101:**11628-33.

31. **Klasse, P. J., and Q. J. Sattentau.** 2002. Occupancy and mechanism in antibody-mediated neutralization of animal viruses. J Gen Virol **83:**2091-108.

32. **Knossow, M., M. Gaudier, A. Douglas, B. Barrere, T. Bizebard, C. Barbey, B. Gigant, and J. J. Skehel.** 2002. Mechanism of neutralization of influenza virus infectivity by antibodies. Virology **302:**294-8.

33. **Kwong, P. D., R. Wyatt, J. Robinson, R. W. Sweet, J. Sodroski, and W. A. Hendrickson.** 1998. Structure of an HIV gp120 envelope glycoprotein in complex with the CD4 receptor and a neutralizing human antibody. Nature **393:**648-59.

34. **Langeveld, J. P., J. I. Casal, E. Cortes, G. van de Wetering, R. S. Boshuizen, W. M. Schaaper, K. Dalsgaard, and R. H. Meloen.** 1994. Effective induction of neutralizing antibodies with the amino terminus of VP2 of canine parvovirus as a synthetic peptide. Vaccine **12:**1473-1480.

35. **Langeveld, J. P., J. I. Casal, C. Vela, K. Dalsgaard, S. H. Smale, W. C. Puijk, and R. H. Meloen.** 1993. B-cell epitopes of canine parvovirus: distribution on the primary structure and exposure on the viral surface. J Virol **67:**765-772.

36. **Lawrence, C. M., S. Ray, M. Babyonyshev, R. Galluser, D. W. Borhani, and S. C. Harrison.** 1999. Crystal structure of the ectodomain of human transferrin receptor. Science **286:**779-782.

37. **Ledford, R. M., N. R. Patel, T. M. Demenczuk, A. Watanyar, T. Herbertz, M. S. Collett, and D. C. Pevear.** 2004. VP1 sequencing of all human rhinovirus serotypes: insights into genus phylogeny and susceptibility to antiviral capsid-binding compounds. J Virol **78:**3663-74.

38. **Liebermann, H., R. Mentel, U. Bauer, P. Pring-Akerblom, R. Dolling, S. Modrow, and W. Seidel.** 1998. Receptor binding sites and antigenic epitopes on the fiber knob of human adenovirus serotype 3. J Virol **72:**9121-30.

39. **Lopez de Turiso, J. A., E. Cortez, A. Ranz, J. Garcia, A. Sanz, C. Vela, and J. I. Casal.** 1991. Fine mapping of canine parvovirus B cell epitopes. J Gen Virol **72:**2445-2456.

40. **Ludert, J. E., M. C. Ruiz, C. Hidalgo, and F. Liprandi.** 2002. Antibodies to rotavirus outer capsid glycoprotein VP7 neutralize infectivity by inhibiting virion decapsidation. J Virol **76:**6643-51.

41. **Martella, V., A. Cavalli, N. Decaro, G. Elia, C. Desario, M. Campolo, G. Bozzo, E. Tarsitano, and C. Buonavoglia.** 2005. Immunogenicity of an intranasally administered modified live canine parvovirus type 2b vaccine in pups with maternally derived antibodies. Clin Diagn Lab Immunol **12:**1243-5.

42. **Martella, V., A. Cavalli, A. Pratelli, G. Bozzo, M. Camero, D. Buonavoglia, D. Narcisi, M. Tempesta, and C. Buonavoglia.** 2004. A canine parvovirus mutant is spreading in Italy. J Clin Microbiol **42:**1333-6.

43. **McKenna, R., N. H. Olson, P. R. Chipman, T. S. Baker, T. F. Booth, J. Christensen, B. Aasted, J. M. Fox, M. E. Bloom, J. B. Wolfinbarger, and M. Agbandje-McKenna.** 1999. Three-dimensional structure of Aleutian mink disease parvovirus: implications for disease pathogenicity. J Virol **73:**6882-91.

44. **Meunier, P. C., B. J. Cooper, M. J. Appel, and D. O. Slauson.** 1985. Pathogenesis of canine parvovirus enteritis: the importance of viremia. Vet Pathol **22:**60-71.

45. **Mochizuki, M., R. Harasawa, and H. Nakatani.** 1993. Antigenic and genomic variabilities among recently prevalent parvoviruses of canine and feline origin in Japan. Vet Microbiol **38:**1-10.

46. **Nakamura, K., M. Sakamoto, Y. Ikeda, E. Sato, K. Kawakami, T. Miyazawa, Y. Tohya, E. Takahashi, T. Mikami, and M. Mochizuki.** 2001. Pathogenic potential of canine parvovirus types 2a and 2c in domestic cats. Clin Diagn Lab Immunol **8:**663-668.

47. **Nakamura, M., K. Nakamura, T. Miyazawa, Y. Tohya, M. Mochizuki, and H. Akashi.** 2003. Monoclonal antibodies that distinguish antigenic variants of canine parvovirus. Clin Diagn Lab Immunol **10:**1085-9.

48. **Nakamura, M., Y. Tohya, T. Miyazawa, M. Mochizuki, H. T. Phung, N. H. Nguyen, L. M. Huynh, L. T. Nguyen, P. N. Nguyen, P. V. Nguyen, N. P. Nguyen, and H. Akashi.** 2004. A novel antigenic variant of canine parvovirus from a Vietnamese dog. Arch Virol **149:**2261-9.

49. **Nybakken, G. E., T. Oliphant, S. Johnson, S. Burke, M. S. Diamond, and D. H. Fremont.** 2005. Structural basis of West Nile virus neutralization by a therapeutic antibody. Nature **437:**764-9.

50. **Osiowy, C., and R. Anderson.** 1995. Neutralization of respiratory syncytial virus after cell attachment. J Virol **69:**1271-4.

51. **Padron, E., V. Bowman, N. Kaludov, L. Govindasamy, H. Levy, P. Nick, R. McKenna, N. Muzyczka, J. A. Chiorini, T. S. Baker, and M. Agbandje-McKenna.** 2005. Structure of adeno-associated virus type 4. J Virol **79:**5047-58.

52. **Palermo, L. M., S. L. Hafenstein, and C. R. Parrish.** 2006. Purified feline and canine transferrin receptors reveal complex interactions with the capsids of canine and feline parvoviruses that correspond to their host ranges. Journal of virology **80:**8482-92.

53. **Palermo, L. M., K. Hueffer, and C. R. Parrish.** 2003. Residues in the apical domain of the feline and canine transferrin receptors control host-specific

binding and cell infection of canine and feline parvoviruses. J Virol **77:**8915-8923.

54. **Parker, J. S. L., W. J. Murphy, D. Wang, S. J. O'Brien, and C. R. Parrish.** 2001. Canine and feline parvoviruses can use human or feline transferrin receptors to bind, enter, and infect cells. J. Virol. **75:**3896-3902.

55. **Parrish, C. R.** 1991. Mapping specific functions in the capsid structure of canine parvovirus and feline panleukopenia virus using infectious plasmid clones. Virology **183:**195-205.

56. **Parrish, C. R., C. Aquadro, M. L. Strassheim, J. F. Evermann, J.-Y. Sgro, and H. Mohammed.** 1991. Rapid antigenic-type replacement and DNA sequence evolution of canine parvovirus. J Virol **65:**6544-6552.

57. **Parrish, C. R., and L. E. Carmichael.** 1983. Antigenic structure and variation of canine parvovirus type-2, feline panleukopenia virus, and mink enteritis virus. Virology **129:**401-414.

58. **Parrish, C. R., Carmichael, L.E., Antczak, D.F.** 1982. Antigenic relationships between canine parvovirus type-2, feline panleukopenia virus and mink enteritis virus using conventional antisera and monoclonal antibodies. Arch.Virol. **72: 267-278**.

59. **Parrish, C. R., J. R. Gorham, T. M. Schwartz, and L. E. Carmichael.** 1984. Characterisation of antigenic variation among mink enteritis virus isolates. Am. J. Vet. Res. **45:**2591-2599.

60. **Parrish, C. R., P. Have, W. J. Foreyt, J. F. Evermann, M. Senda, and L. E. Carmichael.** 1988. The global spread and replacement of canine parvovirus strains. J Gen Virol **69 (Pt 5):**1111-6.

61. **Parrish, C. R., P. H. O'Connell, J. F. Evermann, and L. E. Carmichael.** 1985. Natural variation of canine parvovirus. Science **230:**1046-1048.

62. **Pollock, R. V. H., and L. E. Carmichael.** 1982. Maternally derived immunity to canine parvovirus infection: transfer, decline and interference with vaccination. J Am Vet Med Assoc **180:**37-42.

63. **Rimmelzwaan, G. F., J. Carlson, F. G. UytdeHaag, and A. D. Osterhaus.** 1990. A synthetic peptide derived from the amino acid sequence of canine parvovirus structural proteins which defines a B cell epitope and elicits antiviral antibody in BALB c mice. J Gen Virol **71:**2741-2745.

64. **Rossmann, M. G., Y. He, and R. J. Kuhn.** 2002. Picornavirus-receptor interactions. Trends Microbiol **10:**324-31.

65. **Rota, J. S., K. B. Hummel, P. A. Rota, and W. J. Bellini.** 1992. Genetic variability of the glycoprotein genes of current wild-type measles isolates. Virology **188:**135-42.

66. **Rota, J. S., Z. D. Wang, P. A. Rota, and W. J. Bellini.** 1994. Comparison of sequences of the H, F, and N coding genes of measles virus vaccine strains. Virus Res **31:**317-30.

67. **Sagazio, P., M. Tempesta, D. Buonavoglia, F. Cirone, and C. Buonavoglia.** 1998. Antigenic characterization of canine parvovirus strains isolated in Italy. J Virol Methods **73:**197-200.

68. **Saphire, E. O., P. W. Parren, R. Pantophlet, M. B. Zwick, G. M. Morris, P. M. Rudd, R. A. Dwek, R. L. Stanfield, D. R. Burton, and I. A. Wilson.** 2001. Crystal structure of a neutralizing human IGG against HIV-1: a template for vaccine design. Science **293:**1155-9.

69. **Sheshberadaran, H., and E. Norrby.** 1986. Characterization of epitopes on the measles virus hemagglutinin. Virology **152:**58-65.

70. **Sheshberadaran, H., E. Norrby, and K. W. Rammohan.** 1985. Monoclonal antibodies against five structural components of measles virus. II.

Characterization of five cell lines persistently infected with measles virus. Arch Virol **83:**251-68.

71. **Simpson, A. A., P. R. Chipman, T. S. Baker, P. Tijssen, and M. G. Rossmann.** 1998. The structure of an insect parvovirus (Galleria mellonella densovirus) at 3.7 A resolution. Structure **6:**1355-67.

72. **Skehel, J. J., and D. C. Wiley.** 2000. Receptor binding and membrane fusion in virus entry: the influenza hemagglutinin. Annu Rev Biochem **69:**531-569.

73. **Smith, D. J., A. S. Lapedes, J. C. de Jong, T. M. Bestebroer, G. F. Rimmelzwaan, A. D. Osterhaus, and R. A. Fouchier.** 2004. Mapping the antigenic and genetic evolution of influenza virus. Science **305:**371-376.

74. **Smith, T. J., E. S. Chase, T. J. Schmidt, N. H. Olson, and T. S. Baker.** 1996. Neutralizing antibody to human rhinovirus 14 penetrates the receptor-binding canyon. Nature **383:**350-4.

75. **Steinel, A., E. H. Venter, M. Van Vuuren, C. R. Parrish, and U. Truyen.** 1998. Antigenic and genetic analysis of canine parvoviruses in southern Africa. Onderstepoort J Vet Res **65:**239-42.

76. **Strassheim, L. S., A. Gruenberg, P. Veijalainen, J.-Y. Sgro, and C. R. Parrish.** 1994. Two dominant neutralizing antigenic determinants of canine parvovirus are found on the threefold spike of the virus capsid. Virology **198:**175-184.

77. **Truyen, U., J. F. Evermann, E. Vieler, and C. R. Parrish.** 1996. Evolution of canine parvovirus involved loss and gain of feline host range. Virology **215:**186-189.

78. **Truyen, U., A. Gruenberg, S. F. Chang, B. Obermaier, P. Veijalainen, and C. R. Parrish.** 1995. Evolution of the feline-subgroup parvoviruses and the control of canine host range in vivo. J. Virol. **69:**4702-4710.

79. **Truyen, U., and C. R. Parrish.** 1992. Canine and feline host ranges of canine parvovirus and feline panleukopenia virus: distinct host cell tropisms of each virus in vitro and in vivo. J Virol **66:**5399-5408.

80. **Tsao, J., M. S. Chapman, M. Agbandje, W. Keller, K. Smith, H. Wu, M. Luo, T. J. Smith, M. G. Rossmann, R. W. Compans, and C. R. Parrish.** 1991. The three-dimensional structure of canine parvovirus and its functional implications. Science **251:**1456-1464.

81. **Varghese, R., Y. Mikyas, P. L. Stewart, and R. Ralston.** 2004. Postentry neutralization of adenovirus type 5 by an antihexon antibody. J Virol **78:**12320-32.

82. **Verdaguer, N., G. Schoehn, W. F. Ochoa, I. Fita, S. Brookes, A. King, E. Domingo, M. G. Mateu, D. Stuart, and E. A. Hewat.** 1999. Flexibility of the major antigenic loop of foot-and-mouth disease virus bound to a Fab fragment of a neutralising antibody: structure and neutralisation. Virology **255:**260-268.

83. **Vossen, M. T., E. M. Westerhout, C. Soderberg-Naucler, and E. J. Wiertz.** 2002. Viral immune evasion: a masterpiece of evolution. Immunogenetics **54:**527-42.

84. **Walters, R. W., M. Agbandje-McKenna, V. D. Bowman, T. O. Moninger, N. H. Olson, M. Seiler, J. A. Chiorini, T. S. Baker, and J. Zabner.** 2004. Structure of adeno-associated virus serotype 5. J Virol **78:**3361-71.

85. **Waner, T., A. Naveh, I. Wudovsky, and L. E. Carmichael.** 1996. Assessment of maternal antibody decay and response to canine parvovirus vaccination using a clinic-based enzyme-linked immunosorbent assay. J Vet Diagn Invest **8:**427-432.

86. **Weichert, W. S., J. S. Parker, A. T. Wahid, S. F. Chang, E. Meier, and C. R. Parrish.** 1998. Assaying for structural variation in the parvovirus capsid and its role in infection. Virology **250:**106-17.

87. **West, A. P., Jr., A. M. Giannetti, A. B. Herr, M. J. Bennett, J. S. Nangiana, J. R. Pierce, L. P. Weiner, P. M. Snow, and P. J. Bjorkman.** 2001. Mutational analysis of the transferrin receptor reveals overlapping HFE and transferrin binding sites. J Mol Biol **313:**385-97.

88. **Wikoff, W. R., G. Wang, C. R. Parrish, R. H. Cheng, M. L. Strassheim, T. S. Baker, and M. G. Rossmann.** 1994. The structure of a neutralized virus: canine parvovirus complexed with neutralizing antibody fragment. Structure **2:**595-607.

89. **Wobus, C. E., B. Hugle-Dorr, A. Girod, G. Petersen, M. Hallek, and J. A. Kleinschmidt.** 2000. Monoclonal antibodies against the adeno-associated virus type 2 (AAV-2) capsid: epitope mapping and identification of capsid domains involved in AAV-2-cell interaction and neutralization of AAV-2 infection. J Virol **74:**9281-93.

90. **Xie, Q., W. Bu, S. Bhatia, J. Hare, T. Somasundaram, A. Azzi, and M. S. Chapman.** 2002. The atomic structure of adeno-associated virus (AAV-2), a vector for human gene therapy. Proc Natl Acad Sci U S A **99:**10405-10.

91. **Xie, Q., and M. S. Chapman.** 1996. Canine parvovirus capsid structure, analyzed at 2.9 Å resolution. J Mol Biol **264:**497-520.

92. **Yuan, W., and C. R. Parrish.** 2000. Comparison of two single-chain antibodies that neutralize Canine Parvovirus: analysis of an antibody-combining site and mechanisms of neutralization. Virology **269:**471-480.

CHAPTER THREE

Structure analysis of eight antibodies with variable neutralizing abilities bound to canine and feline parvoviruses.

Christian Nelson, Susan Hafenstein, Tsao Sun, Valorie Bowman, Colin Parrish, and Michael Rossmann.

[Susan Hafenstein and her collaborators were responsible for the electron microscopy and image reconstructions, and Susan helped to write parts of the materials and methods and results. I was responsible for purification of monoclonal antibodies and production of Fabs and shipment of materials, and sequencing of the variable domains of the light and heavy chains of these antibodies]

3.1 Abstract.

The host antibody response is important for protection from and clearance of viral infection, yet the structures on nonenveloped viral capsids that elicit this antibody response are not well understood. We have examined by cryo-electron microscopy and image reconstruction the binding sites of five mouse and three rat IgG Fab fragments on the surface of canine parvovirus and feline panleukopenia virus capsids. We find that these antibodies cluster to two main sites on the surface of the virus, but that each antibody has a unique interaction with the virus. Many of those Fab footprints overlap with the binding site of transferrin receptor, the cellular receptor for these viruses. This suggests that competition for receptor binding may be a mechanism of neutralization for these antibodies, however five Fabs do not neutralize infectivity despite binding the capsid with approximately full occupancy. Structural differences between the Fabs that were neutralizing and those that were non-neutralizing were not readily apparent. These footprints also cover ~70% of the surface accessible areas of the capsid, and suggest that the two antigenic regions of the capsid may overlap and be larger than previously suggested.

3.2 Introduction.

Antibodies are specialized molecules that bind specific epitopes on viral proteins or other antigenic molecules, often with high affinity. An understanding of the antigenic structures of viral proteins is critical for the rationale design of new anti-viral vaccines and of gene therapy vectors, as well as furthering our understanding of virus neutralization (3, 27). During a viral infection the proteins of the virus will bind to the surface immunoglobulin on the surface of B cells. In a naive animal those would be surface IgM, and the crosslinking of the receptors by the multimeric viral epitopes may stimulate a rapid response in the B cells, and the production of IgM.

Upon continuing antigen exposure, and in the presence of T cell help, the cells will undergo class switching and selection, along with somatic hypermutation of antibody variable domain genes. These mutations during B cell development selects for high affinity antibodies; however, the neutralizing ability of the antibody is not considered during this selection process (22). Therefore, an understanding of viral epitopes and host antibody responses may aid the production of vaccines with altered epitopes which generate highly neutralizing antibodies (10). Alternatively, for gene therapy applications, the benefit would come from the preparation of less immunogenic vectors that would allow re-administration of vector without mounting a large immune response (2, 14, 17, 29, 48).

For mapping antigenic sites on nonenveloped viruses, much work has been done on the human rhinovirus 14 (HRV14) (reviewed in (32-34)). A combination of structural and biochemical data demonstrated that there were four main antigenic sites on the virus, termed neutralizing immunogenic sites (NIms) (30, 31). Cryoelectron microscopy (cryo-EM) and X-ray diffraction yielded important insight into epitopes that bound the antibodies and that led to neutralization. Cryo-EM reconstructions on high and low neutralizing antibodies revealed that electrostatic interactions contributed most to epitope selection, and many more residues were important for antibody binding than those seen from escape mutation analysis. Interestingly, the neutralizing and non-neutralizing Fabs bound to very similar areas of the capsid, and shared several charged residues in their epitopes, but differ in their orientation (35-37). It was also shown that the orientation was determined by the charge interactions between the virus and antibody, and that the CDR loops of the antibody deform and intercalate readily into deep crevasses on the surface of the virus.

Although many mechanisms of neutralization have been proposed, recent studies have suggested antibodies neutralize viruses by a simple occupancy model (3,

4, 33). This model suggests that the requirements for effective neutralization include antibody binding to the virus that prevents receptor binding, and the antibodies must bind the virus with high affinity. The need for high affinity fits well with the maturation process of antibodies, and the mass of an intact IgG or IgM appears well-suited to compete for receptor binding, even if the antibody binds elsewhere on the capsid. In HRV14, one antigenic site lies further away from the receptor binding site but is still able to neutralize the virus (6, 7) It has been suggested that since a single IgG is equal to the radius of an HRV14 virion (150 Å), IgG binding to one location could sterically block binding to sites elsewhere on the capsid (33). There is however, no definitive consensus on how neutralization of viruses is achieved.

Canine parvovirus is a nonenveloped virus with a 25 nm icosahedral capsid (40). The capsid is composed of sixty copies of two isoforms of the same capsid protein, VP1 or VP2. These proteins are identical, except that VP1 contains an additional 143 residues at its N-terminus. The capsid structure has been solved to 2.9 Å resolution, and the core structural element is β-barrel that is similar to many other nonenveloped viruses (40, 46). The surface structure of this virus is composed of elaborate loops that connect the strands of this β-barrel. The longest of these loops, the GH loop, forms a large raised region on the capsid over the 3-fold axis of symmetry and is referred to as the 3-fold spike. This region of the capsid contains residues that are important for receptor and antibody binding (11, 38).

The major antigenic sites on CPV have been mapped by escape mutant analysis, and demonstrated that most amino acid substitutions clustered to two main sites on the surface of the capsid that were called sites A and B. Site A involved residues close to the 3-fold axis of symmetry around residues 93, 222, and 224. Site B clustered closer to the 2-fold axis and involved residues 299, 300, and 302 (38). One site B antibody, MAb 8, has been directly visualized binding to CPV by cryo-EM and

image reconstructions of capsid-Fab complexes, and a pseudo atomic resolution co-structure was generated by fitting of the solved CPV capsid and a homology model of the Fab structure (45). The epitope defined by the antibody footprint largely confirmed the results from the escape mutation analysis of site B antibodies. The N-terminus of VP2, residues 1-23, as well as other residues on the surface of the capsid (residues 91, 172, 283, 297, and 498, 549, 573) have been reported as a B-cell epitope (16, 19).

CPV binds and uses the transferrin receptor (TfR) to infect cells. TfR is a type II membrane protein that is present as a homodimer on the surface of cells (8). CPV interacts with residues in the apical domain of TfR, and residues important for the specific binding of the canine TfR have been mapped by natural variation and by site directed mutagenesis and include residues 93, 300, 305, and 323 (11, 13, 23). These residues are present within both the A and B antigenic sites, and those are separated by 20-30 Å on the surface of the capsid (40). A soluble form of the feline TfR has been generated by recombinant baculovirus expression and the TfR-CPV complex visualized by cryo-EM and image reconstructions (9, 12). That reconstruction verified the footprint of TfR binding on the surface of the virus, and showed that TfR makes extensive interactions with the viral capsid, and overlaps both sites A and site B.

The eight antibodies studied here have been previously examined for their ability to neutralize CPV and FPV (21). These Fabs fragments all bound to CPV with similar relative affinities, as determined by solid phase binding assays. All of the IgGs of these antibodies were able to neutralize CPV, but the Fabs were divided into neutralizing and non-neutralizing groups. The neutralizing Fabs neutralized virus at <100 Fabs per capsid and directly competed with TfR for binding to CPV at lower Fab to capsid ratios than the non-neutralizing Fabs. The IgGs of these antibodies all were neutralizing, and those may have inhibited infectivity by aggregating particles through

the cross-linking of the bivalent antibody, and perhaps by the larger mass of the IgG compared to the Fab; two of the IgGs were previously shown to crosslink and aggregate capsids (47).

In this study we present the structures for eight Fab-CPV complexes by cryo-EM and image reconstruction. The binding sites of the antibodies confirmed the general features revealed by escape mutant analysis, and showed no major changes in the capsids after binding, at least at the resolution of these reconstructions. This work also shows that most of the surface exposed regions of the capsid appear to serve as a functional epitope.

3.3 Materials and methods.

Virus production and purification. Virus production and purification were performed as previously described (1). Briefly, inoculums were generated from transfection of Norden laboratory feline kidney cells (NLFK) with an infectious clone of CPV-2 or FPV (24). NLFK cells were maintained in a 1:1 mixture of McCoy's 5A and Liebovitz L15 media with 5% fetal bovine serum. These inoculums were amplified by several passages in NLFK cells and then used to infect roller bottles. At 48 hpi, roller bottles were frozen and thawed three times and the cellular debris was scraped off of the walls of the bottles. Capsids were precipitated with polyethylene glycol 8000 (PEG), and full and empty capsids were purified by banding on 10 to 40% sucrose gradients. Capsids were passed through a Sepharose CL-4B column in 50 mM PIPES.NaOH (pH 7.6), 150mM NaCl for further purification.

Monoclonal antibody production, purification, and generation of Fabs. The production and characterization of the hybridomas used here have previously been described (25, 26). MAbs and Fabs were generated according to previously published results (21). Briefly, hybridomas were grown in Dulbecco's minimal essential

medium, non-essential amino acids, and 5% FBS. These cultures were expanded and placed into gas permeable cell culture bags (Nexell, Irving, CA). After culture the cellular debris was removed by centrifugation, the supernatant was 0.22 μm filtered and dialyzed into phosphate buffer in a 10 kDa cut-off membrane spiral dialysis cassette (Millipore, Billeria, MA). MAbs were then purified from this supernatant by Protein G affinity chromatography on an AKTA FPLC (GE Healthcare, Piscataway, NJ). Fabs were generated from these purified Mabs as according to manufactures recommended protocols (Pierce, Rockford, IL). Briefly, the protein was digested with papain, the Fc fragment removed by chromatography on protein A, and the monomeric Fab was isolated by chromatography on Sepahdex G100.

Sequencing of variable domains of antibodies. mRNA from hybridomas were purified using the RNeasy purification kit (Qiagen, Valencia, CA). This mRNA was either further processed immediately, or aliquoted and stored at -80°C until used. cDNA and amplified products were generated using the one-step RT-PCR kit (Invitrogen, Carlsbad, CA). Primers were designed for variable domain amplification using mouse IgG database (MRC Center for protein engineering, http://www.mrc-cpe.cam.ac.uk). Rat IgG primers were designed from degenerate primers of published sequences. PCR products were then cloned into pGEM T-easy (Promega, Madison, WI). Plasmid inserts were then sequenced using T7 or SP6 primers. The variable sequences of MAb 8 and MAb 14 have been previously described, and these sequences were re-determined in this study (45, 47). The heavy chain of antibody 6 proved refractory to sequencing and was not determined.

Data collection and cryo-EM reconstruction. Purified Fab molecules were incubated with virus at room temperature for 1 h at a ratio of four Fab molecules per potential binding site on the virus (240:1). Small aliquots of this mixture were applied to carbon-coated grids and frozen in liquid ethane at -186°C. Electron micrographs

were recorded on Kodak SO-163 film by using a Phillips CM300 FEG microscope. Micrographs were digitized with a Zeiss PHODIS microdensitometer at 7-micron intervals. The scans were averaged in boxes of 2 × 2 pixels. The final averaged pixel size was 3.11 Å. Particles were selected and corrected for contrast transfer function of the microscope using the program RobEM (http://cryo-EM.ucsd.edu/programs.shtm). The EM reconstruction processes were performed using icosahedral averaging with the programs EMPFT and EM3DR (http://bilbo.bio.purdue.edu/~baker/programs/programs.html). The cryo-EM density of native canine parvovirus was used as an initial starting structure. The final resolution was estimated by using maps of the reconstructed cryo-EM density representing the viral capsid between radii 70 and 140 Å and then determining where the Fourier shell correlation fell below 0.5 using the CUTPIFMAP, FFT, and EMRESOL programs written by Chuan Xiao (http://bilbo.bio.purdue.edu/~viruswww/Rossmann _home/river_programs/). The same cryo-EM reconstruction procedure was used for each complex and for a reconstruction of the native virus.

Crystallization of Fab 14 and structural solution. Fab14 was crystallized in 25% PEG 5K and 0.1 M HEPES (pH 7.5). It was in space group C2, with the unit cell parameters a = 168.604, b= 39.885, c= 70.745, and α = 94.58°, with one molecule (one heavy chain and one light chain fragment) per asymmetrical unit. Molecular replacement using 12E8 structure (Protein Data Bank (PDB) 12E8) as a search model found one solution with R factor of 0.497 and a correlation coefficient of 0.425. Further rigid body refinement improved the R factor to 0.473. The Fab14 structure was refined at 2.5Å, with $R_{working}$ factor of 0.232, and R_{free} factor of 0.278.

Structure and homology models for Fab. For each Fab, the amino acid sequence corresponding to the variable domain (VL and VH) was submitted to Web

Antibody Modeling (http://antibody.bath.ac.uk/) in order to obtain a 3-D homology model. The resulting 3-D model was substituted for the variable domain of a mouse antibody fragment (1AIH) to create a homology model.

Difference map and fitting the Fab structure into the cryo-EM densities. The program EMfit was used to calibrate the exact magnification of each of the cryo-EM reconstructions of virus complexed with Fab by comparing it with a map derived from the X-ray crystallographically determined coordinates of CPV or FPV (PDB accession numbers 1C8D and 1FPV, respectively). A difference map was calculated for each virus-Fab complex by setting to zero the density within a radius of 3Å surrounding each atom in the virus X-ray structure. The crystal structure of Fab 14, or a homology model of Fab was fitted into the difference map and each fitting was refined using the program EMfit (http://bilbo.bio.purdue.edu/~viruswww/Rossmann_home/softwares/emfit.php). For Fab 6, the weighting factor for steric collisions was set to 0 in order to refine the fit. Residues in the virus-Fab interface were identified as those in CPV or FPV that had any atoms less than 4.0Å from any atom in the fitted Fab structure. The buried surface area was calculated using CCP4 programs *areaimol* and *surface* (http://www.ccp4.ac.uk/html/areaimol.html).

3.4 Results.

Cryo-EM structures and fitting of Fab structures into the cryo-EM density to determine the interactions. Cryo-EM reconstructions were determined for complexes between the virus capsids and each of 8 different Fabs generated from MAbs (Figure 3.1)(Table 3.1). FPV was used for all reconstructions, except for Fab 14, which only binds to CPV (25). For seven of the reconstructions, the cryo-EM density corresponding to Fab was approximately equal in magnitude to that of the

Figure 3.1.

Cryo-EM and image reconstructions of eight monoclonal antibodies against FPV and CPV. FPV was used for all reconstructions, except for Fab14, which only binds CPV. For each antibody, the cryo-EM reconstruction is shown on the top and the antibody footprint on the asymmetric unit is shown on the bottom. For the footprint, the capsid residues involved in binding are highlighted and outlined in black. Site A antibodies are shown in red, and site B antibodies are shown in blue.

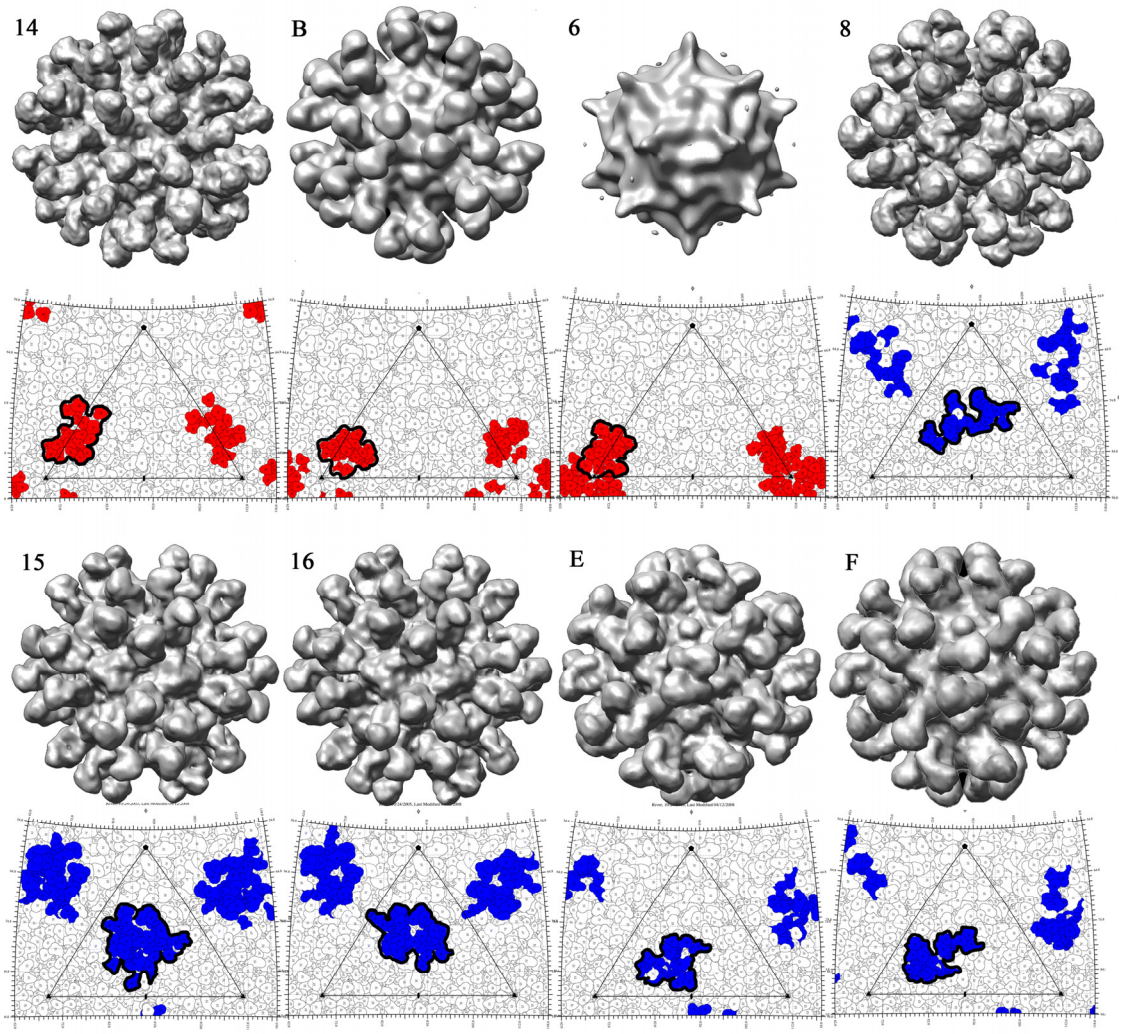
14
B
6
8
15
16
E
F

Table 3.1.

Monoclonal antibodies used to generate FAb for the structural studies.

Antibody	**Source**	**Epitope**	**Specificity**
14	Mouse	**A**	CPV only
B	Rat	**A**	CPV and FPV
8	Mouse	**A**	CPV and FPV
15	Mouse	**B**	CPV and FPV
16	Mouse	**B**	CPV and FPV
E	Rat	**B**	CPV and FPV
F	Rat	**B**	CPV and FPV

virion capsid, indicating that most of the 60 possible Fab binding sites was occupied. For the complex of Fab 6 and FPV a lower Fab density was seen, as the Fab bound very close to the threefold axis of symmetry and steric hindrances between the bound Fabs allowed only 1 Fab to bind per 3-fold axis. The resolutions of the reconstructions varied from 8 to 18Å, correlating to the number of particles used for each reconstruction.

In order to more accurately determine antibody footprints on the virus, pseudoatomic structures were generated. Using the known X-ray crystal structure of CPV or FPV (1C8D and 1FPV respectively) the density corresponding to virus was removed from each cryo-EM map (see methods). This provided a Fab difference density map to fit the Fab structures into. Since only the X-ray structure of Fab 14. was solved, homology models for the remaining 7 antibodies were built, based on the sequences of the variable domains (see materials and methods). To verify the usefulness of these homology models, the structure of the homology model of Fab 14 obtained from the variable domain sequences was compared to the crystal structure of Fab 14. These were both seen to be in good general agreement (data not shown). The placement of each homology model into the electron density difference map was refined using EMfit. No visible elbow angle change was noticed between the EM structure and the crystal structure of the fitted Fab 14.

The structure of CPV (1C8D) was fitted into the corresponding virus cryo-EM density by superimposing the icosahedral symmetry elements. Antibody footprints were then assigned based on proximity of atoms on the surface of the virus and Fabs, where atoms within 4.0 Å of each other were considered interacting (Figure 3.1). The buried surface areas for these Fabs ranged from 700-900$Å^2$. A mentioned above, for the Fab 6 and FPV complex steric interference resulted in only one Fab binding per each threefold-spike, so that only 20 Fabs were bound overall.

In the reconstructions of complexes with Fab 14, B, 8, 15 and 16, the Fab structure extends away from the surface of the virus with the long axes in a radial direction (Figure 3.1). The Fab portion of an entire IgG structure was fitted into each reconstruction to assess whether bivalent binding was possible across the icosahedral two fold axes, but in each case the Fab was oriented in such a way that bivalent binding is not possible. However, the fitting of full-length IgG showed there was sufficient length to the IgG flexible loops connecting the two Fab arms to allow crosslinking of particles. This is consistent with previously published reports for antibodies 14 and 8, which showed crosslinking of viral particles (47). For Fab E and F, the Fab structure is less upright, leaning into the surface of the capsid, making contact between heavy chain framework residues and the virus surface. Thus the Fab is oriented such that the long axes extend at lower angle relative to the surface of the virus, so each Fab blocks access to another region of the capsid surface that is not actually within the footprint of that Fab.

Characterization of the antigenic surface of the virus. Previously published reports identified two main antigenic sites on the virus, by escape mutational analysis. Site A mapped close to the 3-fold axis of symmetry and involved residues 93, 222, and 224, while Site B was further down the spike and involved residues 299, 300, and 302. To compare how accurately the escape mutant analysis predicted the actual antibody footprints, the shared areas of each antibody were displayed on the asymmetric unit (Figure 3.2). These footprints were found to be in good general agreement with the escape mutants, and also identified several more residues in the shared antibody footprint. For site A, these include residues 93, 222, 224, 225, 323, 423, 425-428, while site B had residues 298-302, and 387.

Nature of antigenic sites. The footprints of the antibodies covered a total of ~70% of the capsid surface (Figure 3.3). The combined footprint can also be

Figure 3.2.

The shared binding domains of site A and B antibodies, displayed on one asymmetric unit. Site A is colored in blue and site B is colored in red.

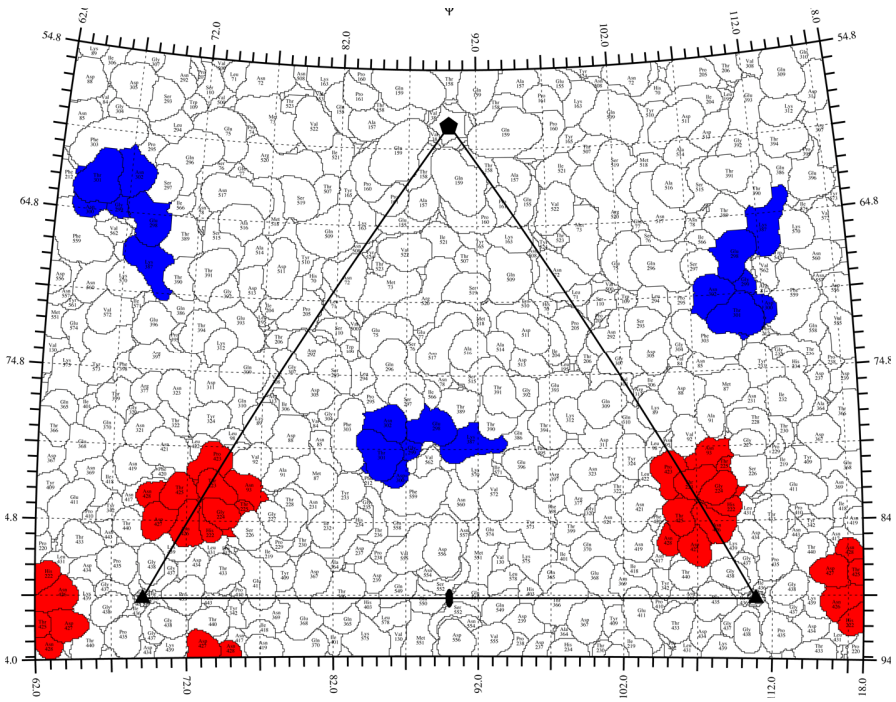
54.8
64.8
74.8
4.8
4.0
72.0
82.0
92.0
102.0
112.0
54.8
64.8
74.8
84
94
72.0
82.0
92.0
102.0
112.0
18.0

Figure 3.3.

The combined binding domain of A and B site antibodies displayed on one asymmetric unit. Site A antibodies are displayed in red, and site B are displayed in blue.

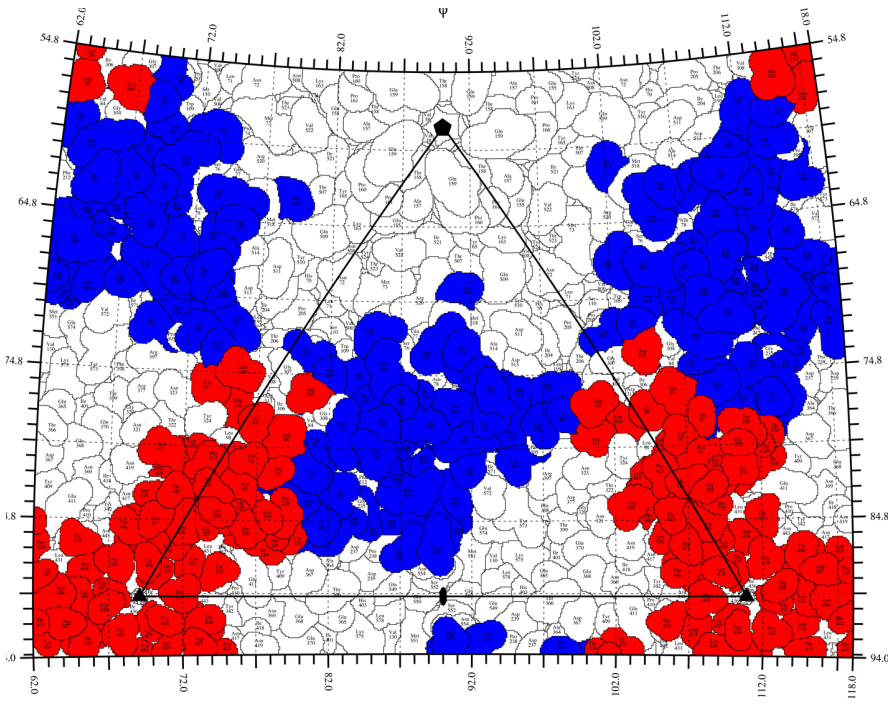
Ψ
54.8
64.8
74.8
84.8
94.0
62.0
72.0
82.0
92.0
102.0
112.0
118.0

displayed according to a radial density map (Figure 3.4). These footprints were examined for their properties, including surface charge, hydrophobicity and hydrophilicity. Amino acid identity of entire CPV surface included 42% polar, 27% charged, 32% hydrophobic amino acids; within the footprints of the B-site binding Fab the exposed residues were 52% polar, 23% charged, 24% hydrophobic; within the A site they were 46% polar, 20% charged, 34% hydrophobic.

3.5 Discussion.

In this study we present the complex interactions of eight antibody Fab fragments with FPV or CPV. We show that each of these eight Fab fragments make a unique interaction with the viral surface, but that there is clustering of these footprints to specific parts of the capsid. Previously, escape mutation analysis has shown that binding of these antibodies are controlled by a specific set of residues on the surface of the virus (38). Site A was shown to be on the three-fold spike and binding of antibodies to this region was controlled by residues 93, 222, and 224.

All of the site A antibodies share these residues in their combined footprint, as well as residues 225, 323, 423, 425-428 (Figure 3.2). Site B mapped further from the 3-fold spike and binding to this region was controlled by residues 299, 300, and 302. The combined site B antibody footprint contained these residues as well as 298, 301, 302, and 387 (Figure 3.2). It is not known whether all of these shared residues contribute to the binding of these antibodies, or are included due to their close proximity to critical residues. Also possible is that mutation of these additional residues would result in non-viable viruses that would not be amplified during escape mutant analysis.

Figure 3.4.

The combined outline of the antibody footprints displayed on a radial structure of the asymmetric unit. Red colors denote amino acids that are further from the center of the capsid, while blue denotes amino acids in recessed areas of the capsid.

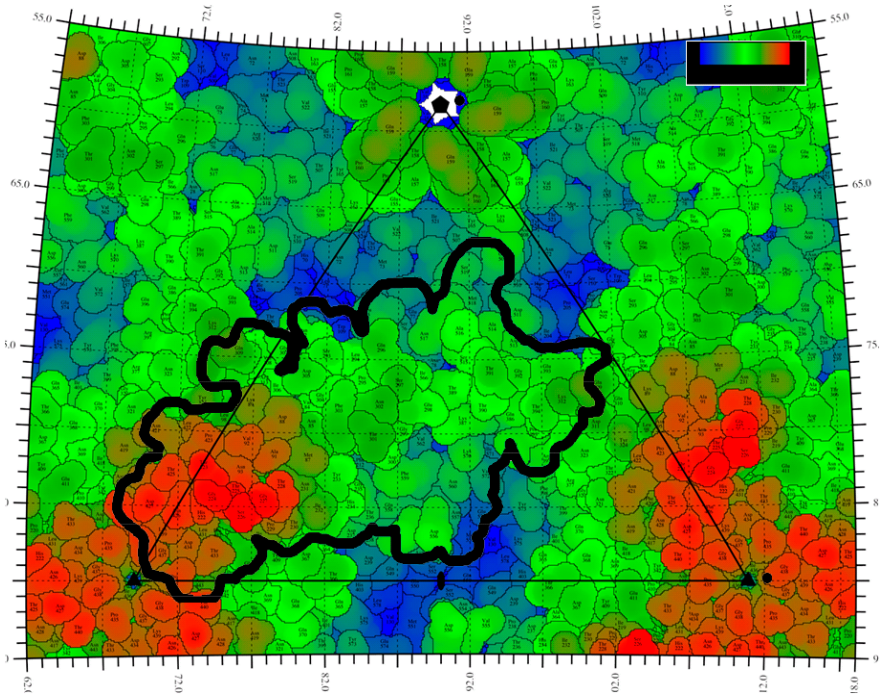

Pseudo-atomic structures were generated by fitting in known atomic resolution structures of CPV and Fab 14. This method has been highly successful in determining virus receptor interactions for structures that are not normally able to be solved by X-ray diffraction of complex crystals (5, 18, 28, 41). For the other seven Fabs whose crystal structure was not determined, we used homology modeling to estimate the structure of the variable domain of these antibodies (44). This method was validated by a comparison of the structure of variable domains of the crystal structure of Fab14 and the predicted homology model. This method was useful, as it was not practical to crystallize and solve atomic resolution structures for all eight antibodies.

The objective of this study was to further understand the structural features that contribute to antibody selection. It is becoming apparent that the most tractable method for studying virus-antibody epitope is through a structural approach, and more recent work is beginning to define these interactions (reviewed in (33)). By examining eight monoclonal antibodies, we hoped to elucidate common structural features that comprise viral epitopes. No distinct features were obvious in the two antigenic sites with respect to charge or hydrophobicity. Also, no specific arrangement of charged or hydrophobic residues were readily seen that could explain the preferential use of site A and B as epitopes. Site A and B antibodies share common area binding domains with each other, all antibodies clearly have unique interactions with the capsid. It appears that the combined antibody sites represent the surface area that is accessible to antibody binding (Figure 3.4). The remaining sites on the virus are in either recessed canyons such as the 2-fold dimple, or large protruding domains, such as the 5-fold cylinder.

A secondary goal was to gain further insight into the structural basis of antibody neutralization. Previous studies have examined the ability of these antibodies to neutralize CPV and FPV (21). All intact IgGs were able to neutralize

CPV and FPV, whereas only 3 Fab fragments of these IgGs were able to neutralize either virus. Rat antibodies F and E were shown to be neutralizing at ~<100 Fabs per capsid, and one mouse antibody (Fab 16) neutralized at ~500 Fabs per capsid. All of these Fabs had similar affinities, suggesting that the epitope may be important for determining neutralization. The three neutralizing Fabs are site B antibodies, yet a comparison of these neutralizing footprints compared to non-neutralizing footprints do not yield any obvious insight into the mechanism of neutralization by these antibodies. All of these Fabs bound with similar affinities and similar levels of occupancy, except Fab 6, which bound once per three-fold axis. The angle of antibody binding for Fab F and E are more skewed across the two fold axis, and this may occlude critical residues that the other antibodies do not block (Figure 3.1). Both antigenic sites overlap the receptor binding domain, as determined by Cryo-EM and image reconstructions (9, 20). Structural asymmetry in CPV has been proposed recently, and this may help explain how antibody F and E neutralize CPV. Both of these antibodies lean across the two-fold axis and therefore have the possibility to occlude a unique site on CPV that antibodies may otherwise not be able to bind. Therefore, if CPV were to bind to this unique vertex, then only antibody E and F would effectively compete with TfR for binding to capsids. Other antibodies are able to less effectively compete with TfR binding and indicates that TfR may bind regions outside this asymmetric site, or regions of TfR protrude outside of this site. However, these antibodies are non-neutralizing and therefore must be less effective in blocking TfR binding.

What are the highest affinity antibody binding areas on parvovirus capsids, and are these selected for during B-cell maturation? Since the hybridomas used in this study were generated from mice and rats that had been repeatedly immunized with antigen, the IgGs used here represent the high affinity response of the vertebrate immune system. It is therefore possible common overlap regions of the A and B sites

could represent the highest affinity sites on the virus. Another possibility is that antibodies selection is confined to areas around site A and B due to the usage of particular variable domain gene segments during somatic recombination. It has been demonstrated that viral infection will stimulate antibody production using a limited subset of antibody variable domain gene segments, and this may limit the antibody response toparticular regions of capsids (15, 39, 42, 43). Phage display or similar studies would be instrumental in determining whether other high affinity sites are available on the capsid. Conversely, it would also be of interest to examine early response (and presumably lower affinity) IgM Fab fragments, to see if they displayed significantly different antigenic sites than the affinity matured IgGs studied here.

3.6 Acknowledgements.

Wendy Weichert and Virginia Scarpino provided excellent technical assistance. Valorie Bowman and TJ Batissti provided excellent technical assistance for electron microscopy.

REFERENCES

1. **Agbandje, M., R. McKenna, M. G. Rossmann, M. L. Strassheim, and C. R. Parrish.** 1993. Structure determination of feline panleukopenia virus empty particles. Proteins **16:** 155-171.
2. **Bangari, D. S., and S. K. Mittal.** 2006. Current strategies and future directions for eluding adenoviral vector immunity. Curr Gene Ther **6:**215-26.
3. **Burton, D. R.** 2002. Antibodies, viruses and vaccines. Nat Rev Immunol **2:**706-13.
4. **Burton, D. R., E. O. Saphire, and P. W. Parren.** 2001. A model for neutralization of viruses based on antibody coating of the virion surface. Curr Top Microbiol Immunol **260:**109-43.
5. **Che, Z., N. H. Olson, D. Leippe, W. M. Lee, A. G. Mosser, R. R. Rueckert, T. S. Baker, and T. J. Smith.** 1998. Antibody-mediated neutralization of human rhinovirus 14 explored by means of cryoelectron microscopy and X-ray crystallography of virus-Fab complexes. J Virol **72:**4610-22.
6. **Colonno, R. J., P. L. Callahan, D. M. Leippe, R. R. Rueckert, and J. E. Tomassini.** 1989. Inhibition of rhinovirus attachment by neutralizing monoclonal antibodies and their Fab fragments. J Virol **63:**36-42.
7. **Colonno, R. J., Condra, J.H., Mizutani, S.** 1989. Interaction of cellular receptors with the canyon structure of human rhinoviruses. Cell Biology of Virus Entry, Replication, and Pathogenesis, Alan R. Liss, Inc. **pp. 75-83**.
8. **Enns, C. A.** 2002. The transferrin receptor, p. 71-94. *In* D. M. Templeton (ed.), Molecular and cellular iron transport. Marcel Dekker, New York.

9. **Hafenstein, S., L. M. Palermo, V. A. Kostyuchenko, C. Xiao, M. C. Morais, C. D. Nelson, V. D. Bowman, A. J. Battisti, P. R. Chipman, C. R. Parrish, and M. G. Rossmann.** 2007. Asymmetric binding of transferrin receptor to parvovirus capsids. Proc Natl Acad Sci U S A **104:**6585-9.

10. **He, Y., J. Li, S. Heck, S. Lustigman, and S. Jiang.** 2006. Antigenic and immunogenic characterization of recombinant baculovirus-expressed severe acute respiratory syndrome coronavirus spike protein: implication for vaccine design. J Virol **80:**5757-67.

11. **Hueffer, K., L. Govindasamy, M. Agbandje-McKenna, and C. R. Parrish.** 2003. Combinations of two capsid regions controlling canine host range determine canine transferrin receptor binding by canine and feline parvoviruses. J Virol **77:**10099-10105.

12. **Hueffer, K., L. M. Palermo, and C. R. Parrish.** 2004. Parvovirus infection of cells by using variants of the feline transferrin receptor altering clathrin-mediated endocytosis, membrane domain localization, and capsid-binding domains. J Virol **78:**5601-5611.

13. **Hueffer, K., J. S. Parker, W. S. Weichert, R. E. Geisel, J. Y. Sgro, and C. R. Parrish.** 2003. The natural host range shift and subsequent evolution of canine parvovirus resulted from virus-specific binding to the canine transferrin receptor. J. Virol. **77:**1718-1726.

14. **Huttner, N. A., A. Girod, L. Perabo, D. Edbauer, J. A. Kleinschmidt, H. Buning, and M. Hallek.** 2003. Genetic modifications of the adeno-associated virus type 2 capsid reduce the affinity and the neutralizing effects of human serum antibodies. Gene Ther **10:**2139-47.

15. **Kallewaard, N. L., B. A. McKinney, Y. Gu, A. Chen, B. V. Prasad, and J. E. Crowe, Jr.** 2008. Functional maturation of the human antibody response to rotavirus. J Immunol **180:**3980-9.

16. **Langeveld, J. P., J. I. Casal, C. Vela, K. Dalsgaard, S. H. Smale, W. C. Puijk, and R. H. Meloen.** 1993. B-cell epitopes of canine parvovirus: distribution on the primary structure and exposure on the viral surface. J Virol **67:**765-772.

17. **Lochrie, M. A., G. P. Tatsuno, B. Christie, J. W. McDonnell, S. Zhou, R. Surosky, G. F. Pierce, and P. Colosi.** 2006. Mutations on the external surfaces of adeno-associated virus type 2 capsids that affect transduction and neutralization. J Virol **80:**821-34.

18. **Lok, S. M., V. Kostyuchenko, G. E. Nybakken, H. A. Holdaway, A. J. Battisti, S. Sukupolvi-Petty, D. Sedlak, D. H. Fremont, P. R. Chipman, J. T. Roehrig, M. S. Diamond, R. J. Kuhn, and M. G. Rossmann.** 2008. Binding of a neutralizing antibody to dengue virus alters the arrangement of surface glycoproteins. Nat Struct Mol Biol **15:**312-7.

19. **Lopez de Turiso, J. A., E. Cortez, A. Ranz, J. Garcia, A. Sanz, C. Vela, and J. I. Casal.** 1991. Fine mapping of canine parvovirus B cell epitopes. J Gen Virol **72:**2445-2456.

20. **Nelson, C. D., E. Minkkinen, M. Bergkvist, K. Hoelzer, M. Fisher, B. Bothner, and C. R. Parrish.** 2008. Detecting small changes and additional peptides in the canine parvovirus capsid structure. J Virol.

21. **Nelson, C. D., L. M. Palermo, S. L. Hafenstein, and C. R. Parrish.** 2007. Different mechanisms of antibody-mediated neutralization of parvoviruses revealed using the Fab fragments of monoclonal antibodies. Virology **361:**283-93.

22. **Neuberger, M. S.** 2008. Antibody diversification by somatic mutation: from Burnet onwards. Immunol Cell Biol **86:**124-32.

23. **Palermo, L. M., K. Hueffer, and C. R. Parrish.** 2003. Residues in the apical domain of the feline and canine transferrin receptors control host-specific binding and cell infection of canine and feline parvoviruses. J Virol **77:**8915-8923.

24. **Parrish, C. R.** 1991. Mapping specific functions in the capsid structure of canine parvovirus and feline panleukopenia virus using infectious plasmid clones. Virology **183:**195-205.

25. **Parrish, C. R., and L. E. Carmichael.** 1983. Antigenic structure and variation of canine parvovirus type-2, feline panleukopenia virus, and mink enteritis virus. Virology **129:**401-414.

26. **Parrish, C. R., Carmichael, L.E., Antczak, D.F.** 1982. Antigenic relationships between canine parvovirus type-2, feline panleukopenia virus and mink enteritis virus using conventional antisera and monoclonal antibodies. Arch.Virol. **72: 267-278**.

27. **Reading, S. A., and N. J. Dimmock.** 2007. Neutralization of animal virus infectivity by antibody. Arch Virol **152:**1047-59.

28. **Rossmann, M. G., M. C. Morais, P. G. Leiman, and W. Zhang.** 2005. Combining X-ray crystallography and electron microscopy. Structure (Camb) **13:**355-62.

29. **Roy, S., P. S. Shirley, A. McClelland, and M. Kaleko.** 1998. Circumvention of immunity to the adenovirus major coat protein hexon. J Virol **72:**6875-9.

30. **Sherry, B., A. G. Mosser, R. J. Colonno, and R. R. Rueckert.** 1986. Use of monoclonal antibodies to identify four neutralization immunogens on a common cold picornavirus, human rhinovirus 14. J Virol **57:**246-57.

31. **Sherry, B., and R. Rueckert.** 1985. Evidence for at least two dominant neutralization antigens on human rhinovirus 14. J Virol **53:**137-43.

32. **Smith, T. J.** 2001. Antibody interactions with rhinovirus: lessons for mechanisms of neutralization and the role of immunity in viral evolution. Curr Top Microbiol Immunol **260:**1-28.

33. **Smith, T. J.** 2003. Structural studies on antibody-virus complexes. Adv Protein Chem **64:**409-53.

34. **Smith, T. J., and T. Baker.** 1999. Picornaviruses: epitopes, canyons, and pockets. Adv Virus Res **52:**1-23.

35. **Smith, T. J., E. S. Chase, T. J. Schmidt, N. H. Olson, and T. S. Baker.** 1996. Neutralizing antibody to human rhinovirus 14 penetrates the receptor-binding canyon. Nature **383:**350-4.

36. **Smith, T. J., N. H. Olson, R. H. Cheng, E. S. Chase, and T. S. Baker.** 1993. Structure of a human rhinovirus-bivalently bound antibody complex: implications for viral neutralization and antibody flexibility. Proc Natl Acad Sci U S A **90:**7015-8.

37. **Smith, T. J., N. H. Olson, R. H. Cheng, H. Liu, E. S. Chase, W. M. Lee, D. M. Leippe, A. G. Mosser, R. R. Rueckert, and T. S. Baker.** 1993. Structure of human rhinovirus complexed with Fab fragments from a neutralizing antibody. J Virol **67:**1148-58.

38. **Strassheim, L. S., A. Gruenberg, P. Veijalainen, J.-Y. Sgro, and C. R. Parrish.** 1994. Two dominant neutralizing antigenic determinants of canine parvovirus are found on the threefold spike of the virus capsid. Virology **198:**175-184.

39. **Tian, C., G. K. Luskin, K. M. Dischert, J. N. Higginbotham, B. E. Shepherd, and J. E. Crowe, Jr.** 2008. Immunodominance of the VH1-46

antibody gene segment in the primary repertoire of human rotavirus-specific B cells is reduced in the memory compartment through somatic mutation of nondominant clones. J Immunol **180:**3279-88.

40. **Tsao, J., M. S. Chapman, M. Agbandje, W. Keller, K. Smith, H. Wu, M. Luo, T. J. Smith, M. G. Rossmann, R. W. Compans, and C. R. Parrish.** 1991. The three-dimensional structure of canine parvovirus and its functional implications. Science **251:**1456-1464.

41. **Wang, G. J., C. Porta, Z. G. Chen, T. S. Baker, and J. E. Johnson.** 1992. Identification of a Fab interaction footprint site on an icosahedral virus by cryoelectron microscopy and X-ray crystallography. Nature **355:**275-8.

42. **Weitkamp, J. H., N. L. Kallewaard, A. L. Bowen, B. J. Lafleur, H. B. Greenberg, and J. E. Crowe, Jr.** 2005. VH1-46 is the dominant immunoglobulin heavy chain gene segment in rotavirus-specific memory B cells expressing the intestinal homing receptor alpha4beta7. J Immunol **174:**3454-60.

43. **Weitkamp, J. H., B. J. Lafleur, and J. E. Crowe, Jr.** 2006. Rotavirus-specific CD5+ B cells in young children exhibit a distinct antibody repertoire compared with CD5- B cells. Hum Immunol **67:**33-42.

44. **Whitelegg, N. R., and A. R. Rees.** 2000. WAM: an improved algorithm for modelling antibodies on the WEB. Protein Eng **13:**819-24.

45. **Wikoff, W. R., G. Wang, C. R. Parrish, R. H. Cheng, M. L. Strassheim, T. S. Baker, and M. G. Rossmann.** 1994. The structure of a neutralized virus: canine parvovirus complexed with neutralizing antibody fragment. Structure **2:**595-607.

46. **Xie, Q., and M. S. Chapman.** 1996. Canine parvovirus capsid structure, analyzed at 2.9 Å resolution. J Mol Biol **264:**497-520.

47. **Yuan, W., and C. R. Parrish.** 2000. Comparison of two single-chain antibodies that neutralize Canine Parvovirus: analysis of an antibody-combining site and mechanisms of neutralization. Virology **269:**471-480.

48. **Zaiss, A. K., and D. A. Muruve.** 2008. Immunity to adeno-associated virus vectors in animals and humans: a continued challenge. Gene Ther **15:**808-16.

CHAPTER FOUR

Detecting small changes and additional peptides in the canine parvovirus capsid structure.

Christian D.S. Nelson, Eveliina Minkkinen, Magnus Bergkvist, Karin Hoelzer, Mathew Fisher, Brian Bothner, Colin R. Parrish. 2008. Detecting small changes and additional peptides in the canine parvovirus capsid structure. Journal of Virology. Electronic early publication on 13 August 2008.

[Eveliina Minkkinen was a visiting masters student who performed spectrofluoremetry on DNA release (Figure 4.8). Magnus Bergkvist was a collaborator at Cornell Nanobiotechology Center who suggested and provided preliminary images of negative staining of CPV. Karin Holezer is a graduate student in Colin Parrish's lab who developed protocols for realtime PCR used in this paper. Matthew Fisher was an undergraduate student in Brian Bothner's laboratory who preformed some of the mass spectrometry measurements]

4.1 Abstract.

Parvovirus capsids are assembled from multiple forms of a single protein, and are quite stable structurally. However, in order to infect cells, conformational plasticity of the capsid is required and this likely involves the exposure of structures that are buried within the structural models. The presence of functional asymmetry in the otherwise icosahedral capsid has also been proposed. Here we examined the protein composition of canine parvovirus capsids, and evaluated their structural variation and permeability by protease sensitivity, spectrofluorometry, and negative staining electron microscopy. Additional protein forms identified included an apparent smaller variant of the virus protein (VP) 1, and a small proportion of a cleaved form of VP2. Only a small percentage of the proteins in intact capsids were cleaved by any of the proteases tested. The capsid susceptibility to proteolysis varied with temperature but new cleavages were not revealed. No global change in the capsid structure was observed by analysis of Trp fluorescence when capsids were heated between 40° and 60°C. However, increased polarity of empty capsids was indicated by bis-ANS binding, something not seen for DNA-containing capsids. Removal of calcium with EGTA or exposure to pHs as low as 5.0 had little effect on the structure, but at pH 4.0 changes were revealed by proteinase K digestion. Exposure of viral DNA to the external environment started above 50°C. Some negative stains showed increased permeability of empty capsids at higher temperatures, but no effects were seen after EGTA treatment.

4.2 Introduction.

The capsids of animal viruses are molecular machines that serve many functions in the viral life cycle. For parvoviruses, a small number of overlapping proteins make up the capsids and serve multiple intricate functions. These include

protecting the genome from the environment, interacting with host receptors and antibodies, targeting the particle to the correct cells and tissues, controlling the process of cell uptake, trafficking the genome to the nucleus during cell infection, and releasing their ssDNA at the correct cellular location for replication. The canine parvovirus (CPV) capsid has been considered to have a superficially simple structure which is assembled from 60 copies of a combination of two proteins, VP1 (84 kDa) and VP2 (67 kDa) (32, 53). About 90% of the protein in the capsid is VP2, and 10% is VP1 which contains the entire VP2 sequence and 143 additional residues at its N terminus (43). The 5-6 copies of the VP1 N-terminal sequence are sequestered from antibody binding and their distribution within the T=1 icosahedron is unknown (31). In full (DNA containing) capsids, some VP2 proteins can be converted to the ~63 kDa VP3 by proteolytic cleavage of approximately 19 amino acids from the N-terminus (57). This cleavage is not seen in empty (no DNA) capsids. CPV is transmitted by the fecal-oral route, and the viruses are stable in the intestinal contents and feces of animals and may persist in the environment for days or weeks before infecting another host (14).

The parvoviruses related to CPV include three variants which have >99% sequence identity, but which differ in host range, receptor binding, and antigenic structure (20, 49). The ancestral feline panleukopenia virus (FPV) of cats mutated to create the original strain of CPV, termed CPV type-2 (CPV-2) which spread around the world in 1978 (40). A variant strain called CPV type-2a (CPV-2a) replaced CPV-2 world-wide during 1979 and 1980, and contained changes of VP2 residues 87, 101, 300 and 305 (35, 37, 41). The CPV-2a variant is antigenically different from CPV-2, has an altered host range for cats (52), and has a reduced binding to the feline transferrin receptor (TfR) (30). Since 1980 a variety of additional mutants have arisen

in the CPV-2a background, including changes of VP2 residues 426 (Asn to Asp; then from Asp to Glu), and 297 (Ser to Ala) (4, 36).

The primary cell receptor for FPV and CPV is the host TfR (33). CPV and FPV capsids both bind the feline TfR, while CPV capsids also bind the canine TfR, and that binding is a primary determinant of canine host range (17, 19). Canine TfR binding is dictated by residues in at least 3 distinct positions on the capsid surface, including VP2 residues 93, 299, and 323 (20, 34). Structural studies of the feline TfR bound to the CPV-2 capsid defined the receptor footprint, and also indicated that the receptor occupied only a few of the 60 potential binding sites on the T=1 capsid (16). Possible reasons for the low occupancy of receptor binding might include inherent asymmetry of the capsid where only a limited number of binding sites are displayed, or structural changes in the capsid induced upon receptor binding which prevent further receptors from attaching. Also, receptors initially bound to the capsid might sterically hinder the binding of additional TfRs, but models predict that 20-24 receptors should still be able to bind to a capsid.

The VP1 and VP2 contain a common core β-barrel structure, where the capsid surface is formed by large loops inserted between some of the β-strands. Prominent surface features include distinct depressions at the twofold axes of icosahedral symmetry and surrounding the fivefold axes, and a raised region around the threefold axes containing the binding sites for canine or feline TfR as well as antibodies (16, 49, 58). Pores with ~10 Å diameter at the fivefold axes of symmetry are each surrounded by a cylinder made up of 5 β-ribbons. The pores are hypothesized to allow exposure of the 5'-end of the viral DNA outside the capsid after DNA packaging (10), and also seem to promote the exposure of the VP2 N-termini in full (i.e. DNA containing) particles (8, 57).

The dynamic properties, flexibility, and alternative structures of viral proteins are important for their various functions. Some type of activation has been shown to be required by many viruses for them to become infectious. Triggers that control infectivity may include receptor binding, proteolysis of viral proteins, exposure to low pH, removal of ions bound within the capsid structure, or specific rearrangement of capsid bonds (such as disulfide bonds) (21, 48). These triggers and the resulting changes in capsid structure can control virus uptake into the cell, allow membrane penetration or fusion, control correct trafficking within the endosomal system, and/or determine the success of cytoplasmic trafficking or nuclear delivery (27, 47).

Structural comparisons of CPV, FPV, and host range variants of those viruses revealed that many of the host range-determining differences were due to altered configurations of hydrogen bonds, with only subtle changes in the overall capsid protein structures (2, 23). However, those changes clearly affect canine TfR binding and in some cases also modify the binding of specific antibodies (15, 30). Their significant functional effects might therefore be the result of alterations in the flexibility of key capsid structures that control receptor or antibody binding (2, 15, 49).

Crystallography studies have shown some flexibility or altered structures of the CPV and FPV capsid proteins when exposed to low pH or after removal of bound Ca^{2+} ions (45). In CPV-2 capsids two Ca^{2+} ions are coordinated by clusters of Asp and His residues, and a third Ca^{2+} binding site is present in FPV and probably CPV-2a (45). Those ions are located at the interfaces between the protein subunits and stabilize certain capsid loops (45). Equivalent ion binding sites are not seen in the same positions of capsids of related parvoviruses, such as the minute virus of mice (MVM) (1, 24). At pHs 6.2 or 5.5 the capsids exhibit only relatively minor structural changes,

with the greatest effect being an increased flexibility of a surface loop between VP2 residues 359 and 372, in part due to the release of the Ca^{2+} (45).

In many parvoviruses the VP1 unique sequence contains a phospholipase A2 (PLA_2) enzyme domain that is required for successful infection. This domain is sequestered in the capsid but becomes exposed during cellular uptake and infection, or after heating to temperatures above 45°C *in vitro* (9, 56, 61). The PLA_2 likely modifies the endosomal membrane to facilitate particle release during infection (12, 50). The VP1 N-terminal sequences also contain basic sequences that resemble classical importin-dependent nuclear localization sequences (NLS) which would also need to be exposed in the cytoplasm (55).

Here we use a variety of methods to examine the structural variability of CPV and related virus capsids, analyzing both wild type capsids and those of specific mutants that affect antibody or TfR binding. The capsids were in general very stable, but low levels of structural variability were detected under certain conditions by broad activity proteinase and by probes for protein polarity. At increased temperatures negative stains showed increased penetration of empty capsids and viral DNA became exposed under conditions where the capsids otherwise remained intact. Minor amounts of previously unrecognized capsid protein forms were also identified within the viral capsids.

4.3 Materials and Methods.

Viruses, cells, and proteins. Viruses include the prototype isolates of CPV type-2 (CPV-2) (CPV-d), FPV (FPV-b) and CPV-2b (CPV-39) (19, 35) as well as mutations with VP2 residue 297 changed from Ser to Ala (FPV S297A, CPV-2 S297A, or CPV-2b S297A), or CPV-2 with VP2 residue 299 changed from Gly to Glu (CPV-2 G299E), or residue 300 changed from Ala to Asp (CPV-2 A300D). Viruses

were isolated from infectious plasmid clones and grown in feline NLFK cells in a 1:1 mixture of McCoy's 5A and Liebovitz L15 media with 5% fetal bovine serum (35).

Capsids were in most cases prepared and purified as reported previously (2). In short, virus was precipitated with polyethylene glycol 8000 (PEG), and full and empty capsids were purified by banding on 10 to 40% sucrose gradients. Capsids were passed through a Sepharose CL-4B column in 50 mM PIPES.NaOH (pH 7.6), 150mM NaCl to remove contaminating proteins and loosely associated peptides. In an alternative method capsids were purified from infected cells by banding in step gradients of Iodixanol (Optiprep, Axis Shield, Oslo, Norway) (11). For the Iodixanol method cells were infected and incubated for 2 days, and then scraped into 0.15M NaCl, 50 mM Tris HCl (pH 7.5) after the initial media had been removed. After freezing and thawing 3 times and 50 U/ml of Benzonase was added and debris pelleted for 20 min at 30,000 ×g. Capsids in the supernatant were then banded in step gradients of 15, 30, 45 and 60% of Iodixanol at 110,000 ×g for 6.5h at 25°C. The virus-containing band was passed through a G100 column, and then separated into full and empty capsid fractions by a linear gradient of 10% to 30% glycerol at 83,000 ×g for 4.5h at 25°C. Particles were passed through Sephadex G100 and Sepharose CL-4B columns in 50 mM PIPES.NaOH (pH 7.6), 150mM NaCl, and virus concentration determined by the micro BCA assay (Pierce, Rockford, IL).

The relative infectivities of the purified full capsid preparations were calculated from the viral genomes per capsid, compared to the infectious titers, and the effects of purification determined by comparing virus in tissue culture medium with the purified full capsids. DNA genome copy numbers were determined by quantitative PCR (Applied Biosystems, Foster City, CA). Primers were designed to bind to a conserved region in the viral genome between nts. 1039 and 1114 of the viral genome (encoding NS1). Absolute copy numbers were inferred from standard curves

of linearized plasmids containing the CPV sequence, and analyzed using a StepOne machine (Applied Biosystems, Foster City, CA). Infectious titers were determined by $TCID_{50}$ analysis (60).

The ectodomains of the feline and canine TfRs were purified after baculovirus expression as described previously (18, 30). The isolation and purification of MAbs F and 15 has been described previously (28, 38, 39).

Proteolytic analysis of CPV capsids. Proteases tested included trypsin, thermolysin, proteinase K, subtilisin, bromelin, and papain (all from Sigma, St. Louis, MO). Proteases were kept at -80°C in their respective storage buffers, and diluted in reaction buffer immediately before each experiment (Table 4.1). Protease activities under various buffer, temperature, pH, or EGTA conditions were calibrated with the Quanticleave assay with FITC-labeled casein (Pierce, Rockford, IL), using a fluorescence plate reader (Tecan Safire, Durham, NC). Most assays were conducted using proteinase K, and the amounts required to give equivalent activities were: 21°C = × 1.51; 37°C = × 1; 45°C = × 0.87; 55°C = × 0.81; pH 7.6 = × 1; pH 6.0 = × 1.92; pH 5.0 = × 3.65; pH 4.0 = × 7.7. Proteinase K activity was not affected by addition of EGTA over the time of the experiment.

Analysis of proteins, cleavage sites and comparison of different viruses. Capsid sensitivity to proteinase K was tested in the presence of 0 to 50 mM EGTA, or at 21, 37, 45, 55°C, or at pHs 7.6, 6.0, 5.0, 4.0. After incubation with proteinase K, Laemmli sample buffer with an excess of specific protease inhibitor was added and samples were placed in a boiling water bath for 5 min. Samples were analyzed in 10% acrylamide gels, stained with Coomassie blue G-250 (Pierce, Rockford, IL) and imaged (Syngene, Frederick, MD). To determine the effects of specific ligands bound to the capsids on the capsid proteolysis patterns, purified feline or canine TfR

Table 4.1.

Conditions used for storage, reaction and inhibition of proteases (5).

Protease	**Specificity**	**Storage buffer**	**Dilution buffer**	**Inhibitor used**
Proteinase K	Hydrophobic aliphatics and aromatics	50mM Tris-HCl (pH 8), 5 mM $CaCl_2$	50mM Tris-HCl (pH 8), 5 mM $CaCl_2$	PMSF
Papain	broad specificity, hydrophobics (P2), not valine (P1)	50 mM Tris-HCl (pH 8)	50 mM Tris-HCl (pH 8)	Sigma protease inhibitor*
Trypsin	Lys, Arg	1mM HCl	50mM Tris-HCl (pH 8)	PMSF
Thermolysin	Bulky Hydrophobics	20 mM $CaCl_2$	50mM Tris-HCl (pH 8), 5 mM $CaCl_2$	EDTA
Subtisilin	Most	50 mM Tris-HCl (pH 8)	50 mM Tris-HCl (pH 8)	PMSF
Bromelain	Nonspecific	50 mM Tris-HCl (pH 8)	50 mM Tris-HCl (pH 8)	TPCK

* Sigma protease inhibitior contains AEBSF, pepstatinA, E-64, bestatin, leupeptin, and aprotinin

ectodomains or Fabs of MAbs F or 15 were incubated with the capsids for 1 hr at 37°C, and then the mixtures treated with proteases at 37°C and analyzed as above.

To determine VP3 N-terminal sequences after proteinase digestions, proteins were transferred to 0.22 μm PVDF membranes (Immobilon Psq, Millipore, Billeria, MA), and N-terminal sequenced (Alphalyse, Palo Alto, CA). Antibodies used for Western blotting included mouse antisera raised against peptides containing VP2 residues 222-238, 292-310, 387-398, or 508-522 which had been conjugated to keyhole limpet hemocyanin. The N-terminal region of VP1 was detected with MAb S2D3 recognizing VP1 residues 2-11 (56).

Identification of proteolytic products in solution or from SDS-PAGE bands was conducted using both electrospray and MALDI ionization to minimize detection bias and increase coverage in mapping experiments. Electrospray instrumentation included an Agilent XCT Plus (Agilent Technologies; Santa Clara, CA), Bruker micrOTOF LC (Bruker Daltonik GmbH; Bremen, DEU), and Waters QToF Premier (Waters Corp.; Milford, MA), all interfaced with reverse-phase HPLC (C18: Phenomenex Inc.; Torrance, CA). MALDI analysis was performed with a variety of sample/matrix ratios and both sinapinic acid and α-Cyano-4-hydroxycinnamic acid, using a Bruker BiFlex III. Identification of protein bands involved in-gel protease digestion followed by mass analysis as above. A detailed protocol for in-gel proteolysis has been previously described (25).

Spectrofluorometric analysis of capsid stability and conformation. Empty or full capsids were concentrated to 0.5 μM in Millipore Amicon Ultra 100 kDa cutoff filters (Millipore, Billerica, MA) in 50 mM PIPES.NaOH (pH 7.6), 150mM NaCl. Assays were carried out using a Cary Eclipse spectrofluorometer (Varian, Palo Alto, CA) with a 1 cm path length. To analyze Trp fluorescence, samples were excited at 295 nm and emissions scanned from 310 to 400 nm or kept fixed at 331 nm (Ex/Em

bandwidth: 5 nm). Capsids were monitored at temperatures between 20 and 77°C. Capsids were also monitored by incubating with 3 μM bis-1-anilino-8-naphthalene sulfonate (bis-ANS) (Invitrogen, Carlsbad, CA) under various conditions. Samples were excited at 395 nm (bandwidth 5 nm) and the emission read at 500 nm (bandwidth 10 nm), and bis-ANS with no added protein was used as a background. The effect of low pH on virus capsids was examined by titrating the sample pH with 0.1N HCl. The effect of ligand binding on capsid structure were determined using purified feline or canine TfR (at a molar ratio of 30 TfR dimers per capsid) or antibody Fabs (at a molar ratio of 60 molecules per capsid). Capsids or purified TfRs and Fabs were also assayed for bis-ANS binding individually.

Exposure of viral DNA. Accessibility of capsid DNA were assayed using the dye TOTO-1 (Invitrogen, Carlsbad, CA). Capsids (8.4 μg/ml) in various pH buffers were heated at temperatures up to 95°C for 10 min, cooled to room temperature, then TOTO-1 was added and the samples excited at 515 nm (5 nm bandwidth) and read at 532 nm (10 nm bandwidth). To verify DNA exposure capsids heated to the indicated temperatures were cooled and then digested with 84 units of micrococcal nuclease for 30 mins at 37^{o}C, and stained for DNA as described above.

Transmission electron microscopy (TEM). Accessibility of different metal salts to the interior of full and empty capsids were examined before and after heating to various temperatures up to 75°C, or after EGTA treatment up to 50 mM. For most experiments, capsids were absorbed to carbon coated TEM grids (Electron Microscopy Sciences, Hatfield, PA) for 5 mins. After excess sample had been removed, stains were added to 5 min then blotted off. Stains used were 2% (w/v) methyl amine tungstate (NanoW) in water (pH 6.8) and 1% (w/v) $NiSO_4$ in water (pH 7.0). In most cases 0.1% bacitracin was added to give an even distribution on the grids. Samples were visualized at 60,000 × magnification in a FEI Tecnai 12 Biotwin

microscope. Ten randomly selected fields were photographed (>400 particles each treatment), and the percentage of capsids penetrated by the stains counted.

4.4 Results.

Protein composition and infectivity of purified capsids. Infectivity per genome was compared for viruses purified by standard PEG precipitation and sucrose gradient centrifugation or by iodixanol and glycerol gradients or viruses in freshly prepared cell culture supernatants. The infectivity of fresh capsids (1:1.3 × 10^{-5} $TCID_{50}$/genome copy) was similar to those of capsids purified using either PEG and sucrose (1:1.6 × 10^{-5} $TCID_{50}$/genome copy) or iodixanol and glycerol (1:1 × 10^{-5} $TCID_{50}$/genome copy). This demonstrates that although the viruses all had low infectivities in these cells, those were not altered during the purification methods used.

SDS-PAGE electrophoresis of all purified capsids examined showed the expected composition of VP1, VP2 (and VP3 in full capsids), as well as small amounts of previously unrecognized 70 kDa, 36.5 kDa and 33 kDa proteins (Figure 4.1 and 4.2). The latter proteins were each present at ~2-3 % of the VP2 protein concentration, but were incorporated into the capsids as they were not susceptible to proteolysis until significant VP2 degradation had occurred (Figures 4.1 and 4.2A). Western blotting and mass spectrometry indicated that these protein fragments were related to VP1 and VP2 (Figure 4.2B and 4.2C), and also showed that the 37 kDa peptide (labeled B), contained the C-terminal portion of VP2, while the 33 kDa peptide (labeled C) contained the VP2 N-terminal sequence (Figure 4.2). The two peptides represent a VP2 molecule incorporated into the capsid that has been hydrolyzed at one position, and between residues 270 and 292. Residue 270 is exposed on the interior wall of the capsid, and most of the residues between that position and residue 292 are buried within the capsid, while residue 292 is exposed on the capsid

Figure 4.1.

Digestion of full and empty particles with proteases and identification of VP3 N-terminus.

A) Sensitivity of the CPV-2 empty capsids to digestion with the proteases listed. Capsids and protease were incubated at 37° for 2 h. Size standards are in kDa. VP1, VP2 and VP3 are labeled. Protease bands are indicated by stars. Arrow heads labeled A, B and C indicate the pre-existing submolar bands detected in the purified capsids.

B) Full capsids treated as for (A).

C) Cleavage sites in VP2 by the different proteases in the VP2 to VP3 conversion. Cleavage sites were determined by N-terminal sequencing or mass spectrometry of the resulting VP3. For thermolysin the major site detected is shown; another unidentified site was also present in lower amounts.

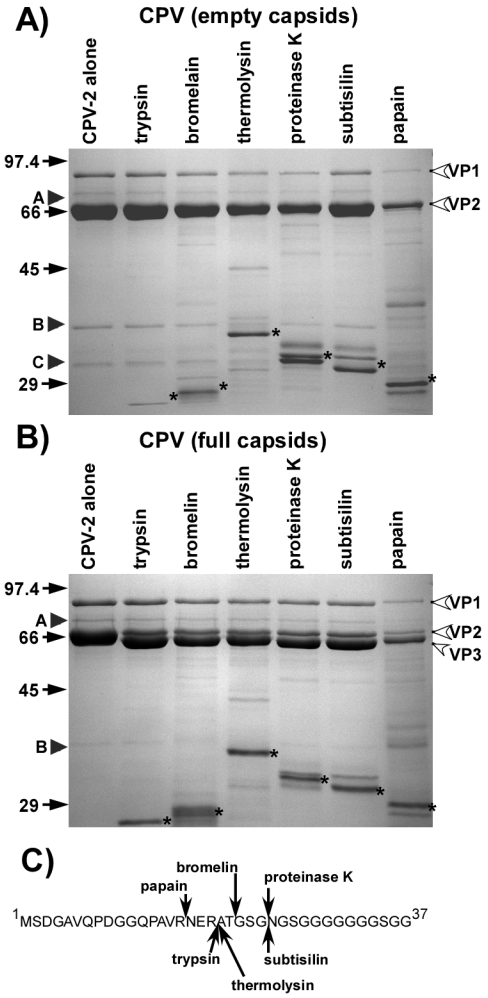
A)
CPV (empty capsids)
CPV-2 alone
trypsin
bromelain
thermolysin
proteinase K
subtisilin
papain
97.4
A
66
45
B
C
29
VP1
VP2
B)
CPV (full capsids)
VP3
C)
bromelin
papain
proteinase K
1MSDGAVQPDGGQPAVRNERATGSGNGSGGGGGGGSGG37
trypsin
subtisilin
thermolysin

Figure 4.2.

Limited proteolysis of CPV and mapping of cleavage fragments.

A) Protein composition of CPV-2 full capsids after incubation with 76 µg/ml of proteinase K at 37°C for up to 2 h. Controls included full capsids incubated alone, proteinase K immediately after thawing or incubated for 2 h at 37°C. Arrow heads labeled A, B and C indicate the pre-existing submolar fragments detected in the purified capsids. New peptides generated by the protease treatment are indicated by solid arrows and are numbered.

B) Approximate mapping of the pre-existing peptides A, B and C, as well as those released by proteinase K treatment (numbers refer to bands marked in (A)). Peptides were identified by Western blotting with anti-peptide sera, or by mass spectrometry after trypsin digestion of the recovered protein band. Precise cleavage sites have not yet been determined. Boxes indicate the specific sequences recognized by anti-peptide anti-sera.

C) Peptide analysis of pre-existing sub-molar peptides of full capsids of CPV-2. One lane of untreated full capsids was Coomassie blue stained. Capsid proteins were transferred and probed with anti-capsid, or anti-peptide sera as indicated. Anti-peptide antisera were made against peptides containing the VP-2 residues indicated.

D) Western blotting for the VP-1 N-terminal peptide (residues 2-13) in full capsids either before or after incubating with proteinase K for 2 h at 37°C. The arrow labeled 2 indicates the submolar fragment that is identified as fragment 2 in (B).

E) Capsid that were treated for 2 h with proteinase K examined in the electron microscope after staining with NanoW.

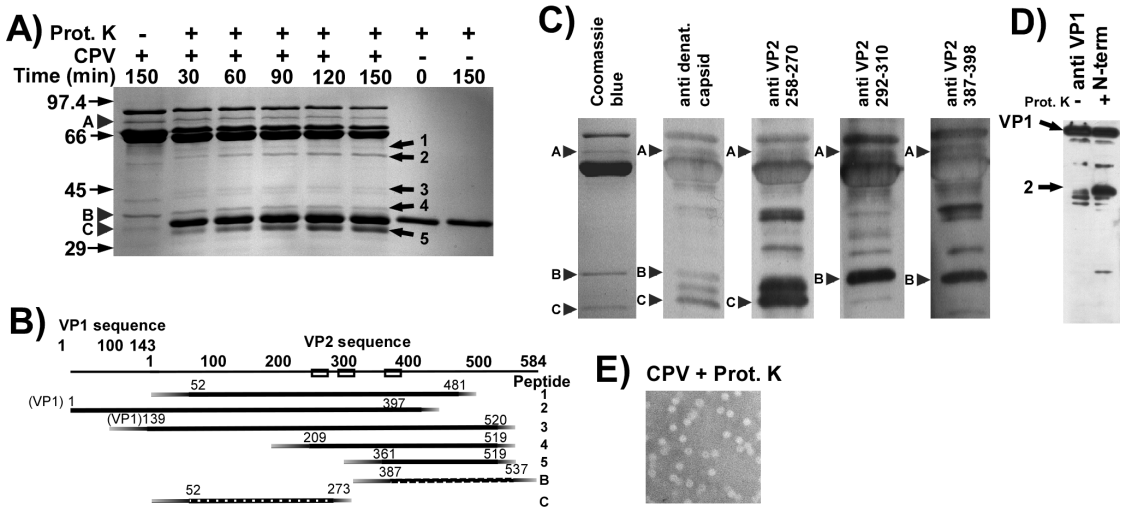
A)
Prot. K - + + + + + + +
CPV + + + + + + - -
Time (min) 150 30 60 90 120 150 0 150
97.4
66
45
29
A
B
C
1
2
3
4
5
B)
VP1 sequence
1 100 143
VP2 sequence
1 100 200 300 400 500 584
Peptide
(VP1) 1
52
481
397
(VP1)139
520
209
519
361
519
387
537
52
273
1
2
3
4
5
B
C
C)
Coomassie blue
anti denat. capsid
anti VP2 258-270
anti VP2 292-310
anti VP2 387-398
A
B
C
D)
Prot. K - +
anti VP1 N-term
VP1
2
E)
CPV + Prot. K

surface. No additional cleavages at similar positions appeared to be made by any of the proteases tested. In full capsids, this new N-terminal fragment was split into 50% of a 33 kDa form and 50% of a 29 kDa form, indicating an N-terminal cleavage similar to VP3, even though those capsid preparations otherwise contained little VP3 (data not shown). The 70 kDa polypeptide has not yet been completely characterized, but may be a truncated form of VP1, as it reacted with antibodies binding VP2 (Figure 4.2C).

Screening of capsid stability by proteolytic cleavage. All proteolytic enzymes tested converted most VP2 in full (but not empty) capsids into VP3 forms (57) (Figure 4.1B). The exact site of cleavage was slightly different for each of the proteases and these were partially mapped using N-terminal sequencing of the N-terminus of the newly generated VP3 fragment (Figure 4.1C) Although proteases were present in large amounts (see Figure 4.1 and 4.2), there was generally little degradation of the capsids during 2 hr of incubation at 37°C (Figure 4.1) and the proteolytic fragments generated represented only a small percentage of the total capsid protein. Proteinase K was selected for more detailed studies due to its broad specificity and activity under the experimental conditions used. Incubating CPV-2 virions for various times with proteinase K at 37°C in pH 7.6 gave a limited number of digestion products (Figure 4.2A). Examining digested capsids by negative staining EM indicated that they were largely intact and that the full particles excluded the NanoW stain (Figure 4.2E). After size exclusion chromatography the cleaved fragments remained incorporated in the capsid (results not shown). Western blotting using specific peptide antibodies and mass spectrometric analysis of trypsin digested protein bands allowed some of the proteolytic fragments to be positioned within the VP1 or VP2 sequences (Figure 4.2B – 4.2D).

Effects of temperature on capsid structure. Proteinase K treatment of the various capsids at higher temperatures demonstrated an increase in the total amount of digestion products, but in most cases no additional peptide fragments (Figure 4.3). FPV and CPV-2b capsids were more sensitive than CPV-2 capsids to digestion at 45 and 55°C (Figure 4.3). CPV-2 and FPV capsids with the VP2 residue 297 changed from Ser to Ala showed an additional peptide of 40 kDa, which was not seen in the wild type forms of those virus capsids, or when the mutation was in the CPV-2b background (Figure 4.3). Changing CPV-2 VP2 residues 299 (Gly to Glu), or 300 (Ala to Asp) alters the alter canine TfR binding, canine host range and antigenic structure of the capsid (17, 19, 23, 34), and the 300 Asp variant of CPV-2 showed loss of a peptide of 23 kDa that fell just below the proteinase K band (Figure 4.3).

All viruses contain 14 Trp residues in VP2 which are mostly sequestered within the capsid structure (29, 59). Tryptophan fluorescence spectra of full and empty CPV-2 particles under physiological conditions were indistinguishable at 22°C (Figure 4.4 A and B). As the temperature was increased, the emission intensity decreased linearly as expected from the thermal quenching of fluorescence (3). At 68-70°C there was an increase and change in the emission maximum wavelength for both empty and full capsid particles, indicating that Trp residues were exposed during particle disintegration (Figure 4.4C). For CPV-2 capsids incubated with bis-ANS, empty capsids displayed a slight increase in binding between 25 and 35°C, then a significant decrease between 35 and 55°C. These changes were not observed for full capsids. Above 68°C there was a dramatic increase of bin-ANS binding to both full and empty capsids as they disintegrated (Figure 4.4D). The observed change between 20 and 55°C for empty capsids was attributed to capsid structural changes, as no change of bis-ANS binding to the BSA control occurred over that temperature range (data not shown).

Figure 4.3.

Temperature sensitivity of CPV and related host range mutants to proteolysis. Susceptibilities of full capsids of CPV-2, FPV, CPV-2a, or mutants of those viruses to proteinase K for 2 h at the temperatures indicated. Gels were stained with Coomassie blue. Size standards are in kDa. Controls include virus incubated without proteinase, fresh proteinase K, or enzyme incubated for 2 h or 37°C. Additional bands seen at in the CPV-2 S297A and FPV S297A samples, or those that differ between CPV-2 and CPV-2 A300D, are indicated by open arrows.

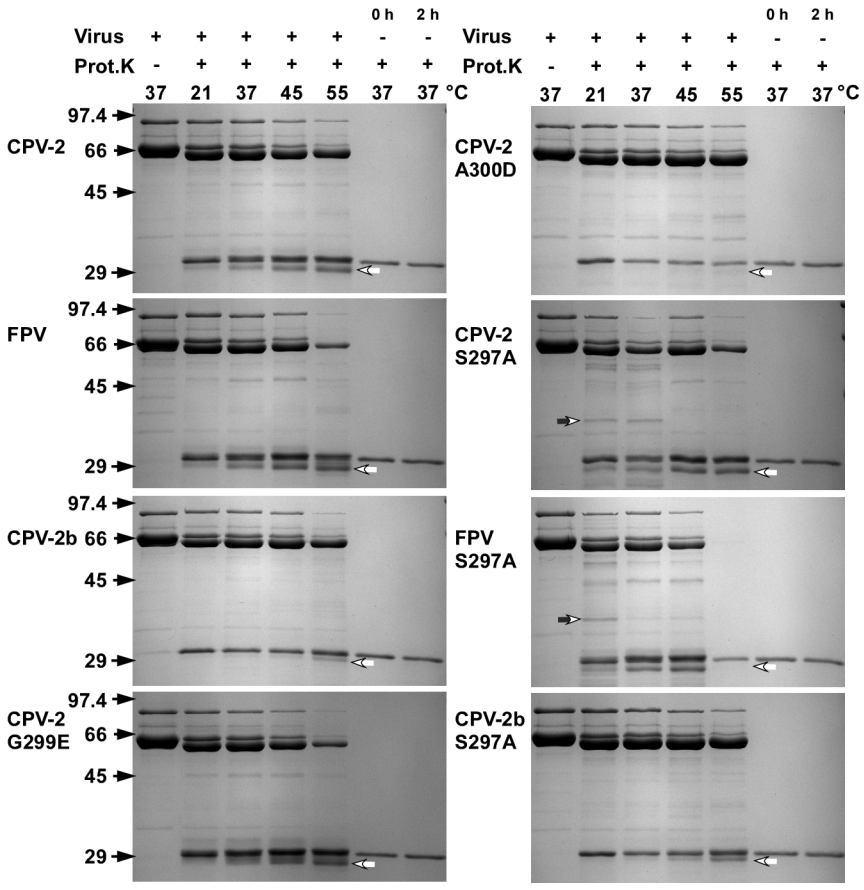
Virus + + + + + - - Virus + + + + + - -
Prot.K - + + + + + + Prot.K - + + + + + +
37 21 37 45 55 37 37 °C 37 21 37 45 55 37 37 °C
0 h 2 h 0 h 2 h
97.4
66
45
29
CPV-2
FPV
CPV-2b
CPV-2 G299E
CPV-2 A300D
CPV-2 S297A
FPV S297A
CPV-2b S297A

Figure 4.4.

Temperature dependence of tryptophan fluorescence and bis-ANS binding to CPV. Trp fluorescence spectra of CPV-2 empty (A) and full (B) capsids at varying temperatures, excited at 295 nm with emission scanned between 310 and 400 nm. C) Trp fluorescence of full and empty CPV-2 particles as temperatures were raised at 0.5°C/min, monitoring emission fluorescence at 331 nm. Data is the mean of three independent experiments ±1 SD.

D) Fluorescence of bis-ANS incubated with CPV-2 full or empty capsids at varying temperatures. Samples were excited at 395 the emission read at 500 nm, as temperatures were raised at 0.5°C/min. Data is the mean of the three independent experiments ±1 SD.

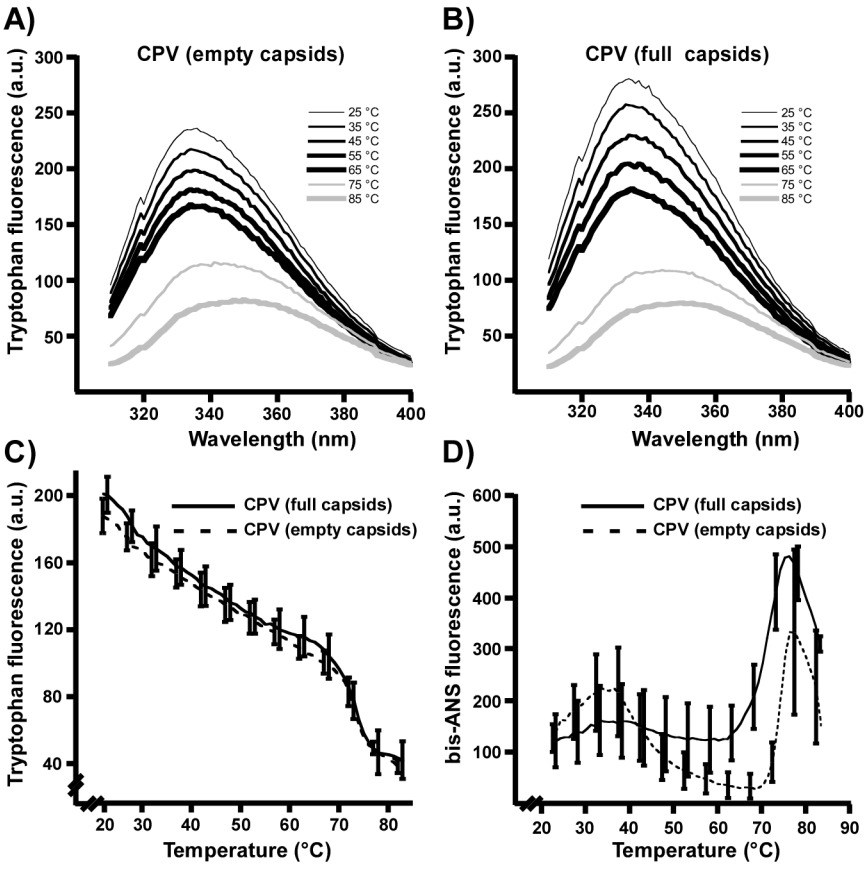
A)
CPV (empty capsids)
Tryptophan fluorescence (a.u.)
Wavelength (nm)
25 °C
35 °C
45 °C
55 °C
65 °C
75 °C
85 °C
B)
CPV (full capsids)
Tryptophan fluorescence (a.u.)
Wavelength (nm)
C)
CPV (full capsids)
CPV (empty capsids)
Tryptophan fluorescence (a.u.)
Temperature (°C)
D)
CPV (full capsids)
CPV (empty capsids)
bis-ANS fluorescence (a.u.)
Temperature (°C)

Effects of pH or EGTA treatment on virus structure. CPV-2 capsids were incubated with proteinase K at 37°C for 2 h in pH 7, 6, 5, and 4 buffers. No significant differences in either protease susceptibility or proteolytic peptide patterns were seen between pHs 7.5 and 5.0, however some alternative cleavages occurred at pH 4 (Figure 4.5A). Trp fluorescence spectroscopy showed no changes in the spectra at any of the pHs tested (Figure 4.5B), although the intensity progressively decreased over the pH range. This indicates no major change in the structure, but that minor. changes such as a relaxation of the capsid structure likely occurred. Binding of bis-ANS increased greatly at low pH (Figure 4.5C). The protein binding properties of bis-ANS itself is generally believed to be pH insensitive (13, 46), although increased binding to positively charged groups can occur at lower pH (22). The bis-ANS binding to BSA increased slightly at lower pH (data not shown), but the effect was considerably less than seen for CPV capsids, indicating that the increased fluorescence from bis-ANS at lower pH resulted from structural changes to the virus.

Proteinase K treatment of CPV-2 capsids incubated with 0, 1, 10, or 50 mM EGTA showed no changes in the digestion levels or peptide patterns (Figure 4.6A), or in the emission wavelength of the Trp fluorescence spectra (Figure 4.6B). Trp fluorescence intensity decreased slightly after initial EGTA treatment, indicating small changes in the local environment of some Trp residues. Binding of bis-ANS to empty capsids gave an increase in intensity at higher concentrations of EGTA that was not seen for full capsids (Figure 4.6C). Control binding to BSA did not change under those conditions (data not shown).

Effects of ligand binding on capsid structure. Incubating full CPV-2 capsids with Fab F or 15, or purified feline TfR ectodomain did not change the virus susceptibility to proteinase K (Figure 4.7A and 4.7B). TfR itself bound very high levels of bis-ANS compared to capsids, and adding bis-ANS to mixtures of CPV-2 capsids and TfR

Figure 4.5.

Effect of low pH on virion stability.

A) Protein composition of CPV-2 capsids incubated with proteinase K for 2 h in the pH buffers indicated. Controls include proteinase K incubated alone for 0 or 2 h, or capsids incubated without proteinase K.

B) Trp fluorescence of CPV-2 full capsids at the pHs indicated.

C) bis-ANS fluorescence of full or empty capsids at various pHs. The dye was added to capsids in the cuvette, and the pH adjusted by the addition of 0.1N HCl. Data is the mean of the three independent experiments ±1 SD.

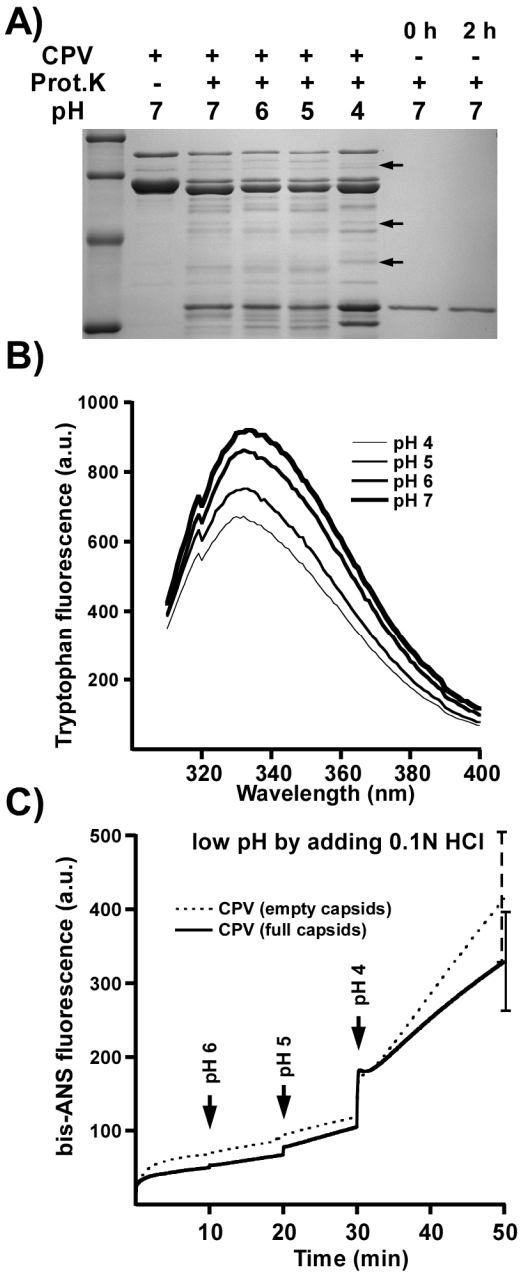
A)
0 h
2 h
CPV + + + + + - -
Prot.K - + + + + + +
pH 7 7 6 5 4 7 7
B)
Tryptophan fluorescence (a.u.)
1000
800
600
400
200
320
340
360
380
400
Wavelength (nm)
pH 4
pH 5
pH 6
pH 7
C)
low pH by adding 0.1N HCl
bis-ANS fluorescence (a.u.)
500
400
300
200
100
CPV (empty capsids)
CPV (full capsids)
pH 6
pH 5
pH 4
10
20
30
40
50
Time (min)

Figure 4.6.

Effect of calcium removal from CPV virions.

A) CPV-2 full capsids incubated with proteinase K in the presence of various concentrations of EGTA. Controls include capsids incubated with neither protease or EGTA, or protease incubated with 0 or 50 mM of EGTA.

B) Trp fluorescence of full capsids in the presence of varying amounts of EGTA.

C) The relative bis-ANS fluorescence of CPV full and empty capsids incubated with varying amounts of EGTA ±1 SD.

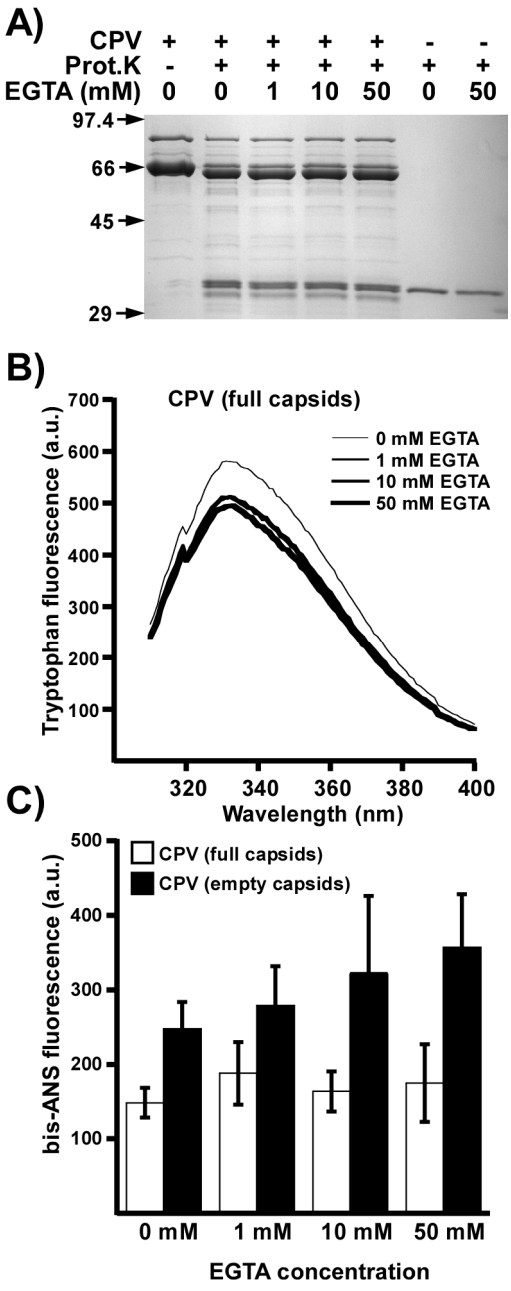
A)
CPV + + + + + - -
Prot.K - + + + + + +
EGTA (mM) 0 0 1 10 50 0 50
97.4
66
45
29
B)
CPV (full capsids)
0 mM EGTA
1 mM EGTA
10 mM EGTA
50 mM EGTA
Tryptophan fluorescence (a.u.)
700
600
500
400
300
200
100
320 340 360 380 400
Wavelength (nm)
C)
CPV (full capsids)
CPV (empty capsids)
bis-ANS fluorescence (a.u.)
500
400
300
200
100
0 mM 1 mM 10 mM 50 mM
EGTA concentration

Figure 4.7.

The effects of the feline TfR ectodomain or antibody Fabs on the CPV-2 full virus capsid structure.

A) CPV-2 full capsids incubated with the purified feline TfR ectodomain, with or without proteinase K treatment. The SDS-PAGE gel was stained with Coomassie blue.

B) Same as for (A), but capsids were incubated with Fabs of MAb 15 or 8.

C) Binding of bis-ANS to full CPV-2 capsids alone, to the feline TfR alone, or the mixture of the two. Results are from 3 separate experiments ±1 SD.

D) Binding of bis-ANS to full CPV-2 capsids alone, to Fab F or Fab 15 alone, or to capsid-Fab mixtures.

The fluorescent results for (C) and (D) cannot be compared directly as the TfR ectodomain bound the dye to much higher levels than the Fabs, so that the photomultiplier was at different settings for each experiment.

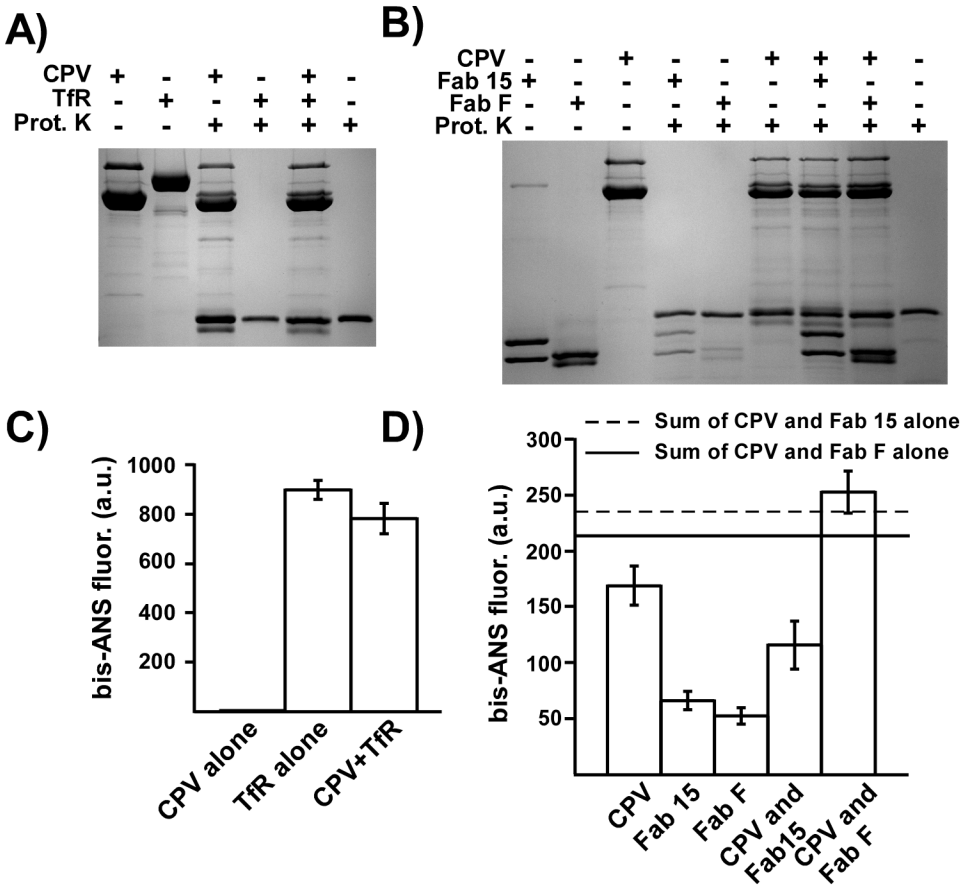
A)
CPV + - + - + -
TfR - + - + + -
Prot. K - - + + + +
B)
CPV - - + - - + + + -
Fab 15 + - - + - - + - -
Fab F - + - - + - - + -
Prot. K - - - + + + + + +
C)
bis-ANS fluor. (a.u.)
1000
800
600
400
200
CPV alone
TfR alone
CPV+TfR
D)
Sum of CPV and Fab 15 alone
Sum of CPV and Fab F alone
bis-ANS fluor. (a.u.)
300
250
200
150
100
50
CPV
Fab 15
Fab F
CPV and Fab15
CPV and Fab F

resulted in a slight decrease in bis-ANS fluorescence (Figure 4.7C). Fab 15 and Fab F bound similar levels of bis-ANS as CPV, and adding the dye to pre-incubated Fab 15 and CPV resulted in a decrease in bis-ANS fluorescence, compared to CPV and Fab 15 alone (Figure 4.7D). Binding of bis-ANS to CPV and Fab F gave a slight increase in fluorescence as compared to the binding to CPV or Fab F individually, suggesting a small change in the structure of one of the components upon ligand binding (Figure 4.7D).

Exposure of viral DNA upon heating. The viral DNA in full CPV-2 capsids became accessible to TOTO-1 dye starting at ~50°C, exposure increased up to 65°C and showed a large increase around 70°C (Figure 4.8). No significant effect of low pH was seen on DNA exposure in that assay. Digestion of heated particles with micrococcal nuclease reduced the DNA signal, indicating DNA externalization occurred, as opposed to dye entering the capsids (data not shown).

Transmission electron microscopy and stain penetration. The permeability of the capsids was examined using NanoW and $NiSO_4$. At 21°C $NiSO_4$ readily entered empty capsids, while NanoW was largely excluded (Figure 4.9). When NanoW was incubated with heat treated empty CPV capsids, penetration increased from 12% at 21°C, to 39% at 37°C, and 79% at 55°C, while at 75°C the particles disassembled. EGTA treatment did not change the staining of empty capsids by NanoW (Figure 4.9C).

4.5 Discussion.

This study confirmed that the CPV capsid is very stable, and showed that subtle changes occur in overall capsid structure, dynamics, and permeability. Some changes appeared to be localized with respect to capsid architecture and may involve only a subset of capsid subunits. The capsid responses to increased temperatures

Figure 4.8.

Staining of the DNA of CPV-2 full capsids with TOTO-1 after heating at various pHs. Capsids were heated for 10 mins, cooled to 21°C, dye added, and the fluorescence determined. There was no statistically significant difference between the exposure of the DNA at any of the pHs tested.

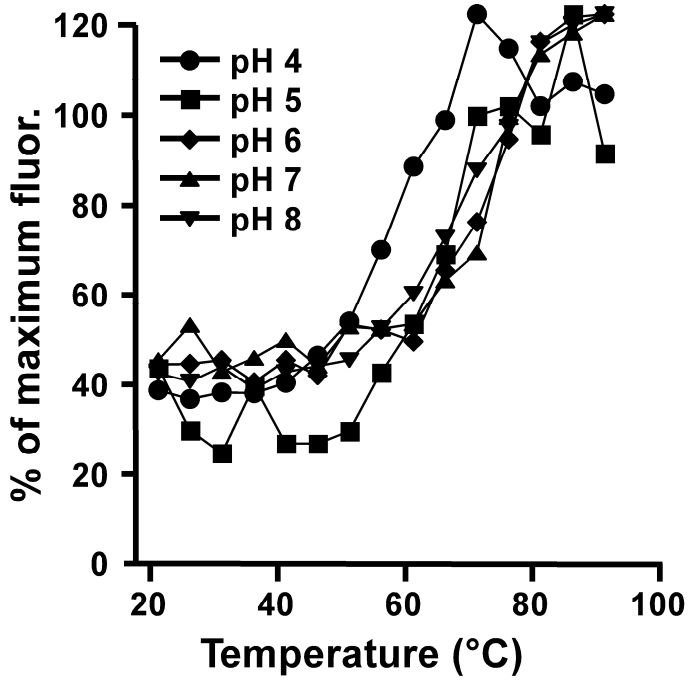
120
100
80
60
40
20
0
% of maximum fluor.
pH 4
pH 5
pH 6
pH 7
pH 8
20
40
60
80
100
Temperature (°C)

Figure 4.9.

Permeability of CPV full and empty particles to negative stains.

A) Negative staining of CPV-2 full or empty capsids (as indicated) with $NiSO_4$ or nanoW.

B) Negative staining of CPV-2 empty capsids with NanoW after heating to various temperatures for 10 mins.

C) Negative staining of CPV-2 empty capsids with NanoW in the presence or absence of 10 mM EGTA.

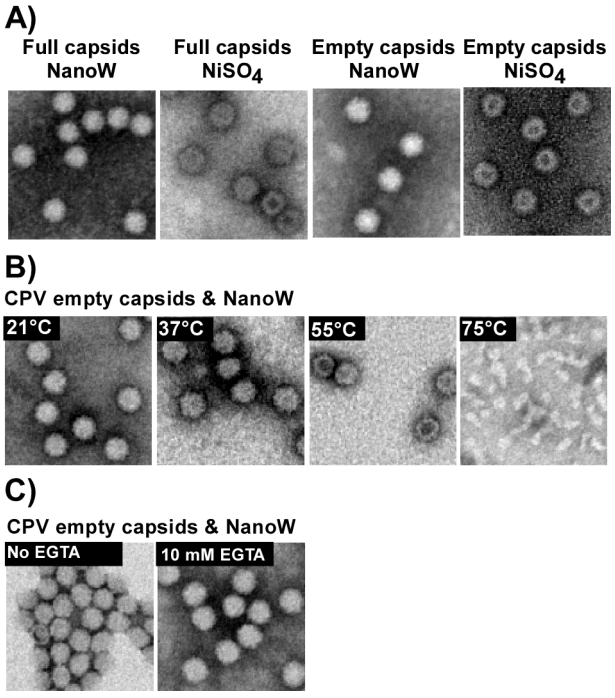
A)
Full capsids NanoW
Full capsids $NiSO_4$
Empty capsids NanoW
Empty capsids $NiSO_4$
B)
CPV empty capsids & NanoW
21°C
37°C
55°C
75°C
C)
CPV empty capsids & NanoW
No EGTA
10 mM EGTA

provided evidence of coordinated changes in the capsid, in particular by higher DNA exposure of full capsids, and by reduced bis-ANS binding and increased NanoW penetration of empty capsids. However, proteinase K treatments showed only small increases in overall capsid sensitivity, although a higher proportion of VP2 was cleaved to VP3 in full capsids, likely due to more ready transport of the VP2 N-termini to the outside of the capsid through the fivefold pore.

The full and empty capsids were indistinguishable by Trp fluorescence, despite the known interactions of the DNA with the interior of the full capsid (59). The 14 Trp residues in the VP1/VP2 common region are mostly buried within the structure, and therefore would report predominantly changes to the overall capsid conformation (29). Studies of VP2-only MVM virus-like particles showed changes in Trp emission intensity when heated between 40 and 55°C (7), but those could not be detected in our studies. This could therefore reflect structural differences between the capsids of MVM and CPV, or between the VP2-only capsids examined in that study and the VP1/VP2 CPV particles examined here. The bis-ANS binds to exposed hydrophobic regions of the capsid and can indicate structural changes (46). Our results show a clear difference in bis-ANS binding between the empty and full capsids, and those could reflect the differences in stability reported for full and empty MVM capsids (6), or to the dye entering the empty but not full capsids. The full and empty capsids did, however, disintegrate at the same temperature.

VP2 cleavage to VP3, as well as low pH treatment, has been reported to alter exposure of the VP1 N-terminus in MVM (11, 26, 44). Here we saw little effect of lower pH on the CPV structure, with the main change in proteinase K cleavages only at pH 4.0, while viral DNA exposure to TOTO-1 was not affected by low pH. We previously showed using X ray crystallography that at pH 6.2 or 5.5 there was reduced

Ca^{2+} bound and small changes in the arrangements of surface loops of the capsids (43).

Triggers activating capsids or envelope proteins of other viruses for infection include exposure to low pH, removal of bound ions, and/or protease digestion (27, 47). In studies of adeno-associated virus capsids or those of other viruses, uniform cleavages of the capsid protein(s) was seen after trypsin treatment (54). The CPV-related viruses replicate in the lymphoid tissues and in the small intestinal epithelial cells, and viruses are shed in the feces of infected animals. Thus, the virus must resist digestive proteases and proteolytic enzymes produced by the intestinal flora. For CPV and FPV even broad-specificity proteases cleaved only a small proportion of the capsid subunits at select positions. The structures of CPV-2 and FPV differ in the inter- or intra-chain bonds of VP2 residues 93 and 323 (15), and in the numbers of bound Ca^{2+} ions (120 or 180, depending on the virus) (45). The CPV-2a/b capsids also vary from CPV-2 at VP2 residues 87, 101, 300, and 305, but showed no differences in the peptides generated after proteinase K digestion.

The Ser to Ala change of VP2 residue 297 which emerged in the CPV-2a/b-derived virus background after 1990 (36) gave an additional sub-molar fragment when present in CPV-2 and FPV capsids, but not when present in CPV-2b (Figure 4.3 and 4.10). Several capsid protein changes near residue 297 affect binding to the canine TfR and to some antibodies. The changes involved include Gly300 which likely increases the flexibility of the loop, and Asp300 (in CPV-2a) which would reduce its flexibility through the formation of new hydrogen bonds in the structure (Figure 4.10A and 4.10B). The differences in the loop and surrounding structures were likely reflected in the loss of the 23 kDa peptide in the 300 Asp mutant (19, 23, 34). A consequence of this cleavage of the surface loop of the capsid would be that the particles would now contain a small number of positions with a different surface

Figure 4.10.

The positions of one of the protease cleavage sites in the structure of the capsid, and the protein or capsid relationships to the known antibody and receptor binding sites.

A and B) Comparison of the structures of 300Ala (A) found in CPV-2 and the 300Asp (B) variant, showing the differences in the bonding and likely flexibility of the loops involved. Residue 297 is shown as a Ser, and when this is changed to an Ala in FPV or CPV-2 an additional submolar cleavage can occur (Figure 4.3). The four loops shown are those that make up the region of the capsid surface around VP2 residue 300. Colors indicate the 3 different VP2 molecules involved, and numbers indicate the VP2 residues involved in hydrogen bonding in this region. The submolar cleavage of the loop around residue 300 is controlled by the presence of Ala300 in CPV-2 which allows cleavage, while 300Asp is not cleaved.

C) The location of the VP2 residues 297 and 300 on the capsid surface, relative to known TfR and antibody binding sites. The three VP2 molecules that surround the cleavage site are colored. The triangle indicates one asymmetric unit of the viral capsid. The binding footprints of 3 different antibodies (white lines) or of the feline TfR (magenta) on the capsid surface are shown, to indicate the relationship of the cleaved loop to the binding sites of those ligands.

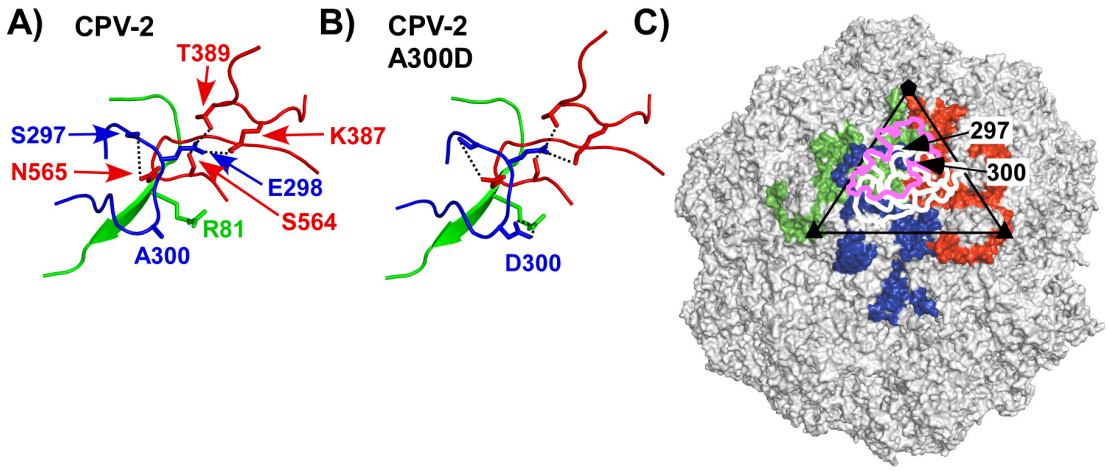
A)
CPV-2
T389
S297
K387
N565
E298
S564
R81
A300
B)
CPV-2
A300D
D300
C)
297
300

structure and charge. That cleavage is within the footprint of many antibody binding sites, and closely adjacent to the TfR binding site on the capsid (Figure 4.10C).

We have shown that feline TfR bound to only a small number of sites on the CPV-2 capsid (16). Possible explanations include intrinsic asymmetry of capsid sites controlling TfR binding, or changes in capsid morphology induced after TfR binding that prevent the attachment of additional TfRs. In these studies no changes were seen in the capsid structure after TfR binding. Sources of pre-existing asymmetry in full capsids could include the exposed 5'-end of the viral DNA, variable number of exposed VP2 or VP3 N-termini, and the 5-6 copies of VP1.

Here we show that purified full and empty capsids also incorporate about 1-3 copies per virion of a 70 kDa capsid protein variant that is likely a shorter form of VP1, and a VP2 cleaved at a single site. The 70 kDa protein may represent a minor capsid protein form, perhaps similar to the VP2 protein of the adeno-associated viruses, or to the intermediate size minor capsid proteins of bovine parvovirus and minute virus of canines (42, 51). Another source of asymmetry would also be the introduction of cleavages of loops within the capsid surface through specific protease cleavage, and in many cases those could interfere with binding of either receptor and antibodies, or of both ligands (Figure 4.10).

These results show that the capsid of the parvoviruses undergoes subtle changes upon heating which are associated with the permeability of the capsids but which do not dramatically alter the structure, and this was particularly true for the infectious DNA-containing capsids. More physiological treatments such as low pH, removal of Ca^{2+}, or binding of receptor of antibodies showed few changes in our assays, suggesting that those may act as triggers, but that dramatic changes are not likely to be present. This emphasizes the likely role of changes in permeability that release internal components such as the viral DNA and the N-terminus of VP1. The

presence of such exposed components and also of the very low copy number protein forms also suggests new sources of asymmetry which may be involved in the functions of the capsids, and we are examining these effects in our future studies.

4.6 Acknowledgements.

We thank Virginia Scarpino and Wendy S. Weichert for excellent technical assistance. Supported by a grant AI33468 from the National Institutes of Health to CRP.

REFERENCES

1. **Agbandje-McKenna, M., A. L. Llamas-Saiz, F. Wang, P. Tattersall, and M. G. Rossmann.** 1998. Functional implications of the structure of the murine parvovirus, minute virus of mice. Structure **6:**1369-1381.
2. **Agbandje, M., R. McKenna, M. G. Rossmann, M. L. Strassheim, and C. R. Parrish.** 1993. Structure determination of feline panleukopenia virus empty particles. Proteins **16:** 155-171.
3. **Albani, J. R.** 2004. Structure and dynamics of macromolecules: absorption and fluorescence studies. Elsevier, Amsterdam.
4. **Buonavoglia, C., V. Martella, A. Pratelli, M. Tempesta, A. Cavalli, D. Buonavoglia, G. Bozzo, G. Elia, N. Decaro, and L. Carmichael.** 2001. Evidence for evolution of canine parvovirus type 2 in Italy. J Gen Virol **82:**3021-5.
5. **Carey, J.** 2000. A systematic and general proteolytic method for defining structural and functional domains of proteins. Methods Enzymol **328:**499-514.
6. **Carrasco, C., A. Carreira, I. A. Schaap, P. A. Serena, J. Gomez-Herrero, M. G. Mateu, and P. J. de Pablo.** 2006. DNA-mediated anisotropic mechanical reinforcement of a virus. Proc Natl Acad Sci U S A **103:**13706-11.
7. **Carreira, A., M. Menendez, J. Reguera, J. M. Almendral, and M. G. Mateu.** 2004. In vitro disassembly of a parvovirus capsid and effect on capsid stability of heterologous peptide insertions in surface loops. J Biol Chem **279:**6517-25.
8. **Chapman, M. S., and M. G. Rossmann.** 1995. Single-stranded DNA-protein interactions in canine parvovirus. Structure **3:**151-162.
9. **Cotmore, S. F., M. D'Abramo A, C. M. Ticknor, and P. Tattersall.** 1999. Controlled conformational transitions in the MVM virion expose the VP1 N-

terminus and viral genome without particle disassembly. Virology **254:**169-181.

10. **Cotmore, S. F., and P. Tattersall.** 1989. A genome-linked copy of the NS-1 polypeptide is located on the outside of infectious parvovirus particles. J Virol **63:**3902-11.
11. **Farr, G. A., S. F. Cotmore, and P. Tattersall.** 2006. VP2 cleavage and the leucine ring at the base of the fivefold cylinder control pH-dependent externalization of both the VP1 N terminus and the genome of minute virus of mice. J Virol **80:**161-71.
12. **Farr, G. A., L. G. Zhang, and P. Tattersall.** 2005. Parvoviral virions deploy a capsid-tethered lipolytic enzyme to breach the endosomal membrane during cell entry. Proc Natl Acad Sci U S A **102:**17148-53.
13. **Flanagan, M. T., and S. Ainsworth.** 1968. The binding of aromatic sulphonic acids to bovine serum albumin. Biochim Biophys Acta **168:**16-26.
14. **Gordon, J. C., and E. J. Angrick.** 1986. Canine parvovirus: environmental effects on infectivity. Am J Vet Res **47:**1464-7.
15. **Govindasamy, L., K. Hueffer, C. R. Parrish, and M. Agbandje-McKenna.** 2003. Structures of host range-controlling regions of the capsids of canine and feline parvoviruses and mutants. J Virol **77:**12211-21.
16. **Hafenstein, S., L. M. Palermo, V. A. Kostyuchenko, C. Xiao, M. C. Morais, C. D. Nelson, V. D. Bowman, A. J. Battisti, P. R. Chipman, C. R. Parrish, and M. G. Rossmann.** 2007. Asymmetric binding of transferrin receptor to parvovirus capsids. Proc Natl Acad Sci U S A **104:**6585-9.
17. **Hueffer, K., L. Govindasamy, M. Agbandje-McKenna, and C. R. Parrish.** 2003. Combinations of two capsid regions controlling canine host range

determine canine transferrin receptor binding by canine and feline parvoviruses. J Virol **77:**10099-10105.

18. **Hueffer, K., L. M. Palermo, and C. R. Parrish.** 2004. Parvovirus infection of cells by using variants of the feline transferrin receptor altering clathrin-mediated endocytosis, membrane domain localization, and capsid-binding domains. J Virol **78:**5601-5611.

19. **Hueffer, K., J. S. Parker, W. S. Weichert, R. E. Geisel, J. Y. Sgro, and C. R. Parrish.** 2003. The natural host range shift and subsequent evolution of canine parvovirus resulted from virus-specific binding to the canine transferrin receptor. J. Virol. **77:**1718-1726.

20. **Hueffer, K., and C. R. Parrish.** 2003. Parvovirus host range, cell tropism and evolution. Curr Opin Microbiol **6:**392-398.

21. **Johnson, J. E.** 2003. Virus particle dynamics. Adv Protein Chem **64:**197-218.

22. **Korte, T., and A. Herrmann.** 1994. pH-dependent binding of the fluorophore bis-ANS to influenza virus reflects the conformational change of hemagglutinin. Eur Biophys J **23:**105-13.

23. **Llamas-Saiz, A. L., M. Agbandje-McKenna, J. S. L. Parker, A. T. M. Wahid, C. R. Parrish, and M. G. Rossmann.** 1996. Structural analysis of a mutation in canine parvovirus which controls antigenicity and host range. Virology **225:**65-71.

24. **Llamas-Saiz, A. L., M. Agbandje-McKenna, W. R. Wikoff, J. Bratton, P. Tattersall, and M. G. Rossman.** 1997. Structure determination of minute virus of mice. Acta Cryst. **D53:**93-102.

25. **Maaty, W. S., A. C. Ortmann, M. Dlakic, K. Schulstad, J. K. Hilmer, L. Liepold, B. Weidenheft, R. Khayat, T. Douglas, M. J. Young, and B. Bothner.** 2006. Characterization of the archaeal thermophile Sulfolobus

turreted icosahedral virus validates an evolutionary link among double-stranded DNA viruses from all domains of life. J Virol **80:**7625-35.

26. **Mani, B., C. Baltzer, N. Valle, J. M. Almendral, C. Kempf, and C. Ros.** 2006. Low pH-dependent endosomal processing of the incoming parvovirus minute virus of mice virion leads to externalization of the VP1 N-terminal sequence (N-VP1), N-VP2 cleavage, and uncoating of the full-length genome. J Virol **80:**1015-24.

27. **Marsh, M., and A. Helenius.** 2006. Virus entry: open sesame. Cell **124:**729-40.

28. **Nelson, C. D., L. M. Palermo, S. L. Hafenstein, and C. R. Parrish.** 2007. Different mechanisms of antibody-mediated neutralization of parvoviruses revealed using the Fab fragments of monoclonal antibodies. Virology **361:**283-93.

29. **Pakkanen, K., J. Karttunen, S. Virtanen, and M. Vuento.** 2008. Sphingomyelin induces structural alteration in canine parvovirus capsid. Virus Res **132:**187-91.

30. **Palermo, L. M., S. L. Hafenstein, and C. R. Parrish.** 2006. Purified feline and canine transferrin receptors reveal complex interactions with the capsids of canine and feline parvoviruses that correspond to their host ranges. Journal of virology **80:**8482-92.

31. **Paradiso, P. R.** 1983. Analysis of the protein-protein interactions in the parvovirus H-1 capsid. J.Virol. **46:**94-102.

32. **Paradiso, P. R., S. L. I. Rhode, and I. I. Singer.** 1982. Canine parvovirus: a biochemical and ultrastructural characterization. J. Gen. Virol. **62:**113-125.

33. **Parker, J. S. L., W. J. Murphy, D. Wang, S. J. O'Brien, and C. R. Parrish.** 2001. Canine and feline parvoviruses can use human or feline transferrin receptors to bind, enter, and infect cells. J. Virol. **75:**3896-3902.

34. **Parker, J. S. L., and C. R. Parrish.** 1997. Canine parvovirus host range is determined by the specific conformation of an additional region of the capsid. J. Virol. **71:**9214-9222.

35. **Parrish, C. R.** 1991. Mapping specific functions in the capsid structure of canine parvovirus and feline panleukopenia virus using infectious plasmid clones. Virology **183:**195-205.

36. **Parrish, C. R., C. Aquadro, M. L. Strassheim, J. F. Evermann, J.-Y. Sgro, and H. Mohammed.** 1991. Rapid antigenic-type replacement and DNA sequence evolution of canine parvovirus. J Virol **65:**6544-6552.

37. **Parrish, C. R., C. F. Aquadro, and L. E. Carmichael.** 1988. Canine host range and a specific epitope map along with variant sequences in the capsid protein gene of canine parvovirus and related feline, mink and raccoon parvoviruses. Virology **166:**293-307.

38. **Parrish, C. R., and L. E. Carmichael.** 1983. Antigenic structure and variation of canine parvovirus type-2, feline panleukopenia virus, and mink enteritis virus. Virology **129:**401-414.

39. **Parrish, C. R., Carmichael, L.E., Antczak, D.F.** 1982. Antigenic relationships between canine parvovirus type-2, feline panleukopenia virus and mink enteritis virus using conventional antisera and monoclonal antibodies. Arch.Virol. **72: 267-278**.

40. **Parrish, C. R., and Y. Kawaoka.** 2005. The origins of new pandemic viruses: the acquisition of new host ranges by canine parvovirus and influenza A viruses. Annu Rev Microbiol **59:**553-86.

41. **Parrish, C. R., P. H. O'Connell, J. F. Evermann, and L. E. Carmichael.** 1985. Natural variation of canine parvovirus. Science **230:**1046-1048.

42. **Qiu, J., F. Cheng, F. B. Johnson, and D. Pintel.** 2007. The transcription profile of the bocavirus bovine parvovirus is unlike those of previously characterized parvoviruses. J Virol **81:**12080-5.

43. **Rhode III, S. L.** 1985. Nucleotide sequence of the coat protein gene of canine parvovirus. J. Virol. **54:**630-633.

44. **Ros, C., C. Baltzer, B. Mani, and C. Kempf.** 2005. Parvovirus uncoating in vitro reveals a mechanism of DNA release without capsid disassembly and striking differences in encapsidated DNA stability. Virology **345:**137-147.

45. **Simpson, A. A., V. Chandrasekar, B. Hebert, G. M. Sullivan, M. G. Rossmann, and C. R. Parrish.** 2000. Host range and variability of calcium binding by surface loops in the capsids of canine and feline parvoviruses. J Mol Biol **300:**597-610.

46. **Slavik, J.** 1982. Anilinonaphthalene sulfonate as a probe of membrane composition and function. Biochim Biophys Acta **694:**1-25.

47. **Smith, A. E., and A. Helenius.** 2004. How viruses enter animal cells. Science **304:**237-42.

48. **Steven, A. C., J. B. Heymann, N. Cheng, B. L. Trus, and J. F. Conway.** 2005. Virus maturation: dynamics and mechanism of a stabilizing structural transition that leads to infectivity. Curr Opin Struct Biol **15:**227-36.

49. **Strassheim, L. S., A. Gruenberg, P. Veijalainen, J.-Y. Sgro, and C. R. Parrish.** 1994. Two dominant neutralizing antigenic determinants of canine parvovirus are found on the threefold spike of the virus capsid. Virology **198:**175-184.

50. **Suikkanen, S., M. Antila, A. Jaatinen, M. Vihinen-Ranta, and M. Vuento.** 2003. Release of canine parvovirus from endocytic vesicles. Virology **316:**267-80.

51. **Trempe, J. P., and B. J. Carter.** 1988. Alternate RNA splicing is required for synthesis of Adeno-associated virus VP1 capsid protein. J Virol **62:**3356-3363.

52. **Truyen, U., J. F. Evermann, E. Vieler, and C. R. Parrish.** 1996. Evolution of canine parvovirus involved loss and gain of feline host range. Virology **215:**186-189.

53. **Tsao, J., M. S. Chapman, M. Agbandje, W. Keller, K. Smith, H. Wu, M. Luo, T. J. Smith, M. G. Rossmann, R. W. Compans, and C. R. Parrish.** 1991. The three-dimensional structure of canine parvovirus and its functional implications. Science **251:**1456-1464.

54. **Van Vliet, K., V. Blouin, M. Agbandje-McKenna, and R. O. Snyder.** 2006. Proteolytic mapping of the adeno-associated virus capsid. Molecular Therapy **14:**809-21.

55. **Vihinen-Ranta, M., L. Kakkola, A. Kalela, P. Vilja, and M. Vuento.** 1997. Characterization of a nuclear localization signal of canine parvovirus capsid proteins. Eur J Biochem **250:**389-394.

56. **Vihinen-Ranta, M., D. Wang, W. S. Weichert, and C. R. Parrish.** 2002. The VP1 N-terminal sequence of canine parvovirus affects nuclear transport of capsids and efficient cell infection. J Virol **76:**1884-91.

57. **Weichert, W. S., J. S. Parker, A. T. Wahid, S. F. Chang, E. Meier, and C. R. Parrish.** 1998. Assaying for structural variation in the parvovirus capsid and its role in infection. Virology **250:**106-17.

58. **Wikoff, W. R., G. Wang, C. R. Parrish, R. H. Cheng, M. L. Strassheim, T. S. Baker, and M. G. Rossmann.** 1994. The structure of a neutralized virus:

canine parvovirus complexed with neutralizing antibody fragment. Structure **2:**595-607.

59. **Xie, Q., and M. S. Chapman.** 1996. Canine parvovirus capsid structure, analyzed at 2.9 Å resolution. J Mol Biol **264:**497-520.

60. **Yuan, W., and C. R. Parrish.** 2000. Comparison of two single-chain antibodies that neutralize Canine Parvovirus: analysis of an antibody-combining site and mechanisms of neutralization. Virology **269:**471-480.

61. **Zadori, Z., J. Szelei, M.-C. Lacoste, P. Raymond, M. Allaire, I. R. Nabi, and P. Tijssen.** 2001. A viral phospholipase A2 is required for parvovirus infectivity. Developmental Cell **1:**291-302.

CHAPTER FIVE

Summary and conclusions

The studies reported in this thesis had two main objectives: To better characterize the capsid interactions with antibodies of the host immune system, and to biochemically characterize the changes that might occur in the capsid structure during infection. The first studies demonstrated that antibodies make complex interactions even with these structurally simple viruses, and suggested that as IgGs, these antibodies neutralize CPV by cross-linking capsids together, and to a lesser extent by steric hindrance of the capsid interaction with the TfR. However, neither of these mechanisms completely explains the results presented. It is likely that other mechanisms contribute to neutralization of CPV by these antibodies, such as steric hindrance of asymmetric sites on the CPV capsid by the highly neutralizing antibodies, as described below. The studies of capsid stability demonstrate that CPV is extremely stable under many conditions, but that small changes can be identified and those are likely of biological relevance.

Due to its structural and genetic simplicity, CPV and the related host range mutants are particularly good models for studying the basic properties of virus-host interactions. CPV capsids can be produced in large quantities, and the genome is amenable to mutation. These viruses use TfR to bind and enter cells, and this receptor normally enters cells using one of the better characterized endocytic pathways. A number of high resolution structures of wildtype CPV and related viruses and mutants have been determined under various conditions. Finally, a large number of monoclonal antibodies have been prepared against the capsids and those are available for study.

Viruses of vertebrates make extensive interactions with the host immune system during infection, and part of this immune response is the production of anti-viral antibodies that in many cases prevent or mitigate viral infection. In this thesis, I have further characterized a selected panel of eight monoclonal antibodies, and

determined their interactions with CPV and FPV. I have shown that all eight of these intact IgG antibodies are able to neutralize the virus, but that only three of the Fab fragments of these antibodies were able to do so. Since these IgGs cannot bivalently bind the virus, the IgGs likely neutralize CPV through cross-linking of capsids, and also through the increased avidity that comes from the multiple interactions of the IgGs with the capsids. Furthermore, the increased mass of the intact IgG compared to the Fab may allow it to block access to residues that are not in its own specific epitope. The two highly neutralizing Fabs that neutralize the virus do so at ratios of <100 Fabs per capsid, while the other Fabs do not neutralize at ratios as high as ~2000 Fabs per capsid. In our solid phase binding assays, all of these Fabs bound with about the same relative affinity, suggesting that neutralization is a special property of the antibodies beyond just binding and blocking receptor attachment. From our structural studies, the neutralizing Fabs do not bind to drastically different regions of the capsid compared to the non-neutralizing Fabs, although in some cases their angle of binding is more skewed across the two-fold axis than other antibodies.

There are several possibilities that could explain the difference for neutralization abilities between these Fabs. It is possible that these neutralizing Fabs interact with capsids in a way that the non-neutralizing Fabs do not. We did not observe any conformational changes in the Fab-CPV reconstructions and by biochemical analysis, indicating that Fab binding did not induce detectable pronounced changes in the virus. The possibility of structural asymmetry in CPV has been raised recently, since TfR binds CPV capsids with low occupancy, despite an excess of TfR added in those experiments. It has therefore been suggested that there may be a small number of "special" sites on the virus that TfR but not antibodies bind to. In this model, the neutralizing Fabs leaning across the two-fold axis would sterically interfere with receptor binding, while the non-neutralizing Fabs would be

less able to compete, despite a large number of Fabs bound. Fabs missing from a few vertices on the virus would not be seen in the cryoEM reconstructions, since sixty fold icosahedral averaging was used to solve those structures. Since the neutralizing Fabs are skewed across the two fold axis, they may block TfR binding to these adjacent special sites. This model is supported by the fact that TfR binds with low occupancy to capsids, the two neutralizing Fabs compete with TfR binding at lower Fab to capsid ratios, and that the non-neutralizing Fabs do not block infectivity at high molar ratios of Fabs to CPV. However, all of the Fabs studied are able to compete with receptor binding to some degree. This indicates that receptor binding may require some interaction with residues outside of these special sites, or regions of TfR protrude away from these special sites and clash with other, non-neutralizing antibodies. However, since these antibodies do not neutralize CPV, this interaction would clearly be less effective than these which occlude the asymmetric position on CPV.

A second possibility that may explain the differing ability of these Fabs to neutralize virus could be related to subtle differences in their binding abilities. For the competition experiments of Fabs and TfR binding of the capsids in *in vitro* binding assays and on cells, the virus and antibody were incubated for one hour at 37°C, and then overlaid onto cells or plates for 1 h. The unbound virus was washed away and measurements taken. Conversely, for the neutralization experiments, virus and antibody were mixed for 1h at 37°C, then incubated with cells for 48 h. Since TfR endocytosis is such a rapid event, any virus that disengages an antibody and binds to receptor would be expected to be rapidly taken up into cells. Therefore, small differences between the off rates of these Fabs could result in differences in neutralization that were not seen in the competition experiments, since the time interval during the neutralization experiments was much greater. However, the non-

neutralizing Fabs do not decrease infectivity at high antibody concentrations, and this would be expected if binding kinetics were the sole explanation for neutralization.

Clearly, more work needs to be done to resolve these issues, and several areas of future research will hopefully identify mechanisms of neutralization of CPV by antibodies. First, an accurate measurement of the binding affinities and kinetics of Fabs and TfR for CPV and their related host range mutants is critical. The use of surface plasmon resonance would be ideal, since this would allow measurement not only of affinity, but also on and off rates. Analytical ultracentrifugation of CPV and TfR pre-incubated with concentrations of TfR well above the dissociation constant would be useful for determining stoichiometry of binding. Unfortunately, it would be difficult to demonstrate the absence one or two antibodies on the CPV capsid by analytical ultracentrifugation. Further characterization of these special sites, and their interactions with CPV and TfR would be critical. For example, it is possible that clustering of VP1 molecules around one vertex is responsible for asymmetry in CPV. Studies involving chemical cross-linking of the capsid could help to resolve distribution of VP1; VP1 has been shown to preferentially cross-link in the related parvovirus H-1, and may be a more general trend in the Parvoviridae family. Alternative approaches, such site-directed spin labeling in the N-terminus of VP1 and detection with electron paramagnetic resonance spectroscopy or double electron-electron resonance would help to localize distances between VP1 N-termini. These methods have been used extensively to determine distances between specific residues in other proteins.

The shared binding footprints of the eight Fabs overlap the areas that are sites where escape mutations are found; however, the distinctions between the A and B sites are not as clear as previously thought. The combined footprints of these eight antibodies cover most of the accessible surface of the virus. As a future study, I would

propose immunizing mice with capsids containing escape mutation substitutions in both site A and B, and cleaved N-termini of VP2, to see whether other sites on the virus could serve as functional epitopes in the absence of the major antigenic sites, and whether these antibodies are neutralizing. I also propose to sequence the variable domains of more of the monoclonal antibody library against CPV. These sequences could then be used to characterize what gene segments preferentially contribute to anti-CPV antibody selection in mice. It would be interesting to see whether these antigenically altered viruses promoted the use of other antibody gene segments during selection of reactive B cells. Finally, all of the virus-Fab structures solved so far involve high affinity IgGs, and it would be interesting to examine the low affinity IgM antibodies that are produced early in the response to see if those also bind around the two antigenically variable A and B structures of the capsid. These proposed studies will hopefully provide a mechanistic understanding into the viral structures that determine the selection and maturation of antiviral antibodies.

The second aim of this thesis was to examine the effects on the virus capsid structure of various conditions that CPV encounters during endocytic uptake and release from endosomes. Since CPV binds TfR, is trafficked through recycling and/or late endosomes, I focused on the effects of receptor binding, low pH, and calcium removal on the capsid. Low pH had little pronounced structural effect on CPV, which is consistent with X-ray diffraction data. Intrinsic tryptophan fluorescence showed that the hydrophobic environment of the Trp residues was not significantly altered at lower pH, although the fluorescence intensity was reduced, indicating that these residues may be more flexible and that they are partially quenched in the capsid at lower pH. Binding of the hydrophobic dye bis-ANS to CPV capsids and also studies using limited proteolysis with proteinase K both showed that the surface structure of this virus is unchanged until ~pH 4. In addition, release of viral DNA was not pH

dependant, indicating that other factors are important in its release. These results are consistent with structural data, which showed that only small changes in some surface loops at pH 6.2. Low pH in the endosome is necessary for CPV infection, but at this point the role of low pH is not understood - whether this is due to a direct effect of pH on the capsid or receptor structure, or to some other role of low pH in the viral infectious process, or perhaps the low pH causes capsid changes that are not detectable in these assays, is not known.

Calcium removal also does not cause large conformational changes to the structure of full particles in solution by limited proteolysis, tryptophan fluorescence, and bis-ANS binding. Empty particles do show increased binding of bis-ANS under EGTA treatments, but is unclear whether this occurred on the surface of capsids, or (more likely) that the bis-ANS more readily gains access to the interior of the empty capsids compared to the full particles. This again is consistent with the structural data, where only small changes are seen at high EGTA concentrations.

I showed that TfR binding to CPV capsids did not cause global conformational changes detectable by bis-ANS binding or limited proteolysis. Previously, we had shown that TfR binds CPV with low occupancy despite a molar excess of TfR, and had hypothesized that this occurred because of conformational changes to the virus, or due to a low number of potential binding sites present on the virus. In light of the work presented here, it appears more likely that inherent asymmetry in CPV is a more plausible explanation for this phenomenon.

What changes to the CPV capsid are actually required for infection? As demonstrated in this presented work, it appears large conformational changes do not occur in the capsid under conditions encountered during infection. This therefore is quite a different result from those reported for many other viruses where the viral proteins or capsids undergo major uniform changes in conformation at low pH, after

proteinase cleavage or ion removal. At the very least however, the 3' end of the viral ssDNA genome needs to become exposed to engage host polymerases. The capsids must also deploy some membrane-lytic or modifying structure to allow escape from endosomes. The PLA2 domain of VP1ur may fulfill this role. Specific assays should be designed to identify the physiological factors that cause VP1ur externalization. Furthermore, an understanding of how the PLA2 activity modifies endosomal membranes to promote infection is critical. Understanding the mechanisms and structural controls of release of the VP1ur would also be important, and might be facilitated by the generation of pseudo atomic structures on heated virions that have exposed their VP1ur. These studies may also help to identify whether the VP1ur is released from one specific region on the capsid with respect to TfR binding or ssDNA release, or is randomly distributed. Heating to 60°C causes not only externalization the VP1ur, but also part of the ssDNA genome. Cryo-EM and image reconstructions would therefore also be able to visualize these transitioned particles, and would help explain the relationship between DNA and VP1ur release. Also, if TfR binding and VP1ur release are similarly arranged, this may act to orient the release of their PLA2 towards the endosomal membrane. Similar studies have been done in poliovirus, which appears to release its RNA through a pore in the endosomal membrane surrounded by poliovirus receptor molecules, and presumably the externalized VP4 molecules.

I also showed that some mutations in a region of the capsid around VP2 residue 300 determine it protease sensitivity. The A300D substitution forms an additional stabilizing hydrogen bond, which would cause surface loop 3 to be less flexible in solution, and this loop is then not cleaved by proteinase K. There are no large structural differences between CPV and FPV, but those viruses differ in their ability to bind canine TfR. It is therefore possible that flexibility of the loop

containing residue 300 is determining differences in host range, since this A300D substitution (and the structurally related VP2 residue 299 change from Gly to Glu) results in less infectivity in canine cells through alterations in canine TfR binding. Several avenues of research could address this issue. First, high resolution structures of the CPV-TfR complex should be generated. This will allow us to determine whether the capsid substitutions that control host range directly control the interactions with the TfR. If no direct interaction is shown, then binding to TfR may be controlled by flexibility of this loop. Introduction of cysteine residues in this flexible loop could allow us to specifically control flexibility through the formation of disulfide bonds, and allow us to assay the ability of these capsids to bind TfR. This will help to further understand the fine tuning of the CPV-TfR interaction.

Finally, I identified three proteins that are incorporated into the capsid at a low molar ratio compared to VP1 or VP2. Two of these proteins correspond to a VP2 that is cleaved in one position. Mass spectrometry and Western blotting with anti-peptide anti-sera predicts that this cleavage occurs between residues 280-290. Interestingly, none of the proteases used in these experiments generated a similar cleavage in the capsids. The other identified protein (about 70kDa) likely corresponds to a lower molecular variant of VP1 and may be the result of alternate splicing of the VP1 mRNA. Future studies should continue to characterize these proteins and to explain their roles (if any) in the viral life cycle. For the cleaved VP2, residues involved in this cleavage should be identified and mutants at that position prepared and assayed for their infectivity and stability. Since this cleavage most likely occurs after capsid assembly, the protease or other host (or viral) factor that is responsible for this cleavage should be identified and knocked out or inhibited to determine its effect on viral infectivity. If the higher molecular weight peptide is indeed a splice variant of

VP1, then the acceptor/donor sequences of that splice could be mutated and the effect on infectivity should be determined.

This thesis has increased our understanding of the interactions that CPV makes with antibodies, receptors, and other host factors during viral infection. The methods developed and presented in this thesis are tractable and can readily be adapted to address other questions involving antibody-virus interactions and structural changes to viral capsids.